

# **Hepatic NK cell education in monobenzene-induced contact hypersensitivity**

Doctoral thesis  
to obtain a doctorate (PhD)  
from the Faculty of Medicine  
of the University of Bonn

**Larissa Helen Mühlenbeck**

from Bergisch Gladbach

2021

Written with authorization of  
the Faculty of Medicine of the University of Bonn

First reviewer: Prof. Dr. Gunther Hartmann

Second reviewer: Prof. Dr. Sven Burgdorf

Day of oral examination: 14.04.2021

For the Institute of Clinical Chemistry and Clinical Pharmacology, University Hospital Bonn

Director: Prof. Dr. Gunther Hartmann

## Table of Contents

List of abbreviations .....	6
1. Introduction .....	9
1.1 Immunity - the innate and adaptive immune compartments.....	9
1.2 Natural killer cells - protection through innate immunity.....	12
1.3 Human and mouse NK cells .....	14
1.4 NK cell development.....	15
1.5 NK cells and their innate and adaptive relatives .....	17
1.5.1 NK vs. ILC1 cells.....	17
1.5.2 NK vs. cytotoxic CD8+ T cells (CTLs) .....	19
1.5.3 Transcription factors T-bet and Eomesodermin (Eomes) .....	19
1.6 Memory NK cells bridge innate and adaptive immunity .....	20
1.7 Hapten-induced contact hypersensitivity (CHS) in mice .....	21
1.7.1 CHS mimics symptoms of allergic contact dermatitis (ACD) .....	21
1.7.2 The CHS response.....	22
1.7.2.1 The sensitization phase of CHS.....	23
1.7.2.2 The CHS elicitation phase.....	24
1.7.3 NK cells can drive hapten-specific memory responses .....	27
1.7.4 Monobenzene - vitiligo inducer and melanoma immunotherapy agent .....	28
1.8 Aims of the thesis .....	31
2. Material and methods .....	33
2.1 Mice .....	38
2.2 Induction of contact hypersensitivity (CHS) .....	38
2.3 Validation of CHS establishment through elicitation of the ear .....	38
2.4 Immune cell isolation from the liver.....	39
2.5 Immune cell isolation from the inguinal lymph node (ILN).....	39

2.6	Immune cell isolation from the ear and ear homogenate extraction.....	39
2.7	Serum preparation from whole blood.....	40
2.8	Flow cytometry.....	40
2.9	NK cell purification through MACS- and FACS-based cell sort.....	41
2.10	Adoptive NK cell transfer experiments.....	41
2.10.1	Adoptive transfer of <i>ex vivo</i> MBEH-exposed cNK cells.....	41
2.11	NK cell co-culture with B16.F10 melanoma cells.....	42
2.11.1	Enzyme-linked immunosorbent assay (ELISA).....	42
2.11.2	CellTiter-Blue® cell viability assay.....	43
2.12	Sequencing.....	43
2.12.1	RNA single cell sequencing.....	43
2.12.2	3'-RNA bulk sequencing of cNK cells.....	44
2.12.3	ATAC sequencing of cNK cells.....	45
2.13	Statistics.....	46
2.14	General software.....	47
3.	Results.....	48
3.1	Distinction and response of hepatic NK cells upon MBEH sensitization.....	48
3.2	Elicitation response of MBEH-sensitized mice.....	52
3.2.1	Ear swelling as indicator of successful MBEH sensitization.....	52
3.2.2	Multiple immune cell subsets respond during MBEH-induced elicitation.....	53
3.3	Local and systemic immune cell signaling during MBEH elicitation.....	58
3.3.1	The cytokine and chemokine milieu in the elicited ear.....	58
3.3.2	Cytokine and chemokine concentration in the serum.....	59
3.4	Adoptive transfer of hepatic NK cell populations and initiation of..... MBEH-induced CHS.....	60
3.4.1	Adoptive transfer of mature hepatic NK cell populations reveals..... subset specificity in MBEH-induced CHS.....	60

3.4.2	The ear swelling upon adoptive transfer of hepatic NK1.1+,CD49b+ cells from MBEH-sensitized mice arises from cell specificity	62
3.5	Adoptive transfer of <i>in vitro</i> MBEH-exposed hepatic cNK cells can induce an elicitation response in naïve recipient mice	65
3.6	MBEH sensitization of mice modifies hepatic NK cell features <i>in vitro</i>	68
3.6.1	MBEH sensitization does not change the spontaneous IFN- $\gamma$ and granzyme B secretion of hepatic NK1.1+,CD49b+ NK cells	68
3.6.2	<i>In vivo</i> MBEH sensitization modulates NK cell control of B16.F10 melanoma cells <i>ex vivo</i>	69
3.7	RNA single cell sequencing reveals transcriptional identity of hepatic NK1.1+ cells from naïve and MBEH-sensitized mice	72
3.8	Sensitization with MBEH <i>in vivo</i> induces transient transcriptional changes in hepatic cNK cells	75
3.9	MBEH sensitization of mice establishes epigenetic changes in hepatic cNK cells	80
4.	Discussion	84
5.	Abstract	92
6.	List of figures	94
7.	List of tables	96
8.	References	97

**List of abbreviations**

ADCC	antibody-dependent cell-mediated cytotoxicity
AhR	aryl hydrocarbon receptor
APC (fluorophore)	allophycocyanin
APC (immunity)	antigen presenting cell
ATAC seq	assay for transposase-accessible chromatin using sequencing
BM	bone marrow
CCL	CC chemokine ligand
CD	cluster of differentiation
CHS	contact hypersensitivity
CMV	cytomegalovirus
CTL	cytotoxic T lymphocyte
CXCL	CXC chemokine ligand
CXCR	CXC chemokine receptor
DAMP	damage-associated molecular pattern
DC	dendritic cell
dDC	dermal dendritic cell
DNA	deoxyribonucleic acid
DNAM-1	DNAX accessory molecule 1
DNFB	1-fluoro-2,4-dinitrobenzene
EDTA	ethylenediaminetetraacetic acid
ELISA	enzyme-linked immunosorbent assay
Eomes	eomesodermin
FACS	fluorescence-activated cell sorting

FITC	fluorescein isothiocyanate
FSC	forward scatter
GM-CSF	granulocyte macrophage colony-stimulating factor
IFN	interferon
IL	interleukin
ILC	innate lymphoid cell
ILN	inguinal lymph node
KC	keratinocyte
LC	langerhans cell
LN	lymph node
MACS	magnetic activated cell sorting
MBEH	monobenzene
MCMV	murine cytomegalovirus
MHC	major histocompatibility complex
MIC therapy	monobenzene imiquimod CpG therapy
mNK	mature natural killer
NK	natural killer
NLRP3	NACHT, LRR and PYD domains-containing protein 3
NOD	nucleotide-binding oligomerization domain
Oxa	oxazolone (4-ethoxymethylene-2-phenyloxazol-5-one)
PAMP	pathogen-associated molecular pattern
PBS	phosphate-buffered saline
PE	phycoerythrin
PE/Cy7	phycoerythrin cyanine 7 conjugate
PerCP	peridinin chlorophyll protein complex
PRR	pattern recognition receptor

p-value	probability value
RAG	recombination-activating gene
RNA	ribonucleic acid
ROS	reactive oxygen species
Rpm	revolutions per minute
RT	room temperature
SEM	standard error of the mean
S1PR	sphingosine-1-phosphate receptor
SSC	sideward scatter
T-bet	T-box transcription factor TBX21
TCR	T cell receptor
T <sub>H</sub> cell	T helper cell
TLR	toll-like receptor
TNCB	2,4,6-trinitro-1-chlorobenzine
TNF $\alpha$	tumor necrosis factor alpha
TRAIL	TNF-related apoptosis-inducing ligand
VSV	vesicular stomatitis virus



## 1. Introduction

### 1.1 Immunity - the innate and adaptive immune compartments

Every living organism is constantly exposed to potentially toxic molecules, bacterial, fungal, and viral pathogens. “Immunity” describes the ability of organisms to resist their negative impacts (Murphy and Weaver, 2016). Classically, the immune system of vertebrates can be divided into the innate and the adaptive immune compartments (Klein, 1989), which act in concert and comprise tissue-resident as well as circulating immune cells that survey the environment and are tightly regulated to prevent self-damage and autoimmunity (Murphy and Weaver, 2016).

The innate immune system represents the first line of defense and evolutionarily conserved arm of the immune system found across all species (Buchmann, 2014). It is mostly unspecific and characterized by rapid responses, including the immediate production and secretion of effector molecules like cytokines, chemokines, reactive oxygen species (ROS) and antimicrobial peptides. Innate immunity provides three mechanisms of protection:

1. Anatomical barriers, such as the epithelium lining the skin, the lung or the gut, which prevents the invasion of immediate threats like foreign particles, toxins, noxious chemicals, microbes, and pathogens (Murphy and Weaver, 2016).

2. Innate immune cells, including granulocytes (basophils, eosinophils, neutrophils), monocytes, macrophages, dendritic cells (DCs), natural killer cells (NKs), and innate lymphoid cells (ILCs). Innate immune cells possess germline-encoded pattern recognition receptors (PRR) (Janeway, 1989; Medzhitov et al., 1997) on their surface, which allow the recognition of molecular patterns in the extracellular milieu, including some commonly found on pathogens. The toll-like receptor (TLR) family represents a very well characterized group of PRRs that release (pro)inflammatory cytokines following pathogen recognition and whose signaling through NF $\kappa$ B is conserved from *Drosophila* flies to humans (Medzhitov et al., 1997; Takeda et al., 2003). In general, PRRs include the pathogen-associated molecular patterns (PAMPs) and damage-associated molecular patterns (DAMPs), described as components released by the host cell during self-damage or death. PRR recognition activates innate immune cells and induces the phagocytosis of

pathogens, transformed, or infected cells. The activation of phagocytes promotes cytotoxicity and the secretion of inflammatory chemo- and cytokines, which attract and recruit lymphocytes of the adaptive immune system.

3. The complement system, consisting of a large number of plasma proteins whose interaction with one another induces phagocyte stimulation and clearance of damaged cells, microbes, or foreign material, by inducing a series of inflammatory responses that support the clearance of infection (Murphy and Weaver, 2016). Neutrophils, DCs, monocytes, and macrophages rapidly incorporate and neutralize pathogens by phagocytosis. Following phagocytosis, DCs and macrophages internalize and break down pathogenic proteins into small peptides, which are then loaded on major histocompatibility complex (MHC) structures and allow these cells to act as antigen presenting cells (APCs), revealing the foreign peptides to other immune cells and inducing the adaptive immune response (Murphy and Weaver, 2016).

In the adaptive immune system, T and B lymphocytes are the most prevalent immune cell types (Murphy and Weaver, 2016). These are characterized by their high adaptive specificity and their capacity to develop immunological memory. The latter is defined as the capability of the immune system to respond faster and with a higher magnitude to a stimulus previously encountered, e.g. a pathogen. The humoral component of adaptive immunity are antibodies secreted by B lymphocytes that, like innate immunity, can activate the complement system and specifically bind to a wide variety of antigens.

Most immune cells of the innate and adaptive immune compartments develop in the bone marrow (BM) from hematopoietic stem cells (HSC). Through the process of hematopoiesis, the HSC in the BM can differentiate into a myeloid or a lymphoid progenitor. Whereas the common myeloid progenitor gives rise to erythrocytes, granulocytes (basophils, neutrophils, eosinophils), monocytes, macrophages, dendritic cells, and mast cells, the lymphoid progenitor develops into T or B lymphocytes (Szilvassy, 2003), NK or other innate lymphoid cells (ILCs) (Constantinides et al., 2014). Whereas T cells are generated in the thymus, B lymphocytes originate from the BM. Once mature, both cellular subsets can distinguish between host and foreign molecules because autoreactive cells were either removed or tolerized in relation to self-antigens (de Boer and Hogeweg, 1987). Once maturation is complete, they migrate through the

lymphatic system and blood stream and then mostly reside in secondary lymphatic organs like the spleen and lymph nodes (LNs). The latter are connected to an extended network of lymphatic vessels and capillaries, which span the whole body. Innate and adaptive immune cells reside and interact in the LNs, receive activation and survival signals, and are recruited to sites of infection or distress. Besides innate and adaptive immune signaling, LNs form active barriers that prohibit the spread of pathogens through lymphatics (Bogoslowski and Kubes, 2018).

In contrast to innate immunity, the antigen-specific receptors of T and B lymphocytes are generated throughout the lifetime of the organism by randomized recombination of segments encoding receptor DNA sequences, called somatic recombination. In this process, a few hundred different gene segments are recombined and used to generate a near indefinite number of unique receptors, referred to as V(D)J-recombination.

As adaptive immune cells, T cells recognize small peptides presented on the MHC molecules through the T cell receptor (TCR) and can be divided into the cytotoxic T lymphocytes (CTL) and T helper ( $T_H$ ) cells. Foreign structures, like pathogen-derived peptides, can be detected by CTLs. These bind to the peptide-MHC class I complex and are characterized through expression of the cluster of differentiation co-receptor CD8. CD8+ T cells release cytotoxic granules and induce cell contact-mediated apoptosis to kill target cells. Other foreign structures are detected and processed by APCs and can be recognized by  $T_H$  cells through the interaction between the TCR and the peptide-MHC class II complex. These cells express the co-receptor CD4 and can further differentiate upon activation.

Activated  $T_H$  cells can promote the activation of the other subset of adaptive immune cells, the B cells. These cells bind the antigen via their membrane-bound or soluble B cell receptor, called immunoglobulin (Ig) or antibody (DeFranco, 1987). These antibodies consist of a constant and a variable region: while the variable region forms the antigen-binding site, the constant region determines the antibody class (IgM, IgG, IgD, IgA, IgE). B cell activation induces antigen internalization, antigen breakdown into small peptides, peptide loading on the MHC class II complex, and presentation on the B cell surface. Further, B cell stimulation can induce the differentiation into a memory B cell or a plasma cell, which secretes antibodies that specifically bind the encountered antigen.

## 1.2 Natural killer cells - protection through innate immunity

Due to their “natural” cytotoxicity against tumor cells, “natural killer” (NK) cells were discovered in 1975 (Herberman et al., 1975; Kiessling et al., 1975). Upon identification as a separate lymphocyte lineage, they were characterized based on their spontaneous cytotoxicity against tumor cells and cytokine production (Trinchieri, 1989). NK cells survey the host organism for stressed, mutated, and infected cells, and can rapidly kill endangering cells without previous priming or antigen specificity.

Activation, signaling, and the effector function of NK cells rely on the balance of activating and inhibitory signals (Murphy and Weaver, 2016). Through the expression of a variety of inhibitory and activating surface receptors, NK cells can discern between healthy, foreign, or transformed cells. To assess whether a cell is a health risk, NK cells examine the surface-expressed receptor landscape of cells for MHC-I receptors. These receptors are constitutively expressed by healthy cells at steady-state conditions. NK cells are educated to tolerate these cells as “self” cells that belong to the host and do not represent a threat for the host integrity. Hence, the expression of MHC-I receptors prevents cells from NK-induced lysis, whereas missing MHC-I expression activates NK cells and induces NK cytotoxic activity against these cells, a mechanism of action known as “missing self-hypothesis” (Kärre et al., 1986).

The MHC-I receptor is detected by inhibitory receptors of NK cells, like the lectin-like Ly49 dimers in the mouse, the killer cell immunoglobulin-like receptors (KIRs) in humans, and the lectin-like CD94-NKG2A heterodimers in mice and humans (Anfossi et al., 2006; Fernandez et al., 2005; Kim et al., 2005; Parham, 2005; Yokoyama and Plougastel, 2003; Yu et al., 2007).

In addition to inhibitory receptors, NK cells also possess activating receptors, which detect the presence of ligands on cells in distress, such as the stress-induced self-ligands recognized by NKG2D (Bauer et al., 1999; Glässner et al., 2012). Additionally, target cell apoptosis can be induced through upregulation of Fas ligand (FasL) and TNF-related apoptosis-inducing ligand (TRAIL) on NK cells that bind to Fas- or TRAIL receptors, respectively, on the target cell surface (Glässner et al., 2012) (Figure 1).

Further danger signaling molecules are infectious non-self ligands, like the cytomegalovirus (CMV)-encoded protein m157 that is recognized by Ly49H in the mouse

(Arase et al., 2002; Davis et al., 2008; Smith et al., 2002) and TLR ligands expressed by NK cells (Sivori et al., 2004).

Once activated, NK cells can directly act on target cells and alarm the immune system through cytokine secretion. Upon stimulation through target cell contact or IL-12/IL-18 stimulation, NK cells secrete the pro-inflammatory cytokines IFN- $\gamma$  (Scharton and Scott, 1993) and TNF- $\alpha$  (Fauriat et al., 2010) or interleukins like IL-10 (Mehrotra et al., 1998), the eosinophil-activating factor IL-5 (Warren et al., 1995), and the hematopoietic growth factor and immune modulator granulocyte/macrophage-colony stimulating factor (GM-CSF) (Levitt et al., 1991). In addition, activated NK cells secrete chemokines, like CCL3 (MIP-1 $\alpha$ ) and CCL5 (RANTES) (Roda et al., 2006).

The immediate NK cytotoxicity and ability to target and kill transformed or infected cells result from the exocytosis of NK granules, which contain perforin and granzyme B. While the perforin protein creates pores in the cell membrane of the target cell, granzymes are proteases that enter the target cells through the perforin-induced pores. Once in the cytosol of the target cell, granzyme B targets caspase-3, initiates DNA fragmentation and induces cell apoptosis (Shi et al., 1992). Importantly, NK-induced apoptosis of stressed or infected cells can also occur through antibody-dependent cellular cytotoxicity (ADCC) since stressed or infected cells can be opsonized by antibodies to alert the immune system (Figure 1). By this antibody-coating, phagocytosis is facilitated and if such an antibody binds to its antigen on the target cell surface, this antibody can be recognized by the activating NK cell receptor Fc $\gamma$ RIII (CD16), resulting in NK cell activation, the release of cytolytic granules, and target cell apoptosis (Werfel et al., 1989).

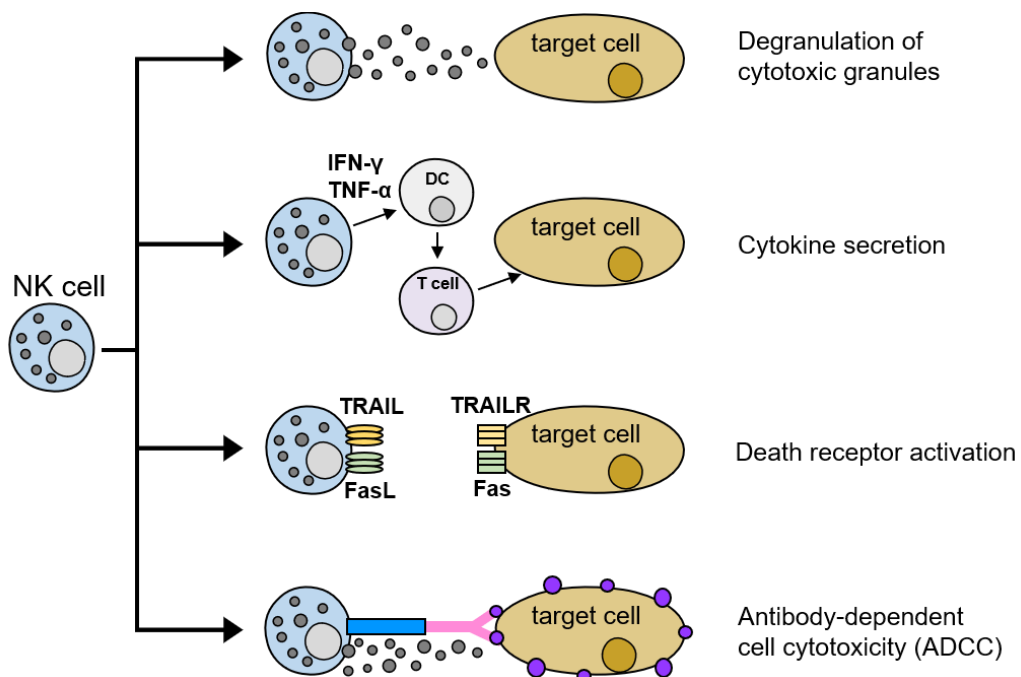


**Figure 1: Overview of NK cell effector mechanisms.** NK cells can induce target cell apoptosis through various mechanisms, comprising the release of cytotoxic granules, secretion of the pro-inflammatory cytokines IFN- $\gamma$  and TNF- $\alpha$  to activate DCs and prime T cells, upregulate FasL and TRAIL, and operate ADCC.

In general, NK recruitment, activation and killing is governed by the cytokine and chemokine micro-environment and the interaction with neighboring cells (Vivier et al., 2004). While NK cell effector functions are modulated by their environment through IL-2, which promotes NK cell proliferation, cytotoxicity and cytokine secretion (Trinchieri, 1989), type I IFN, IL-12, IL-15, and IL-18 are also potent activators of NK cell effector function (Walzer et al., 2005). Beside other immune cells, DC activation can significantly shape the intensity and quality of the NK cell response (Long, 2007).

### 1.3 Human and mouse NK cells

NK cells recirculate and can be found in many different organs, like the spleen, liver, mucosal tissues, skin, pancreas, uterus, gut, joints and central nervous system (CNS) where they amplify the local immune response and fight infectious agents. Mature NK cells from C57BL/6 mice express NK1.1, NKp46, and by the majority the integrin CD49b (DX5).

The cell surface receptor NK1.1 (Killer cell lectin-like receptor subfamily B, member 1; CD161) is a surface molecule required for NK activation and the induction of target cell lysis (Karlhofer and Yokoyama, 1991), whereas the surface receptor NKp46 (Natural cytotoxicity triggering factor 1; CD335) is expressed by all resting or activated NK cells. P46 molecules were shown to induce cytolytic activity and cytokine production in resting NK cells and NK cell clones (Sivori et al., 1997).

NK cells that lack the CD49b surface marker express the integrin CD49a instead, allowing the discrimination of these two subsets. Both, CD49b and CD49a, belong to the receptor family of integrins, which are involved in cell adhesion and cell-surface mediated signaling (Anderson and Springer, 1987; Ruoslahti and Pierschbacher, 1987; Springer, 1985), conveying the interactions between cells, among cells and the extracellular matrix and are critical for ligand binding (Elices et al., 1990; Hemler, 1990; Michishita et al., 1993; Springer, 1990).

In mice, mature conventional NK (cNK) cells are defined as NK1.1<sup>+</sup> and CD49b<sup>+</sup>. Other than in mice, in humans, NK cells are phenotypically defined by the surface receptors CD56 and CD16. Whereas CD56<sup>dim</sup>CD16<sup>+</sup> NK cells are highly cytotoxic, CD56<sup>bright</sup>CD16<sup>-</sup> NK cells are less cytotoxic and considered to be an immature subset that can differentiate into CD56<sup>dim</sup> cells (Chan et al., 2007; Romagnani et al., 2007), since CD56<sup>bright</sup>CD16<sup>-</sup> NK cells proliferate more upon stimulation and secrete higher cytokine amounts (Cooper et al., 2001).

#### **1.4 NK cell development**

Although fetal thymus and liver contain bipotent NK/T cell progenitor cells with the ability to become NK cells (Carlyle et al., 1997; Sánchez et al., 1994), NK development primarily takes place in the BM, where the self-renewing hematopoietic stem cell (HSC) gives rise to a multi-potent progenitor (MPP). The MPP can then evolve into the common lymphoid progenitor (CLP), which transitions to the common innate lymphoid progenitor (CILP) that can give rise to NK cells, T and B cells (Kondo et al., 1997), lymphoid tissue inducer progenitors (LTiPs) and innate lymphoid cell precursors (ILCPs) which will become ILC1, ILC2, or ILC3 cells (Vivier et al., 2018).

Throughout their development and maturation, the NK cell fate is determined by different transcription factors. While early stages of NK cell development depend on transcription factors like PU.1 and Nfil3 (Colucci et al., 2001; Gascoyne et al., 2009; Kamizono et al., 2009), Id2 and Tox come into play later (Aliahmad et al., 2010; Yokota et al., 1999), with the expression of T-bet and Eomesodermin (Eomes) controlling the final stages of NK development (Gordon et al., 2012; Townsend et al., 2004) (Figure 2).

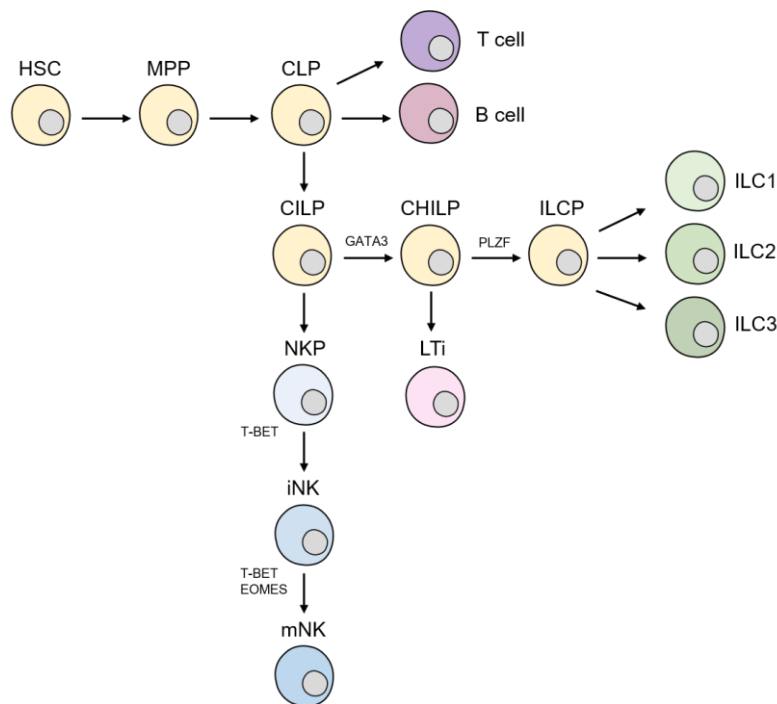


**Figure 2: Schematized ILC development.** Following the HSC and MPP stage, the CLP is formed. From the CLP, T and B lymphocytes, as well as the CILP arise, which can differentiate into the NKP, forming iNK and mNK cells, or the CHILP, resulting in LTi or ILCP from which ILC1, ILC2, and ILC3 cells arise (adapted from Vivier et al., 2018).

However, the CLP expresses CD127 (IL-7R $\alpha$ ), c-kit (CD117), and the common gamma chain (CD132) (Kondo et al., 1997) and transitions through at least three stages before the mature NK (mNK) cell is generated. The CLP can differentiate into the NK progenitor (NKP), which expresses CD122 (IL-2 receptor beta chain), but neither NK1.1 nor CD49b (Rosmaraki et al., 2001). Importantly, CD122 begins to be expressed and is required for sensing of IL-15. Overall, IL-15 plays a critical role in NK development and survival and its signaling, which engages the intracellular molecule STAT5, is required throughout the



life span of the NK cell (Yokoyama et al., 2004). The transition from the NKP to the immature NK (iNK) cell is supported by T-bet, stabilizing the iNK cell which starts to express NK1.1 but not yet CD49b (Gordon et al., 2012; Rosmaraki et al., 2001). When iNK cells gain expression of CD11b, Ly49 receptors, and CD49b, they attain cytotoxicity, produce IFN- $\gamma$  and evolve into mNK cells (Geiger and Sun, 2016; Kim et al., 2002). The highly cytotoxic potential and strong IFN- $\gamma$  secretion of the mNK cell is reached when the mNK cells traffic from the BM into the periphery where they continue to mature while migrating to specific organ sites and are described by the surface receptors CD11b and CD27 (Hayakawa and Smyth, 2006), KLRG1 (Chiossone et al., 2009; Hayakawa and Smyth, 2006; Huntington et al., 2007), as well as CD49b and TRAIL (Gordon et al., 2012; Kim et al., 2002; Takeda et al., 2005).

## **1.5 NK cells and their innate and adaptive relatives**

### **1.5.1 NK vs. ILC1 cells**

In contrast to T and B cells, NK cells recognize transformed and infected cells through germ line-encoded receptors and do not involve gene rearrangement mediated by the (RAG) recombinase (Lanier et al., 1986). Consequently, NK cell numbers are not influenced by genetic deletion of either RAG-1 or RAG-2, whereas T and B cells are completely lost (Mombaerts et al., 1992; Shinkai et al., 1992). However, a subset of developing NK cells was reported to express RAG, with its endonuclease activity eventually being relevant for function and fitness of the mature peripheral NK cell pool (Karo et al., 2014).

Within recent years, further RAG-independent ILCs closely related to NK cells were discovered and classified into the ILC1, ILC2, and ILC3 subset. These three helper ILC subsets differ in their transcription factor expression and cytokine production (Mjösberg and Spits, 2016; Spits et al., 2013; Spits and Di Santo, 2011; Stokic-Trtica et al., 2020). Other than their adaptive counterparts, helper ILCs are predominantly found at barrier sites, in the skin, lung and gut, where they are important regulators of immunity and inflammation (Artis and Spits, 2015). By surface receptor and transcription factor expression NK cells are distinguishable from ILC1s, ILC2s and ILC3s, with the ILC1

subset sharing the most similarities with NK cells. Both share identical surface markers (NK1.1 and NKp46), express the transcription factor T-bet, and can produce large amounts of IFN- $\gamma$  upon activation by the pro-inflammatory cytokines IL-12 and IL-18 (Artis and Spits, 2015; Spits et al., 2013; Spits and Cupedo, 2012). Additionally, they possess related gene-expression patterns (Robinette et al., 2015). In the liver, the ILC1 subset was described during embryogenesis, when a population of innate lymphocytes was found to express the surface marker TRAIL, which at this point is usually not found on NK cells. However, the population size of this TRAIL<sup>+</sup> cell population decreased over time and was finally replaced by BM-derived cNK cells (Takeda et al., 2005).

Today, TRAIL<sup>+</sup> ILC1s are described as separate cell subset that coexists with the Trail-CD49b<sup>+</sup> cNK cells in the adult liver (Seillet et al., 2014; Takeda et al., 2005). Here, transcriptomic analyses of both cells revealed not only similarities but also distinct gene profiles. Liver ILC1 and cNK cells share the surface molecules NKp46, CD122 and NK1.1 but cNK cells also express CX3CR1, CD62L, S1PR1 and S1PR5 with S1P being involved in NK cell retention and egress from the BM and LNs and expression of S1P5 being regulated by T-bet (Daussy et al., 2014; Jenne et al., 2009; Walzer et al., 2007). However, a recent publication challenges this concept, reporting tissue-resident ILC1 cells which exit draining LNs via S1PR1 (Wang et al., 2018). Other than NK cells, which only express CD127 at the iNK stage, the ILC subsets in mice and humans express CD127 also in the periphery (Bernink et al., 2013; Vonarbourg et al., 2010).

Overall, the cytotoxic potential of NK cells seems to be unique, along with some specific cell surface markers and differentially expressed transcription factors between NK and ILC1 cells (Bernink et al., 2013; Fuchs et al., 2013; Klose et al., 2014). In particular, the expression of T-bet and Eomes allows the distinction of NK cells and ILC1s because NK cells critically depend on Eomes for maturation and survival, while ILC1s do not seem to express this transcriptional regulator (Daussy et al., 2014; Gordon et al., 2012). In addition, in NK cell development the transcription factor Nfil3 is expressed as early as in the CLP to promote lineage commitment through regulation of Id2 and Eomes, whereas ILC1s do not require Nfil3 for evolution (Crotta et al., 2014; Male et al., 2014; Seillet et al., 2014). Intriguingly, the exact relation between ILC1 and NK cells is a challenging research

focus since plasticity between those two cell subsets has been reported in the micro-environment of tumors (Gao et al., 2017) and obese mouse livers (Cuff et al., 2019).

### **1.5.2 NK vs. cytotoxic CD8+ T cells (CTLs)**

NK cells and helper ILCs maintain tissue homeostasis and provide the interface between external cues and adaptive immunity. Nevertheless, ILCs and T cells cooperate and complement each other (Bouchery et al., 2015; Hepworth et al., 2015; Kruglov et al., 2013; Rankin et al., 2016) and share similar transcriptional programs and cytokine secretion. While helper ILCs resemble CD4+ T cells, NK cells are often compared to cytotoxic CD8+ T cells due to their similar killing ability through perforin and granzymes. During infection, CD8+ T cells and NK cells are activated through inflammatory cytokines like type I IFNs, IL-12, and antigen-specific receptors. Upon activation, both cell populations produce large amounts of IFN- $\gamma$  (Sun and Lanier, 2010) and following egress from the BM (NK cells) and thymus (T cells), both cell subsets continue to mature in the periphery (Fink and Hendricks, 2011; Hayakawa and Smyth, 2006; Takeda et al., 2005). Here, IL-15 is required by NK cells (Yokoyama et al., 2004) and promotes the clonal expansion of T cells (Ma et al., 2006), protecting memory precursor T cells from cell death during the contraction phase (Schluns and Lefrancois, 2003). Additionally, the transcription factor Runx3 is predominantly expressed in CD8+ T cells and NK cells. In murine developing NK cells, Runx3 initiates transcription of activating receptors like the Ly49s and is suggested to promote the expression of CD122, required for NK maturation (Ohno et al., 2008). Further, ChIP-seq analysis revealed shared and unique transcriptional programs of CD8+ T and NK cells (Lotem et al., 2013).

### **1.5.3 Transcription factors T-bet and Eomesodermin (Eomes)**

Through their shared DNA-binding domain (T-box), T-bet and Eomes both belong to the same family of transcription factors. The transcription factor T-bet is expressed by different lymphocyte lineages comprising innate and adaptive immune cells during type I immune responses (Kallies and Good-Jacobson, 2017; Lazarevic and Glimcher, 2011; Lazarevic et al., 2013; Szabo et al., 2000). T-bet was found to promote the early differentiation as well as terminal maturation of NK cells (Gordon et al., 2012; Robbins et al., 2005; Townsend et al., 2004; Werneck et al., 2008) by mediating lymphocyte trafficking and the expression of S1PR required for NK egress (Jenne et al., 2009; Townsend et al., 2004;

Walzer et al., 2007). Importantly, in a model in which NK cells usually control melanoma, T-bet-deficient mice were shown to be more susceptible (Werneck et al., 2008). Moreover, T-bet-deficient mice express higher levels of Eomes, whose deletion in mNK cells resulted in a reversion to the iNK stage where CD49b was not expressed (Gordon et al., 2012).

Besides T-bet, Eomes expression plays a crucial role in cNK cell development and function. It is expressed in resting and activated NK cells, as well as in activated CD8<sup>+</sup> T cells (Kaech and Cui, 2012). Although not expressed by naïve T cells, Eomes was found to be important for the formation of memory CD8<sup>+</sup> T cells (Intlekofer et al., 2005). In general, Eomes facilitates the development of memory cells with a longer survival and the potential for homeostatic proliferation (Banerjee et al., 2010), supports the maintenance of mature NK cells, and fosters NK effector functions by promoting the expression of Ly49 receptors (Gordon et al., 2012).

T-bet and Eomes cooperate to induce a high expression of CD122, the beta chain that binds IL-15 (Intlekofer et al., 2005), critical for NK development and survival (Yokoyama et al., 2004). Beyond a compensatory mechanism of Eomes and T-bet, their downregulation coincides with a diminished cytotoxicity and IFN- $\gamma$  production by NK cells and their genetic ablation resulted in the loss of the characteristic NK antigens NK1.1 and NKp46 (Gordon et al., 2012). Furthermore, these transcription factors are critical for NK cell-mediated cytotoxicity by binding to the granzyme B gene *Gzmb* and the perforin encoding gene *Prf1* (Beima et al., 2006; Intlekofer et al., 2005; Lewis et al., 2007; Miller et al., 2008) and control *Ifng* expression through binding its promotor and enhancer regions (Sekimata et al., 2009) with binding site deletion resulting in the ablation of *Ifng* gene transcription in NK cells (Hatton et al., 2006).

## **1.6 Memory NK cells bridge innate and adaptive immunity**

In recent years, mouse and human NK cells were found to display features of adaptive immune cells that can mount recall responses upon antigen stimulation. This implies that exposed cells respond faster and with a higher magnitude upon re-stimulation, even if the re-exposure takes place weeks or months after the first stimulation. The phenomenon of immunological memory forms the theoretical basis for vaccinations, which prepare immune cells to react specifically to e.g. viral antigen and protect from infection.

Whereas first evidence of antigen-specific recall responses by NK cells was reported in a model of hapten-induced contact hypersensitivity (CHS) with 1-fluoro-2,4-dinitrobenzene (DNFB) and oxazolone (Oxa) (O'Leary et al., 2006), two further types of NK cell "memory" were reported since. These comprise adaptive virus-specific recall responses (Abdul-Careem et al., 2012; Gillard et al., 2011; van Helden et al., 2012; Sun et al., 2009; Sun et al., 2010; Sun and Lanier, 2011) and cytokine-induced NK cell reactivity upon IL-12, IL-15, and IL-18 stimulation (Cooper et al., 2009; Ni et al., 2012; Romee et al., 2012). Especially the (murine) cytomegalovirus (MCMV)-specific NK cell response is well characterized. Here, the recognition of MCMV-infected cells occurs through detection of the viral protein m157 by the NK cell receptor Ly49H in mice (Arase et al., 2002; Dokun et al., 2001; Smith et al., 2002) and by NKG2C in humans, resulting in a memory response upon re-infection (Foley et al., 2012a; Foley et al., 2012b). In accordance with CD8+ T cell memory development (Williams and Bevan, 2007), MCMV-specific NK memory development can be divided into three phases (O'Sullivan et al., 2015). Upon antigen exposure, naïve cells clonally expand and differentiate into effector cells. Following "expansion", the "contraction" phase is entered when the vast majority of effector cells undergo apoptosis and only a small pool of cells survives. These form persistent "memory" cells that maintain their longevity through self-renewal until they re-encounter the specific antigen and can drive strong recall responses (Foley et al., 2012a; Foley et al., 2012b; Lopez-Vergès et al., 2011; Sun et al., 2009).

## **1.7 Hapten-induced contact hypersensitivity (CHS) in mice**

### **1.7.1 CHS mimics symptoms of allergic contact dermatitis (ACD)**

The skin represents the first barrier organ against a variety of environmental challenges and comprises highly specialized immune and non-immune cells which are organized in several layers (Nestle et al., 2009; Pasparakis et al., 2014; Tay et al., 2013). Both, human and mouse skin, can be distinguished into the epidermis and the dermis, with the epidermis being the outermost layer with KCs as most prevalent cell type found at different stages of differentiation (Tay et al., 2013). In humans, NK cells have been shown to migrate to inflamed skin in various conditions, including psoriasis (Ottaviani et al., 2006)

and allergic contact dermatitis (ACD) (Buentke et al., 2002). ACD is a type IV delayed-type CHS reaction that affects 15 - 20 % of the population and is one of the worlds' most prevalent skin diseases (Peiser et al., 2011). To study ACD, the animal model of CHS is applied. Here, mice are treated with haptens, which are small compounds with low molecular weight (<1000 Da) that can enter the skin due to their lipophilic nature. Because of their small size, the haptens used are not immunogenic by themselves. These molecules require the attachment to larger carrier proteins to form hapten-carrier complexes that evoke an immune response (Divkovic et al., 2005; Karlberg et al., 2008). Importantly, haptens have to exert a pro-inflammatory effect in order to activate the innate immune response in the skin and mediate the recruitment, migration and maturation of langerhans cells (LCs) and dermal dendritic cells (dDC), which is a prerequisite for CHS (Bonneville et al., 2007; Grabbe et al., 1996). Recurrent hapten application on the skin of mice induces CHS, characterized by dry, itchy, and red skin and the infiltration of various immune cell populations.

Repeated long-term skin sensitization of mice induces T<sub>H</sub>2 cytokine-mediated chronic dermatitis, with increasing levels of hapten-specific IgE in the serum and locally at the application site, leading to ACD-like skin inflammations (Harada et al., 2005; Kitagaki et al., 1995).

### **1.7.2 The CHS response**

In mice, CHS is induced through the application of chemical haptens. For CHS responses, different haptens can be applied, ranging from DNFB and Oxa to fluorescein isothiocyanate (FITC), 2,4,6-trinitro-1-chlorobenzine (TNCB) and monobenzene (MBEH).

CHS reactions can be divided into two different phases: sensitization and elicitation. During sensitization, the hapten is applied directly to the shaved abdominal skin of mice, which has two major consequences. First, haptens exert a pro-inflammatory function, promoting the activation of innate immunity in the skin and the recruitment, migration, and maturation of cutaneous DCs. Second, haptens modify self-proteins by binding to their amino acid residues. Thereby, new antigenic determinants are generated that prime hapten-induced T cells.

Following sensitization of the (abdominal) skin, the animal is re-exposed to the same antigen which is then applied to a distant site (ear) at a non-irritating dose (elicitation).

As readout of the hapten-specific recall response, the ear swelling, resulting from vasodilation and cell infiltration of e.g. NK cells into the site of inflammation is measured. However, whereas general T cell-driven CHS is relatively well characterized, NK cell-mediated CHS remains a current field of research.

#### 1.7.2.1 The sensitization phase of CHS

Upon skin contact, haptens interact with the KCs in the epidermis. Thereby, KCs are activated and secrete chemical mediators like IL-1 $\beta$ , TNF- $\alpha$ , IL-18, GM-CSF, PGE<sub>2</sub>, and multiple chemokines, including CXCL1, CXCL2, CXCL9, CXCL10, CCL8, CCL17, and CCL27 (Flier et al., 2001; Honda et al., 2009; Karsak et al., 2007; Mori et al., 2008). Together with IL-1 $\beta$ , TNF- $\alpha$ , and IL-18, CXCL10 is of great importance, being the ligand for CXCR3, a receptor strongly expressed on T<sub>H</sub>1 cells. Additionally, the CCL17/22-CCR4 and CCL27-CCR10 signaling axes contribute to T cell recruitment into the skin (Homey et al., 2002; Reiss et al., 2001; Wang et al., 2010). PRR stimulation, comprising membrane-associated TLRs and cytosolic nucleotide-binding oligomerization domain (NOD)-like receptors (NLRs), activates barrier and innate immune cells. Following hapten application to the skin, KCs are activated in an NLR-dependent manner and pyrin domain containing 3 (NLRP3) controls the production of pro-inflammatory cytokines through caspase-1 activation, which causes the release of IL-1 $\beta$  and IL-18 from KCs and APCs and reveals the relevance of danger signaling through NLRP3 for animal sensitization (Watanabe et al., 2008).

The NLR-dependent pathway is further triggered by adenosine triphosphate (ATP) efflux from damaged, haptened cells. As energy carrier in cells, ATP is crucial for NLRP3 activation by haptens because it is released into the extracellular space by stressed, damaged, and dying cells. In the extracellular area, ATP binds to the purinergic receptor P2X7, which is present on different immune and structural cells. When the ion channel ligand-gated receptor P2X7 is bound by ATP, the NLRP3 inflammasome and caspase-1 are activated (Mariathasan et al., 2006; Martinon et al., 2006; Sutterwala et al., 2006). This is critical because deficiency or lack of ATP-P2X7 signaling was shown to result in an impaired sensitization capacity of DCs and the inability to mount a CHS response (Martin et al., 2011; Weber et al., 2010).

In general, haptenated cells are important for CHS establishment due to the release of danger signals. These can be hyaluronic acid (HA), extracellular matrix ligands for TLRs, PGE2, reactive oxygen species (ROS), heparin sulfate, tenascin, B defensins, and fibrinogen (Christensen and Haase, 2012; Honda et al., 2013; McFadden et al., 2011). Especially ROS formation in DCs may result in degradation of the extracellular matrix and induce TLR2, TLR4 and NLRs (Honda et al., 2013; Martin et al., 2008; Martin et al., 2011). Haptens bind to endogenous proteins in the skin and form immunogenic hapten-carrier complexes. These antigens and the local release of soluble cytokines activate dDCs and LCs and direct dDCs to dLNs for maturation and presentation of hapten-antigen to naïve T cells (Cumberbatch and Kimber, 1995; Fukunaga et al., 2008; Honda et al., 2013; Martin et al., 2011). LCs are found in the epidermis abundantly, have antigen-presenting ability *in vitro* and their removal from the tissue by drugs impaired the CHS response (McMinn et al., 1990). Thus, LCs and dDCs may work in a compensatory manner during initiation of CHS (Honda et al., 2010; Noordegraaf et al., 2010) but LCs appear to have a rather regulatory function during sensitization since congenitally LC-depleted mice have an aggravated CHS response (Kaplan et al., 2005), suggesting a suppressive function of LCs in CHS through their production of IL-10 (Igyártó et al., 2009).

Another important mediator of CHS are the mast cells and their conditional depletion via administration of diphtheria toxin reduced FITC- and Oxa-induced (Dudeck et al., 2011), as well as DNFB- and Oxa-induced CHS (Otsuka et al., 2011).

Moreover, neutrophils are recruited to the site of hapten challenge and secrete pro-inflammatory cytokines (Dilulio et al., 1999; Kish et al., 2009). These contribute to DC activation and induce their migration from the exposed skin to the LN, where effector T cells are activated and hapten-specific T cells primed (Bursch et al., 2007; Kaplan et al., 2005). Upon activation and clonal expansion, these effector T cells migrate to the site of hapten challenge and mediate the inflammatory responses (Gorbachev and Fairchild, 2001).

#### 1.7.2.2 The CHS elicitation phase

Elicitation describes the secondary hapten challenge on the ear. Commonly, the elicitation of hapten-sensitized mice can be divided into two phases. Whereas the early elicitation phase peaks after around two hours of challenge and is mostly unspecific, the late



elicitation phase occurs within 24 hours of the challenge and is hapten-specific (Honda et al., 2013). If the concentration of haptens is not high enough to induce the unspecific inflammation early during elicitation, no CHS response will occur (Grabbe et al., 1996). It was reported that without IL-1 $\beta$  and IL-18 production by KCs, DC migration was impaired and T cell priming hindered (Nakae et al., 2003). Besides KCs, neutrophils, and mast cells drive the unspecific inflammation during elicitation, where the release of (pro)inflammatory cytokines and chemokines induces the expression of adhesion molecules on vascular endothelial cells, which then favor the transmigration of T cells from the circulation into the skin. Early after hapten application, the secretion of mast cell-derived histamine increases the vascular permeability (Dudeck et al., 2011) and neutrophils are recruited by CXCL1 and CXCL2 secretion (Biedermann et al., 2000; Honda et al., 2009). Since neutrophil depletion reduces CD8 $^+$  T cell infiltration and impairs CHS, initial neutrophil recruitment is assumed to be a prerequisite for subsequent T cell infiltration (Dilulio et al., 1999; Engeman et al., 2004).

Accessorially, hapten application activates iNKT cells in the liver and promotes the migration of peritoneal B1-like B cells to lymphoid organs and their production of hapten-specific IgM (Campos et al., 2006a; Campos et al., 2006b), which enters the circulation and activates complement C5a (Szczepanik et al., 2003; Tsuji et al., 2002). Consequently, C5a stimulates mast cells and platelets to release serotonin and TNF- $\alpha$ , promoting endothelial activation and inflammation and initiating the elicitation through early T cell recruitment into the targeted skin (Tsuji et al., 2000). Further, hapten-specific T cell recruitment is promoted by the TNF- $\alpha$  and serotonin production by mast cells, which increase the release of CXCL10, CCL1, CCL2, and CCL5 and the upregulation of ICAM-1 and P/E-selectins on endothelial cells (Biedermann et al., 2000; Dudeck et al., 2011; Honda et al., 2013; Otsuka et al., 2011).

During the late elicitation phase, KCs, dDCs, LCs and endothelial cells process haptened antigen and present the antigen to hapten memory T cells that migrated into the dermis early during elicitation (Christensen and Haase, 2012; Kish et al., 2011; Robert and Kupper, 1999). However, LCs seem to fulfill a more regulatory function during elicitation since depletion of epidermal LCs in sensitized mice elicited higher CHS responses (Grabbe et al., 1995).

Through elicitation, hapten-specific effector and memory CD4<sup>+</sup> and CD8<sup>+</sup> T cells are activated. Whereas CD8<sup>+</sup> T cells were shown to be the main effector T cells in CHS, CD4<sup>+</sup> T cells were mostly found to fulfill regulatory functions (Bour et al., 1995; Gocinski and Tigelaar, 1990; Kehren et al., 1999; Martin et al., 2000). Through increase of cytotoxicity with perforin and Fas/FasL interaction, CD8<sup>+</sup> T cells increased tissue damage during CHS elicitation (Kehren et al., 1999) and CD8<sup>+</sup> T cell depletion significantly reduced CHS recall responses upon challenge (Bour et al., 1995). However, the antagonist of the CD8<sup>+</sup> T cells are the T regulatory (T<sub>reg</sub>) cells, which control the immunologic responsiveness in CHS (Kish et al., 2005). T<sub>regs</sub> were shown to traffic into inflamed skin during elicitation (Tomura et al., 2010) and their depletion during sensitization resulted in higher effector CD4<sup>+</sup> and CD8<sup>+</sup> T cell induction and enhanced and prolonged ear swelling (Honda et al., 2011). Also, T<sub>reg</sub> depletion during elicitation induced an enhanced and prolonged ear swelling, pointing towards a critical role in the termination of CHS (Tomura et al., 2010). Utilizing a cell-labeling system with the photo-convertible protein Kaede, the migration of T cells after skin infiltration was tracked and showed that skin-infiltrating T cells moved from the skin to the dLNs in the steady-state and under inflammatory conditions (Tomura et al., 2010).

Overall, DNFB (Dearman et al., 1996), Oxa (Webb et al., 1998), and TNCB (Kitagaki et al., 1997) are considered to be primarily T<sub>H1</sub> IFN $\gamma$ -inducing haptens, whereas FITC is, due to its solvent dibutylphthalate, regarded to be a T<sub>H2</sub>-inducing hapten (Larson et al., 2010). As described by the “hapten atopy hypothesis”, hapten application stimulates TLR4 through the release of danger signals and mounts a T<sub>H1</sub> response (McFadden et al., 2011). However, repeated and prolonged exposure to haptens may induce a shift of these T<sub>H1</sub> to T<sub>H2</sub> responses because TLR4 stimulation will weakly upregulate TLR2 expression as well. Since TLR2 stimulation induces T<sub>H2</sub> responses and exposure to a hapten can take place multiple times, this weak stimulation of TLR2 may gradually form a strong T<sub>H2</sub> response, downregulating T<sub>H1</sub> cytokines and suppressing TLR4 function. This effect is called “danger limitation effect” (McFadden et al., 2011) and was described for TNCB-induced CHS (Kitagaki et al., 1997). It was shown that the amount and duration of the hapten challenge shaped the character of the CHS response that could occur acute (one challenge), subacute (three challenges) or chronically with the comparison of the acute and chronic treatment revealing a decrease of T<sub>H1</sub> cytokines

(TNF- $\alpha$ , INF $\gamma$ , IL-2, and IL-12), an increase of T<sub>H</sub>2 cytokines (IL-4, IL-5, and IL-13), and an increase of the T<sub>reg</sub> cytokine IL-10 (Röse et al., 2012).

### **1.7.3 NK cells can drive hapten-specific memory responses**

After CHS responses had long been considered to be primarily T cell-mediated (Marchal et al., 1982), in 2006 first evidence of a hapten-specific recall response by NK cells in DNFB- and Oxa-induced CHS was reported (O'Leary et al., 2006). In this study, CHS was induced in immunodeficient mice that lacked T and B cells, NK cells accumulated in the inflamed ears and NK cell depletion abolished the CHS response (O'Leary et al., 2006). Importantly, only hepatic NK cells were observed to mediate CHS responses to sensitizing haptens (O'Leary et al., 2006; Paust et al., 2010; Peng et al., 2013).

In mice, NK cells represent 5 - 10 % of the liver lymphocytes, whereas up to 30 - 50 % of human lymphocytes in the liver are NK cells. It is assumed that only educated NK cells have the potential to acquire immunological memory, since complete deficiency of Ly49 family member receptors can abolish the CHS response (Wight et al., 2018). Until today, two different NK cell subsets were shown to mount hapten-specific recall responses in mice. These two populations differ in their surface receptor and transcription factor expression. For example, application of the contact sensitizer Oxa can induce CHS and was shown to require NK1.1+, CD49a+ NK cells. These represent the minority of the hepatic NK cell population, are known to be liver-resident, and express the aryl hydrocarbon receptor (AhR). Since this subset of liver-resident NK cells is decreased in mice that lack the AhR receptor, the respective NK cell-mediated CHS response is impaired (Zhang et al., 2016). Importantly, these NK cells depend on the transcription factor T-bet (Daussy et al., 2014) and NK cells were shown to accumulate in the skin after hapten administration (O'Leary et al., 2006). Furthermore, this NK cell subset expresses the chemokine receptor CXCR6 (Paust et al., 2010) that binds CXCL16 (Matloubian et al., 2000). These CXCR6+ hepatic NK cells can not only develop a hapten-induced, but also an immunological memory to virus-like particles, like viral proteins from influenza or human immunodeficiency virus (HIV), or inactivated vesicular stomatitis virus (VSV) (Paust et al., 2010). As CD49a+ NK cells rarely leave the liver at steady-state or

recirculate, the mechanism by which these memory NK cells migrate from their priming site to the liver and to the challenge site remains ambiguous.

Whereas only Ahr+, CXCR6+, CD49a+ NK cells were shown to specifically mediate Oxa-induced recall responses upon adoptive transfer (Peng et al., 2013; Zhang et al., 2016), MBEH-induced CHS could be conveyed by hepatic CD49b+ cells (van den Boorn et al., 2016). Hence, these cells could belong to the other hepatic mNK subset, which is AhR-, CXCR6-, CD49b+, referred to as conventional NK (cNK) cell, that circulates throughout the body and expresses the transcription factors T-bet and Eomes (Daussy et al., 2014). Whether this exact subset accounts for MBEH-specific CHS remains to be determined but their nearly absent receptor CXCR6 may explain why CD49b+ cells are less efficient than liver-resident NK cells in Oxa- or FITC-induced CHS models (Peng et al., 2013). Conventional NK cells are described to possess the inhibitory receptor Ly49C/I and Ly49C/I-sensitive peptides were found to induce NK cell recall responses (Wight et al., 2018), making the possibility that the hapten-self protein complexes contain Ly49C/I-sensitive peptides and can be recognized by cNK cells a matter of investigation.

#### **1.7.4 Monobenzene - vitiligo inducer and melanoma immunotherapy agent**

Monobenzene (MBEH), also known as 4-(benzyloxy)phenol or monobenzylether of hydroquinone, belongs to the family of phenols and is soluble in alcohol, diethyl ether and benzene but insoluble in water. It was discovered in 1939 by Oliver et al. (Oliver et al., 1939) and acts as a skin sensitizer (Forman et al., 1953; Lyon and Beck, 1998) which is the most potent skin depigmenting agent described (Boissy and Manga, 2004; Kahn, 1970).

Repeated application of MBEH on the skin can induce symptoms similar to *vitiligo vulgaris* in humans (Becker and Spencer, 1962; Forman, 1953; Mosher et al., 1977) and mice, visible through the formation of white patches on the skin. This MBEH-induced skin depigmentation can spread to distant sites unexposed to MBEH, indicating a progressive systemic reaction against melanocytes (Forman, 1953; Grojean et al., 1982; Lyon and Beck, 1998). Since MBEH treatment can induce vitiligo in healthy individuals when used to lighten the skin tone (Becker and Spencer, 1962; Catona and Lanzer, 1987; Forman, 1953), a 20 % cream formulation was developed and used to completely depigment *vitiligo universalis* patients (Mosher et al., 1977). Additionally, the approach of

an effective melanoma immunotherapy in mice through combination of MBEH with imiquimod and cytosine-guanine oligodeoxynucleotides (CpG) yielded promising results. This treatment, known as MIC therapy, combined MBEH application with the injection of the TLR9 agonist CpG and topic application of the TLR7 agonist imiquimod, which had already been established therapy adjuvants in the melanoma setting (Adams et al., 2008; Lonsdorf et al., 2003; Najjar and Dutz, 2008; Ray et al., 2005; Sidky et al., 1992). As an autoimmune side-effect of melanoma immunotherapy, vitiligo-like leukoderma can occur (Luiten et al., 2005) and is in fact considered an encouraging prognostic sign (Gogas et al., 2006; Quaglino et al., 2010). Hence, MIC therapy was tested in mice and revealed that upon subcutaneous B16.F10 melanoma injection in C57BL/6 wildtype mice melanoma outgrowth was inhibited in up to 85 % of the mice. In this study, between 57 - 64 % of the mice remained tumor-free for more than 100 - or 200 days after injection, with MIC treatment inducing a systemic B16-specific CD8+ T cell- and NK cell response that mostly protected from tumor outgrowth and progression (van den Boorn et al., 2010). Combined with the knowledge that vitiligo development during melanoma therapy associates with a better disease outcome, MBEH application was part of a clinical trial to treat melanoma patients.

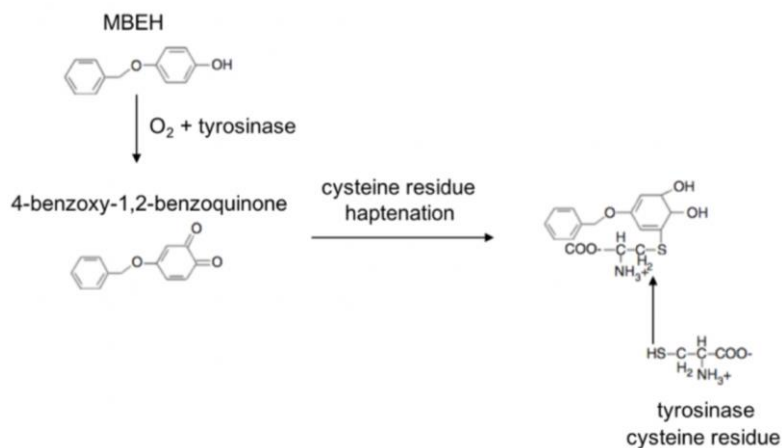


**Figure 3: Chemical principle of MBEH attachment to the tyrosinase enzyme.** MBEH attaches to tyrosinase and other melanosomal proteins through cysteine residue haptination (adapted from van den Boorn et al., 2011).

Recently, a study combined imiquimod treatment with the application of the hapten DNFB and revealed an enhanced CHS response in mice (Ren et al., 2019). Since the active MBEH hapten is only generated in melanocytes, CHS only occurs in pigmented skin (Nordlund et al., 1985). Therefore, the inactive pro-hapten MBEH has to be metabolized by melanocytes. Within the melanocytes, MBEH haptens melanocyte-specific antigens, which induces cytotoxic autoimmunity against pigmented cells (van den Boorn et al., 2011; van den Boorn et al., 2016). The reason therefore is that MBEH acts as an alternative substrate for the tyrosinase enzyme. This key enzyme of the pigment synthesis cascade metabolizes MBEH, which then haptens tyrosinase's cysteine residues and inhibits melanocyte pigment synthesis (van den Boorn et al., 2011) (Figure 3, Figure 4). Also, the MBEH conversion product benzoquinone has been shown to act as a potent skin sensitizer through hapten formation to proteins (Cooksey et al., 1992; Naish and Riley, 1989; Nazih et al., 1993). In addition, the reaction product of hydroquinone, *p*-benzoquinone, induces a T cell-dependent, hapten-specific B cell response *in vivo* (Ewens et al., 1999). The haptening of tyrosinase and other melanosomal proteins by MBEH induces oxidative stress, the autophagocytical digestion of the damaged organelle and the release of antigen containing exosomes (van den Boorn et al., 2016).

In a previous study, the adoptive transfer of a lineage negative hepatic CD49b<sup>+</sup> MACS-purified cell population conferred melanocyte-specific immunity in naïve mice. Further, macrophage infiltration was recorded in MBEH-exposed abdominal skin and the analysis of cutaneous LNs revealed an inflammasome-dependent influx of tissue-resident macrophages. Macrophages, as well as the NLRP3 inflammasome, the adaptor protein ASC, the P2X7 receptor and IL-18 were required for MBEH-specific CHS establishment (van den Boorn et al., 2016). In addition, upon sensitization of mice with Oxa or MBEH, respectively, followed by elicitation with the sensitizing hapten versus the foreign hapten, no cellular cross-priming was observed when these two haptens were exchanged between sensitization and elicitation (van den Boorn et al., 2016), punctuating the different target populations and mechanisms of action of these two haptens.

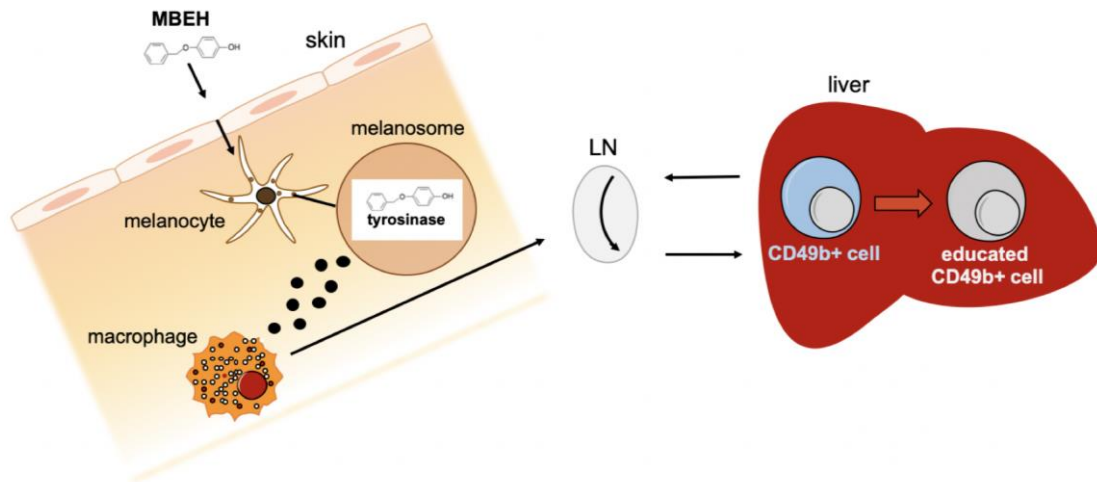


**Figure 4: Hypothesized cell signaling upon MBEH application to the skin of mice.** Following MBEH application to the skin, the small molecule is taken up by epidermal cells. MBEH diffuses further into the skin and haptens tyrosinase and other melanosomal proteins in the melanosome. The physiologically active hapten is generated and activates tissue-resident macrophages, which migrate to the LN and recruit immune cells. Immune cell priming results in specific effector cells that engage in the CHS response in the liver.

### 1.8 Aims of the thesis

By repeated skin application MBEH has been shown to effectively induce melanocyte-specific autoimmunity, leading to a progressive depigmentation in humans and mice (Becker and Spencer, 1962; van den Boorn et al., 2016; Forman, 1953; Mosher et al., 1977). Experiments in mice indicated MBEH as powerful melanoma immunotherapy agent since its use with imiquimod and CpG provoked a systemic response against melanoma cells, involving CD8+ T cells and NK cells, that could largely protect from tumor outgrowth and progression (van den Boorn et al., 2010). As a study from 2016 revealed, adoptive transfer of lineage negative hepatic CD49b+ MACS-purified cells from MBEH-treated mice could confer melanocyte-specific immunity in naïve animals.

Based on these findings we wanted to investigate the following aspects:

With respect to the emerging investigation of the relevance and plasticity of ILC1 and NK cells in health and disease, we wanted to determine if true NK or ILC1 cells in the murine liver develop an educated phenotype or adaptive features in MBEH-induced CHS.

Besides CD49b+ cells, CD49a+ NK cells are described as important mediators in hapten-induced immunity. We aimed to assess which hepatic mature NK subsets respond in the course of MBEH sensitization and can provide naïve mice with a recall response upon adoptive transfer.

The systemic reaction of MBEH has not been described in detail. Thus, immune cell in- and efflux in the liver, ILN, and elicited ear, as well as cytokine and chemokine changes in the elicited ear were measured to define critical mediators during systemic MBEH-induced CHS.

We wanted to characterize the hepatic CD49b+ cell population and define the differences between the naïve (d0) and MBEH-educated cells (d7), comprising changes of their transcriptome, spontaneous cytokine release, chromatin accessibility, and ability to contain B16 melanoma cell outgrowth.

It remains ambiguous if MBEH responsive cells require a comprehensive supply of excitation or whether *in vitro* (*ex vivo*) exposure might exhibit a direct effect on these immune cells. Hence, we wanted to test whether the substance MBEH can directly alter the characteristics of MBEH-responsive CD49b+ innate hepatic immune cells.

Analyzing MBEH-primed hepatic innate immune cells in comparison to their naïve counterparts will show us cellular changes that define innate cells which may be able to develop an “adaptive” phenotype. This knowledge would allow us to specifically generate educated or adaptive immune cells out of the innate immune cell compartment that could be utilized to combat diseases like melanoma.



## 2. Material and methods

**Table 1: Antibodies for immune cell FACS analysis**

<b>Antibody</b>	<b>Source</b>	<b>Clone</b>	<b>Identifier #</b>
Alexa Fluor® anti-mouse I-A/I-E (MHCII)	BioLegend	M5/114.15.2	107622
APC-Cy7 anti-mouse CD4	BioLegend	RM4-5	100526
APC/Fire™ 750 Streptavidin	BioLegend		405250
APC/Fire™ 750 TCR β chain	BioLegend	H57-597	109245
Biotin anti-mouse CD19	BioLegend	6D5	115503
Biotin anti-mouse Ter119/Erythroid cells	BioLegend	TER-119	116203
Brilliant Violet 510® anti-mouse I-A/I-E (MHCII)	BioLegend	M5/114.15.2	107636
BV421 rat anti-mouse CD49b	BD Biosciences	DX5 (RUO)	563063
CD49b monoclonal antibody (DX5) Pe-Cy7	eBioscience	DX5	25-5971-82
CD11b monoclonal antibody PE-Cyanine7	eBioscience	M1/70	25-0112-82
CD3ε anti-mouse APC/Fire™ 750	BioLegend	145-2C11	100362
CD103 monoclonal antibody APC	eBioscience	2E7	17-1031-82
CD45 monoclonal antibody eFluor450®	eBioscience	30-F11	48-0451-82
EOMES monoclonal antibody PE-Cyanine7	eBioscience	Dan11mag	25-4875-82
FITC anti-human/mouse Granzyme B	BioLegend	GB11	515403
FITC anti-mouse CD186 (CXCR6)	BioLegend	SA051D1	151107
FITC anti-mouse Ly-6G/Ly-6C (Gr-1)	BioLegend	RB6-8C5	108406
NK1.1 monoclonal antibody APC	eBioscience	PK136	17-5941-82
NK1.1 monoclonal antibody PE	eBioscience	PK136	12-5941-82

Pacific Blue™ anti-mouse CD45.1	BioLegend	A20	110722
Pacific Blue™ anti-mouse/human CD11b	BioLegend	M1/70	101224
PE anti-mouse CD45.2	BioLegend	104	109808
PE anti-mouse IFN- $\gamma$	BioLegend	XMG1.2	505808
PE anti-mouse SiglecF	BD Biosciences	E50-2440	552126
PE/Cy7 anti-mouse CD11c	BioLegend	N418	117317
PerCP/Cyanine5.5 anti-mouse CD45	BioLegend	30-F11	103132
PerCP/Cyanine5.5 anti-mouse CD8a	BioLegend	53-6.7	100734
PerCP/Cyanine5.5 anti-mouse/human CD11b	BioLegend	M1/70	101228
PerCP/Cyanine5.5 anti-mouse/rat/human CD27	BioLegend	LG.3A10	124214
T-bet monoclonal antibody APC	eBioscience	eBio4B10	17-5825-80
T-bet monoclonal antibody PE	eBioscience	eBio4B10	12-5825-82
Zombie UV™ Fixable Viability Kit	BioLegend		423108

**Table 2: Chemicals, reagents, and enzymes**

<b>Product</b>	<b>Source</b>
Acetone	Merck
Bicoll	Biochrom
BD GolgiPlug™	BD Biosciences Identifier # 555029
$\beta$ -Mercaptoethanol	PAN Biotech
cOmplete™ Mini Protease Inhibitor Cocktail	Merck Identifier # 11836153001
DMF	Sigma-Aldrich
DNase I	Thermo Fisher Scientific
eBioscience™ FoxP3 / Transcription factor staining buffer set	Thermo Fisher Scientific Identifier # 00-5523-00

EDTA (0.5 M, pH 8)	Thermo Fisher Scientific
Ethanol	Roth
FACS Flow	BD Biosciences
Fetal calve serum (FCS)	Gibco
Formaldehyde	Roth
HBSS	Gibco
HEPES buffer	PAN Biotech
Hydrogen peroxide (H <sub>2</sub> SO <sub>4</sub> )	Roth
IL-2	PeptoTech
IL-15	PeptoTech
Insulin-transferrin-sodium selenite media supplement (ITS)	Gibco (Thermo Fisher Scientific)
Invitrogen™ eBioscience™ cell stimulation cocktail (500x)	Invitrogen Identifier # 50-930-5
L-Glutamine	Gibco
Liberase™ TL research grade	Sigma-Aldrich Identifier # 5401020001
Magnesium chloride	Roth
Mouse BD Fc Block™	BD Biosciences
Monobenzene	Tokyo Chemical Industry
NEBNext® High-Fidelity 2x PCR Master Mix	New England BioLabs Identifier # M0541
Non-essential amino acids (NEAA)	Gibco
IGEPAL® CA-630 (Nonidet P-40)	MBL International
Olive oil	Sigma-Aldrich
PBS	Thermo Fisher Scientific
Penicillin/Streptomycin	Gibco
RPMI 1640 medium	Thermo Fisher Scientific
Sodium chloride	Roth
Sodium hydroxide	Roth
Sodium pyruvate	Gibco
T5130-25G (TAPS)	Merck/Sigma-Aldrich
Tris	Roth

Trypsin/EDTA	Gibco
Tween-20	Roth

**Table 3: Kits**

Product	Source
Agilent High Sensitivity DNA Kit	Agilent
cDNA amplification and library kit	10x Genomics
CellTiter-Blue® cell viability assay	Promega (# G8080)
Granzyme B mouse ELISA kit	eBioscience
Mouse IFN-γ ELISA set	BD Biosciences (# 551866)
LEGENDplex mouse anti-virus response panel	BioLegend (# 740622)
LEGENDplex mouse proinflammatory chemokine panel	BioLegend (# 740451)
MinElute reaction cleanup kit	Qiagen (# 28204)
NK cell isolation kit II mouse	Miltenyi Biotec (# 130-096-892)
RNeasy mini kit	Qiagen (# 74104)
QuantSeq 3'-mRNA-Seq Library Prep Kit FWD for Illumina	Lexogen
Single Cell 3' Reagent Kit v2 for reverse transcription	10x Genomics

**Table 4: Buffers**

FACS buffer	2 % FCS; 2 mM EDTA; 0.05 % NaN <sub>3</sub> in PBS
Fixation buffer (FACS)	3.7 % formaldehyde in PBS
Lysis buffer (ATAC seq)	10 mM Tris-HCl (pH 7.4); 10 mM NaCl; 3 mM MgCl <sub>2</sub> ; 0.1 % IGEPAL® CA-630 (Nonidet P-40) in H <sub>2</sub> O

MACS buffer	2 % FCS; 2 mM EDTA in PBS
Permeabilization buffer (FACS)	0.5 % saponin in FACS buffer
TAPS-DMF (ATAC seq)	50 mM TAPS-NaOH (pH 8.5); 25 mM MgCl <sub>2</sub> ; 50 % DMF in H <sub>2</sub> O

**Table 5: Equipment**

Balance, electronic	Sartorius
BD FACS Aria III	BD Biosciences
BD FACS Aria Fusion	BD Biosciences
BD FACSCanto	BD Biosciences
BD LSRFortessa	BD Biosciences
Bioanalyzer 2100	Agilent
Centrifuge 5810R	Eppendorf
Chromium™ Controller	10x Genomics
Digital micrometer (Kroeplin-IP67)	Kroeplin
EDTA-containing microtainer	Sarstedt
EnVision multilabel plate reader	Perkin Elmer
FACS LSR II	BD Biosciences
Gel Bead-In-EMulsions (GEMs)	10x Genomics
HiSeq 2500 System	Illumina
Hollow needle	VWR
MACS cell separator and isolater	Miltenyi Biotec
MACS separation columns	Miltenyi Biotec
Microcentrifuge 5415R	Eppendorf
Micropipettes	Eppendorf
Multichannel pipettes	VWR International
Neubauer chamber	Brand
NovaSeq™ 6000 System	Illumina
Pipetting aid	Integra Biosciences
Qubit™	Thermo Fisher Scientific
Shaker	NeoLab
SimpliAmp Thermal Cycler	Applied Biosystems

Sterile bench	Thermo Fisher Scientific
Syringe (1 ml)	B. Braun Melsungen AG
TapeStation (Agilent high sensitivity D1000)	Agilent
Thermocycler	Analytik Jena
Thermomixer	Eppendorf
Vortex mixer	VELP Scientifica

## 2.1 Mice

Mice were bred and housed under IVC conditions in the House for Experimental Therapy (HET) of the University Hospital in Bonn. C57BL/6J mice were either bought from Charles River Laboratories (Germany) or bred in-house in the facilities of the HET Bonn, where the mice with the congenic marker CD45.1 were bred. Mice were maintained at in-house facilities in Bonn (Germany) under specified pathogen free (SPF) conditions and all procedures were performed according to ethical protocols approved by the local and regional ethical committees. Mice were used for the experiments between the age of 8 - 14 weeks.

## 2.2 Induction of contact hypersensitivity (CHS)

Sensitization was conducted by application of a 20 % MBEH solution (Tokyo Chemical Industry) in a 3:1 acetone:olive oil (AOO) vehicle. For sensitization purposes, 75  $\mu$ l MBEH solution was applied on days d0, d1, d2 and d3 to the shaved abdomen of mice. The solution was allowed to diffuse into the skin for approximately 15 seconds before the residual solution was spread and kneaded into the skin.

## 2.3 Validation of CHS establishment through elicitation of the ear

For elicitation, 25  $\mu$ l of the 20 % MBEH solution in a 3:1 AOO vehicle was carefully applied on the right ear of the mice. For 15 - 20 additional seconds, the solution was allowed to diffuse into the skin. Standard protocol comprised elicitation on d7 and d8 after sensitization on d0 - d3. Prior, during, and after elicitation the ear swelling was measured

using a highly sensitive digital micrometer (Kroeplin-IP67). The difference in ear thickness ( $\Delta$ ) upon treatment was calculated and the mean  $\pm$  SEM depicted.

#### **2.4 Immune cell isolation from the liver**

Isolated livers were thoroughly washed in ice-cold PBS buffer and passed through a 70  $\mu$ m cell strainer (Corning) using ice-cold MACS buffer. Cell suspensions of three livers were pooled in 50 ml MACS buffer and centrifuged at 1000 rpm for 10 minutes at 4 °C. The supernatant was discarded and cells were washed for a second time. The cell pellet was resuspended in 35 ml ice-cold MACS buffer and separated by a Ficoll gradient according to standard protocol (2000 rpm, 20 min, RT, minimal speed-up and slow-down). Lymphocytes were isolated from the Ficoll-interphase, diluted in MACS buffer, centrifuged at 1800 rpm for 10 min at 4 °C and pelleted cells were dissolved in MACS buffer or RPMI medium.

#### **2.5 Immune cell isolation from the inguinal lymph node (ILN)**

Following lymph node isolation, these were passed through a 70  $\mu$ m cell strainer (Corning) using 5 ml ice-cold MACS buffer. The cell suspension was centrifuged at 4 °C with 1500 rpm for 5 min and the cell pellet was FACS stained in MACS buffer or RPMI medium.

#### **2.6 Immune cell isolation from the ear and ear homogenate extraction**

The two skin layers of the ear were separated, minced, put on a 70  $\mu$ m cell strainer (Corning) with 100  $\mu$ l ice-cold PBS and centrifuged at 1500 rpm for 5 min at 4 °C. 5  $\mu$ l cOmplete™ Mini Protease Inhibitor Cocktail (Merck) were added to 50  $\mu$ l of the homogenate and stored at -80 °C until analysis. Skin fragments were digested in 1 ml supplemented RPMI medium (500 ml RPMI1640 medium with 5 ml NEAA, 5 ml L-Glutamine, 5 ml Pen/Strep, 5 ml sodium pyruvate, 12,5 ml HEPES buffer, 500  $\mu$ l  $\beta$ -mercaptoethanol, Liberase™ TL (Sigma-Aldrich) (0.25 mg/ml), and DNase I (Thermo Fisher Scientific) (0.1 mg/ml) for 60 min at 37 °C on a shaker. Digestion was stopped by addition of RPMI medium with 2 % FCS and 5 mM EDTA. Ears were mashed through a

70 µm cell strainer using 5 ml RPMI medium, centrifuged at 1500 rpm for 5 min at 4 °C and pelleted cells were analyzed.

## **2.7 Serum preparation from whole blood**

Following blood draw, 500 µl of whole blood were transferred into EDTA-containing microtainers. The content was mixed, transferred into Eppendorf tubes and kept at 8 °C for approximately 20 min before they were centrifuged at 1,000 x g for 10 min at 4 °C. 50 µl serum were removed and 5 µl cOmplete™ Mini Protease Inhibitor Cocktail (Merck) added prior to storage at -80 °C until analysis.

## **2.8 Flow cytometry**

Cells were incubated in a 96-well round-bottom plate in 30 µl of antibody dilution in MACS or RPMI medium for 20 min in the dark to stain for surface markers. Hereafter, 150 µl of RPMI medium were added and cells washed by centrifugation (400 x g for 3 min at 4 °C). Transcription factor stains were conducted using the eBioscience™ FoxP3/Transcription factor staining buffer set (Thermo Fisher Scientific). For intracellular cytokine staining, cells were re-stimulated in 100 µl RPMI medium with 1 x Invitrogen™ eBioscience™ cell stimulation cocktail (Invitrogen) and BD GolgiPlug™ (BD Biosciences) for 3 h at 37 °C. Extracellular surface stains in 50 µl MACS buffer included Fc block (BD Biosciences) and were incubated on ice for 20 min. Cells were washed with 150 µl HBSS and stained for life/dead in 100 µl HBSS for 20 min on ice, followed by a wash with 150 µl FACS buffer. Fixation was conducted in 100 µl 3.65 % formaldehyde for 20 min at RT in the dark. Cells were washed with 100 µl FACS buffer and permeabilized with 0.1 % NP-40 for 4 min at RT, washed with 100 µl FACS buffer and stained with antibodies for intracellular cytokines in 50 µl FACS buffer for 25 min at RT in the dark, washed and analyzed. Cytokine and chemokine analysis of serum and ear homogenate was conducted with BioLegend LEGENDplex™ kits according to manufacturer's instructions. FACS analysis was performed with a BD FACSCanto, BD FACS LSRFortessa or FACS LSR II (BD Biosciences). Flow cytometric data were analyzed using Flowjo X.10 software (Flowjo LLC).



## **2.9 NK cell purification through MACS- and FACS-based cell sort**

Lymphocyte isolation from the liver was conducted according to 2.4 and hepatic NK cell subsets were MACS-purified or cell-sorted prior to adoptive transfer, RNA single cell or bulk sequencing, and ATAC sequencing. MACS purification was conducted according to the manufacturer's protocol, separating CD49b<sup>+</sup> liver lymphocytes from the rest, with CD49b<sup>+</sup> cells remaining "untouched" since they were not bound by antibodies and passed through the MACS column. FACS-based cell sort was conducted with the BD FACS Aria III and BD FACS Aria Fusion. Here, the 100 µm wide nozzle was used to sort cells, compromising a gentle and efficient cell sort.

## **2.10 Adoptive NK cell transfer experiments**

Standard protocol for the assessment of MBEH-responsive NK cells comprised the sensitization of mice (d0, d1, d2, d3) and the validation if the NK cells isolated on d7 provide a naïve recipient mouse, which receives d7 cells, with the capability of a specific and potent recall response immediately after transfer (d7) on d8 and d9 during elicitation. Therefore, hepatic NK cells were isolated by MACS or FACS-based cell sort and 5 - 8 x 10<sup>4</sup> cells were adoptively transferred from naïve or MBEH-sensitized mice by intravenous injection (i.v.). Hereby, cells were dissolved in a volume of 50 - 100 µl PBS. Prior to adoptive transfer, recipient mice received 25 µl of 20 % MBEH in AOO on the ear (d7). After cell transfer, the ear swelling was measured, comparing the ear thickness prior to the treatment to the ear thickness during and after elicitation with a digital micrometer (Kroeplin). Here, the observance of vasodilation and immune cell infiltration into the ear serves as indication whether MBEH application induces a spontaneous unspecific or rather a strong adaptive response due to previous immune cell priming.

### **2.10.1 Adoptive transfer of *ex vivo* MBEH-exposed cNK cells**

Through *ex vivo* stimulation of hepatic NK1.1<sup>+</sup>,CD49b<sup>+</sup> cNK cells from naïve mice, the effect of direct MBEH contact on NK cells was tested. Therefore, liver lymphocytes were isolated and FACS-sorted. Live, lineage (CD3, CD19, Ter119, TCRβ) negative, and NK1.1<sup>+</sup>,CD49b<sup>+</sup> cells were sorted and washed in supplemented RPMI1640 medium. This medium was supplemented with 10 % FCS, 1 % Pen/Strep, 1 % sodium pyruvate, 1 % L-glutamine, 1 % NEAA, 1 % ITS and 500 µl β-mercaptoethanol. After cell sort and

one wash step in a volume of 1 ml medium and centrifugation at 1000 rpm for 3 min at 8 °C,  $1 \times 10^5$  cells were transferred into a round-bottom 96-well plate and either dissolved in 100  $\mu$ l RPMI medium with 0.1 % ethanol (control) or in 100  $\mu$ l RPMI medium with 0.1 % ethanol and MBEH, resulting in a 10  $\mu$ M MBEH containing medium. Cells were gently dissolved in the respective medium, centrifuged for 1 min at RT with 200 x g to provide cell-cell contact during incubation and placed at 37 °C with 5 % CO<sub>2</sub> for 1 h. Then, cells were centrifuged at RT for 3 min at 200 x g and washed in 150  $\mu$ l twice. Cells were taken up in PBS to ensure a cell concentration of  $2 \times 10^4$  in 50  $\mu$ l and were injected i.v into mice that just had received 25  $\mu$ l of a 20 % MBEH solution in AOO on the right ear (d0). On d1 and d2 elicitation was conducted and the ear swelling measured from d0 - d3. Elicitation was repeated on d7 and d8 (measurement d7 - d10) and d14.

## **2.11 NK cell co-culture with B16.F10 melanoma cells**

To determine the effect of *in vivo* sensitization with MBEH on NK cell reactivity towards melanoma cells, both mature hepatic NK cell subsets were isolated from MBEH-sensitized mice on d7 by FACS sort and added to previously seeded murine B16.F10 melanoma cells (kindly provided by Prof. Thomas Tüting). These experiments were conducted in 96-well flat-bottom culture plates and hepatic NK cells were co-cultured with the target cells at a ratio of 2:1. This culture was conducted in complete RPMI medium with 100 ng/ml IL-15 and 100 U/ml IL-2 (Peprotech). Following 42 h of co-culture, supernatants were analyzed with respect to their IFN- $\gamma$  and granzyme B content (ELISA, 2.11.1) and B16.F10 melanoma cell survival was determined by CellTiter-Blue<sup>®</sup> cell viability assay (2.11.2.).

### **2.11.1 Enzyme-linked immunosorbent assay (ELISA)**

For quantification of the cytokines IFN- $\gamma$  and granzyme B the supernatants were collected after 42 h of B16.F10 melanoma cell/NK cell co-culture. Supernatants were analyzed using ELISA kits according to the manufacturer's protocol. Therefore, ELISA plates were coated with the respective capture antibody in 50  $\mu$ l coating buffer and incubated at 4 °C overnight. Of note, between each incubation step, wells were washed at least three times with ELISA wash buffer. Following overnight plate coating, unspecific binding sites were blocked through 1 h of incubation with 50  $\mu$ l of the respective blocking buffer. Standards and samples were prepared in accordance with the manufacturer's instructions

in a volume of 50  $\mu$ l ELISA buffer and incubated at RT for 2 h. Next, biotinylated detection antibody was added in a volume of 50  $\mu$ l ELISA buffer and incubated at RT for 2 h. Afterwards, streptavidin-HRP was adjoined in 50  $\mu$ l ELISA buffer and incubated at RT for 1 h. Following addition of 50  $\mu$ l of the 1:1 mixed substrate solution, which allowed the HRP-mediated substrate oxidation resulting in the blue-colored product, 50  $\mu$ l of 1 M H<sub>2</sub>SO<sub>4</sub> was adjoined to terminate the reaction and measure the absorbance at 450 nm (with the reference of 570 nm) by a microplate spectrophotometer. Supported by the standard curve, the sample cytokine concentration was calculated.

### **2.11.2 CellTiter-Blue<sup>®</sup> cell viability assay**

To assess the viability of B16.F10 melanoma cells, a CellTiter-Blue<sup>®</sup> assay was performed. This assay is based on the reduction reaction of resazurin into a fluorescent product by metabolically active cells. Therefore, 100  $\mu$ l medium and 20  $\mu$ l CellTiter-Blue<sup>®</sup> reagent were added to the cells after melanoma and NK cell co-culture. Following the addition of the CellTiter-Blue<sup>®</sup> reagent, cells were kept in the incubator at 37 °C and 5 % CO<sub>2</sub> for 3 h. Fluorescence intensity was measured with the EnVision multilabel plate reader (excitation: 560 nm; emission: 590 nm) and cell survival calculated according to the manufacturer's advice.

## **2.12 Sequencing**

### **2.12.1 RNA single cell sequencing**

For single cell sequencing, liver lymphocytes were isolated (2.4), FACS-stained and hepatic lineage negative (CD3-, CD19-, Ter119-) cells were sorted (2.9) with respect to the expression of the surface receptor NK1.1. By FACS gating, debris and doublets were excluded. Following single cell sort by FACS Aria III, cells were collected in PBS that contained 0.04 % w/v BSA (400  $\mu$ g/ml) at a concentration of 500 cells/ $\mu$ l. Chromium<sup>™</sup> Controller was used to partition single cells into nanoliter-scale Gel Bead-In-EMulsions (GEMs) and the Single Cell 3' reagent kit v2 for reverse transcription and cDNA amplification and library construction (10x Genomics) were applied according to the manufacturer specifications. The SimpliAmp Thermal Cycler (Applied Biosystems) was used for amplification and incubation steps. Libraries were quantified by Qubit<sup>™</sup> 3.0

Fluorometer (Thermo Fisher Scientific) and the quality was checked using the Bioanalyzer 2100 with the Agilent High Sensitivity DNA kit (Agilent). Libraries were pooled and sequenced with the NovaSeq™ 6000 System (S1 Cartridge, Illumina) in paired-end mode to reach at least  $5 \times 10^4$  reads per single cell. Approximately 3000 cells were captured and a median gene number per cell of 1700 could be retrieved for both samples. The data were demultiplexed using Cell Ranger software (version 2.0.2) based on 8 base pair 10 x sample indices. The reads were aligned to mouse UCSC mm10 reference genome using STAR aligner. The alignment results were employed to quantify the expression level of mouse genes and to generate a gene-barcode matrix. “Cellranger aggr” command in Cell Ranger was used for aggregating libraries from multiple sequencing runs. Doublets and potentially dead cells were removed according to the percentage of mitochondrial genes, the number of genes and UMIs expressed in each cell. The remaining data were normalized, log-transformed and used for the downstream analysis. Data clustering was performed using Seurat R package (version 2.4). Principle component analysis was operated for dimensionality reduction and t-distributed stochastic neighbor embedding (t-SNE) was applied for data visualization and projection of high dimensional data. Seurat built-in “FindMarkers” function was utilized to find differentially expressed genes.

### **2.12.2 3'-RNA bulk sequencing of cNK cells**

Upon liver lymphocyte isolation cells were FACS stained. Lymphocyte gating and further debris and doublet exclusion depicted the lineage negative (CD3-, CD19-, Ter119-) cells against the surface marker NK1.1. Lineage negative cells were gated and NK1.1+,CD49b- and NK1.1+,CD49b+ stained cells were sorted.

Following FACS-based NK cell sort, RNA purification was carried out with the RNeasy mini kit (Qiagen) according to the manufacturer's instructions. Quantification and quality control were employed by Qubit (Thermo Fisher Scientific), where 20 ng RNA were applied for the sequencing of each sample. Library preparation was carried out with the QuantSeq 3' mRNA-Seq Library Prep Kit (Lexogen) and sequencing with the HiSeq 2500 System (V4) (Illumina) with 10 million raw reads and a length of 1 x 50 base pairs. The TapeStation (Agilent) was used to verify size, quantity, and integrity of the samples. Instruments and kits were used according to the vendor protocols and

bioinformatics were conducted similar to the protocol described for RNA single cell sequencing (2.12.1).

### 2.12.3 ATAC sequencing of cNK cells

Liver lymphocytes were isolated according to 2.4 and FACS-sorted by gating of lineage (CD3, TCR $\beta$ , CD19, Ter119) negative live cells that expressed the surface molecules NK1.1 and CD49b. Each sample comprised between  $1 \times 10^4$  and  $2 \times 10^4$  cells that were spun down with  $500 \times g$  for 5 min at 4 °C. Cells were washed once with 50  $\mu$ l of cold  $1 \times$  PBS buffer and spun down once more. The cell pellet was gently resuspended in 50  $\mu$ l of cold lysis buffer and immediately centrifuged at  $500 \times g$  for 10 min at 4 °C. The supernatant was discarded and it was immediately continued with the transposition reaction. Here, the cell preparation protocol was similar to the procedure described by Buenrostro et al. (Buenrostro et al., 2013). For the transposition reaction, the buffer was prepared according to Picelli et al. (Picelli et al., 2014). The transposition reaction mix comprised 1  $\mu$ l Tn5 (DZNE in-house, UKB) and 4  $\mu$ l 5  $\times$  TAPS-DMF buffer plus 15  $\mu$ l H<sub>2</sub>O (20  $\mu$ l). To resuspend the nuclei the cool cell pellet was gently pipetted and incubated at 37 °C for 30 min. Immediately after transposition, purification was conducted with the Qiagen MinElute kit. Transposed DNA was eluted in 10  $\mu$ l H<sub>2</sub>O and stored at 4 °C overnight. For the amplification of transposed DNA fragments, 10  $\mu$ l transposed DNA, 10  $\mu$ l nuclease-free H<sub>2</sub>O, 2.5  $\mu$ l 25  $\mu$ M customized Nextera PCR Primer 1, 2.5  $\mu$ l 25  $\mu$ M customized Nextera PCR Primer 2 [Barcode] and 25  $\mu$ l NEBNext<sup>®</sup> High-Fidelity 2  $\times$  PCR Master Mix (New England BioLabs) were combined and the PCR program run.

PCR cycle	Temperature (°C)	Duration
1	72	5 min
2	98	30 sec
3	98	10 sec
4	63	30 sec
5	72	1 min
6	Repeat steps 3-5, 11x (12 total)	
7	4 °C	

PCR products were purified with the Qiagen MinElute kit and PCR products eluted in 12  $\mu$ l H<sub>2</sub>O. To validate correct tagmentation and amplification and to determine the concentration, PCR products were analyzed by gel electrophoresis (TapeStation; Agilent) and sequenced thereafter.

For data analysis, single-end 61 base pair short reads were aligned to the mouse genome version mm10 using Bowtie 2 (Langmead and Salzberg, 2012) after trimming of adapter and low-quality sequences by Trimmomatic. Duplicate reads were flagged with Picard (<http://broadinstitute.github.io/picard/>) and the Tn5 offset was removed using the alignmentSieve functionality of the deepTools suite (Ramírez et al., 2016) prior to peak calling with MACS2 (Zhang et al., 2008). Bam file sorting and indexing was performed with SAMtools (Li et al., 2009). Consensus peak regions across all samples were generated with the 'reduce' function of the Bioconductor GenomicRanges package and read counting per sample was performed applying the 'summarizeOverlaps' function of the Bioconductor GenomicAlignments package (Lawrence et al., 2013). Blacklisted genomic regions for mm10 defined by ENCODE were excluded from the analysis and regions were annotated using ChIPseeker (Yu et al., 2015). After filtering for a minimum sum of 50 counts across all samples, differentially-accessible (DA) regions were determined using the Bioconductor DESeq2 package (Love et al., 2014) and independent hypothesis weighting (Ignatiadis et al., 2016).

### **2.13 Statistics**

Experimental data were analyzed using Graphpad Prism software (GraphPad Software) and significance was determined using an unpaired t-test with a two-tailed p value and 95 % confidence interval. Significance was defined as  $p < 0.05$  (\*);  $p < 0.01$  (\*\*);  $p < 0.001$  (\*\*\*) ;  $p < 0.0001$  (\*\*\*\*);  $p > 0.05$  (ns, not significant). Graphs depict the mean  $\pm$  SEM. For comparison of more than two datasets one-way ANOVA was applied.

## 2.14 General software

**Table 6: Software for data analysis and illustration and databases**

BD FACSDiva™ Software	BD Biosciences	<a href="https://www.bdbiosciences.com/en-us/instruments/research-instruments/research-software/flow-cytometry-acquisition/facsdiva-software">https://www.bdbiosciences.com/en-us/instruments/research-instruments/research-software/flow-cytometry-acquisition/facsdiva-software</a>
FlowJo V10	FlowJO	<a href="https://www.flowjo.com/solutions/flowjo/downloads/">https://www.flowjo.com/solutions/flowjo/downloads/</a>
Illustration Toolkits – BIOLOGY Bundle	MOTIFOLIO	<a href="https://www.motifolio.com/mfbiobundle.html">https://www.motifolio.com/mfbiobundle.html</a>
LEGENDplex data analysis software	BioLegend	<a href="https://www.biolegend.com/legendplex">https:// www.biolegend.com/legendplex</a>
Mendeley®	Elsevier	<a href="https://www.mendeley.com/">https://www.mendeley.com/</a>
Prism Graphpad 6	GraphPad Software	<a href="https://www.graphpad.com/scientific-software/prism/">https://www.graphpad.com/scientific-software/prism/</a>
Immunological Genome Project (RNA sequencing)	(Heng et al., 2008)	<a href="http://rstats.immgen.org/Skyline/skyline.html">http://rstats.immgen.org/Skyline/skyline.html</a>

### 3. Results

#### 3.1 Distinction and response of hepatic NK cells upon MBEH sensitization

To characterize and describe the MBEH-responsive hepatic innate immune cell subsets, the two mature NK cell populations (NK1.1+,CD49b- and NK1.1+,CD49b+) in the liver were analyzed with respect to their cell number before (d0), during (d3), and after (d8) sensitization with MBEH. Since a subset of NK1.1+ NK cells is described as specific memory NK cell for the haptens DNFB and Oxa (O’Leary et al., 2006; Peng et al., 2013; Zhang et al., 2016) and MACS-purified CD49b+ cells have been described to mediate a MBEH-specific recall response upon adoptive transfer (van den Boorn et al., 2016), the population size of both hepatic NK1.1+ NK subsets was measured following MBEH sensitization (Figure 5).

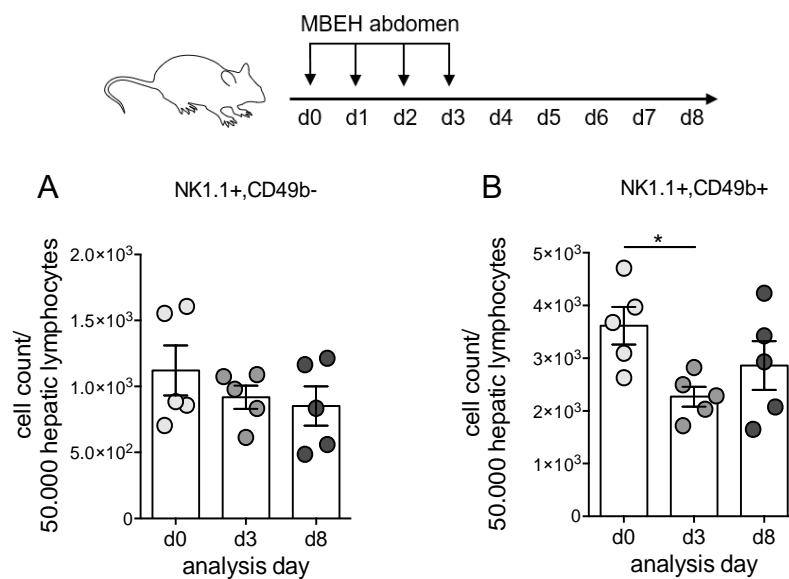


**Figure 5: NK population size before, during, and after MBEH sensitization.** Mice received abdominal MBEH treatment daily on d0 - d3. To verify whether the NK subsets NK1.1+,CD49b- (A) and NK1.1+,CD49b+ (B) expand, contract, or remain unchanged in size, hepatic NK cells were counted and the mean  $\pm$  SEM compared with  $p < 0.05$  (\*) indicating a statistically significant alteration.

By comparison to d0 neither hepatic NK1.1+ NK population had expanded on d3 or d8. On the contrary, the NK1.1+,CD49b- population appeared slightly decreased after MBEH sensitization (Figure 5A) and the NK1.1+,CD49b+ subset went through a significant



contraction between d0 and d3, mostly recovering by d8 (Figure 5B). This observation may indicate a more pronounced effect of abdominal MBEH treatment on NK1.1+,CD49b+ hepatic NK cells than on the CD49b- subset and suggests NK cell education rather than memory development, which is usually associated with a cell subset expansion prior to contraction. Figure 6 illustrates the clear distinction of these two hepatic NK cell populations by FACS analysis. To obtain this subset separation, lymphocytes were gated and only single cells included that were alive and expressed CD45. Gating on the lineage negative cells, the two NK cell subsets were defined by NK1.1 and CD49b expression.

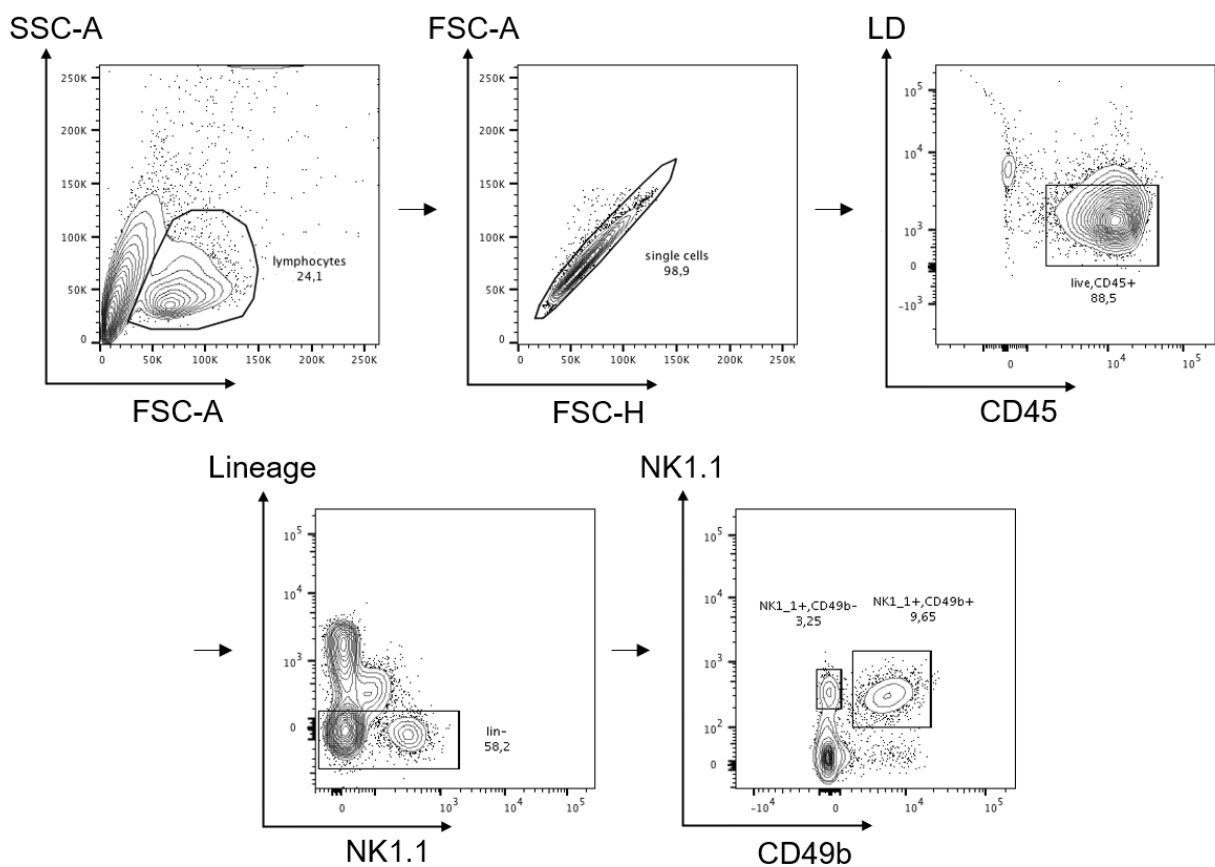


**Figure 6: FACS gating scheme for NK cell analysis.** Live liver lymphocytes (CD45+), which were lineage (CD3, TCR $\beta$ , CD19, Ter119) negative, were further characterized by the expression of NK1.1 and CD49b to distinguish the NK subsets NK1.1,CD49b- and NK1.1+,CD49b+.

In addition to the observance that hepatic NK cells are CD11b+, the mature NK cell subsets were described further by FACS analysis, which confirmed the population

characteristics published. Moreover, NK1.1+,CD49b- NK cells presented CXCR6 on their surface while expressing T-bet and lacking the transcription factor Eomes, whereas NK1.1+,CD49b+ NK cells exhibited Ly49H and expressed the transcription factors T-bet and Eomes (Figure 7). Moreover, in compliance with other studies, CD27 expression was found on NK cells (Hayakawa and Smyth, 2006; Takeda et al., 2000).

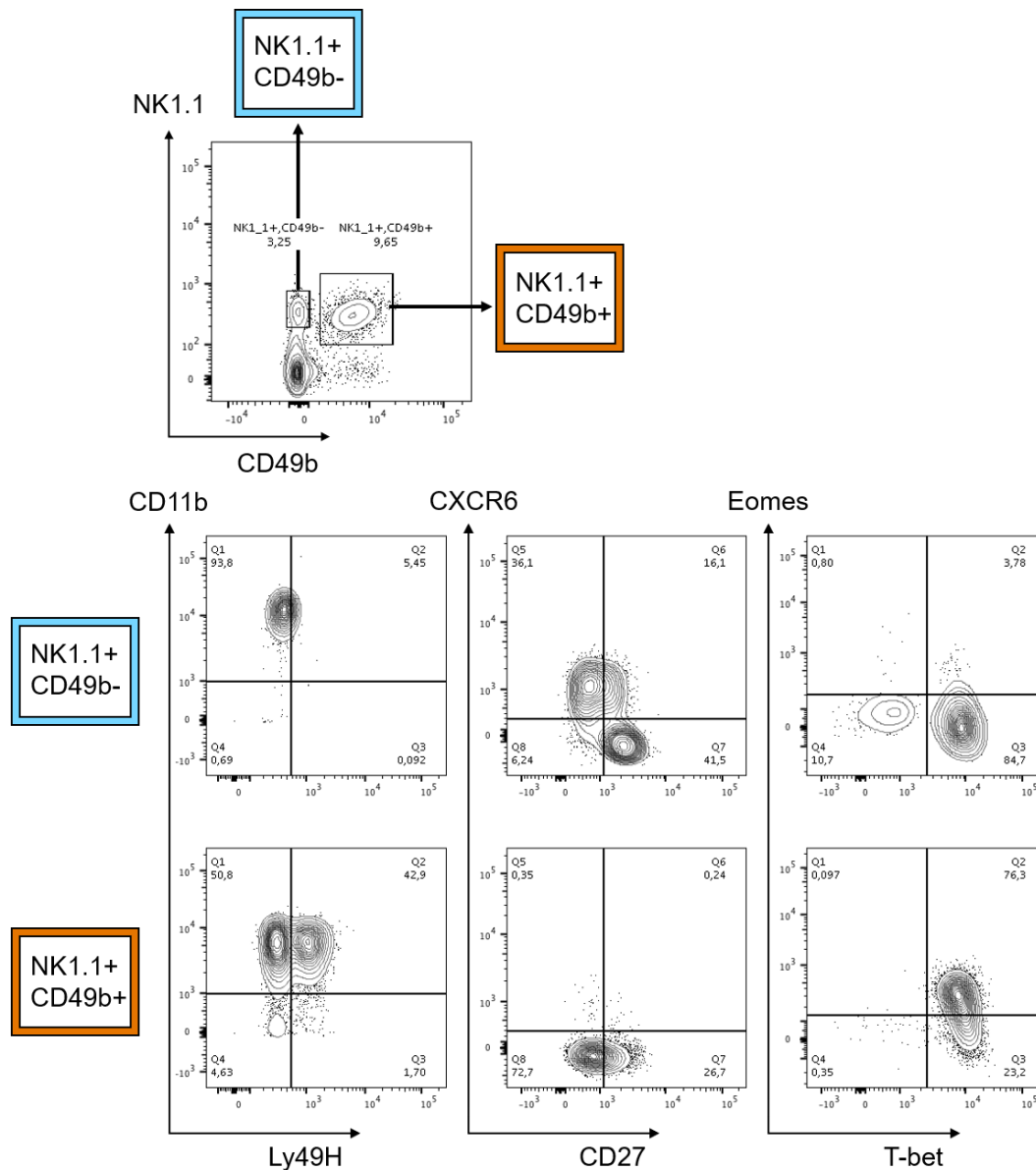


**Figure 7: Features of hepatic lineage (CD3, TCR $\beta$ , CD19, Ter119) negative mature NK subsets (NK1.1+,CD49b-; NK1.1+,CD49b+).** FACS analysis revealed that both cell subsets expressed CD11b but while the NK1.1+,CD49b+ cNK cells possessed the Ly49H receptor and the transcription factors T-bet and Eomes, the CXCR6 receptor was restricted to only T-bet expressing NK1.1+,CD49b- NK cells.

By FACS cell sorting of liver lymphocytes, debris and doublets were excluded and viable lineage negative cells were analyzed with respect to the expression of NK1.1 and CD49b (Figure 8A) and bulk 3'-RNA sequencing could confirm the presence of *Ncr1* (Nkp46) and *Il2rb* (IL-2 receptor subunit beta) in both mature NK subsets (Figure 8B).

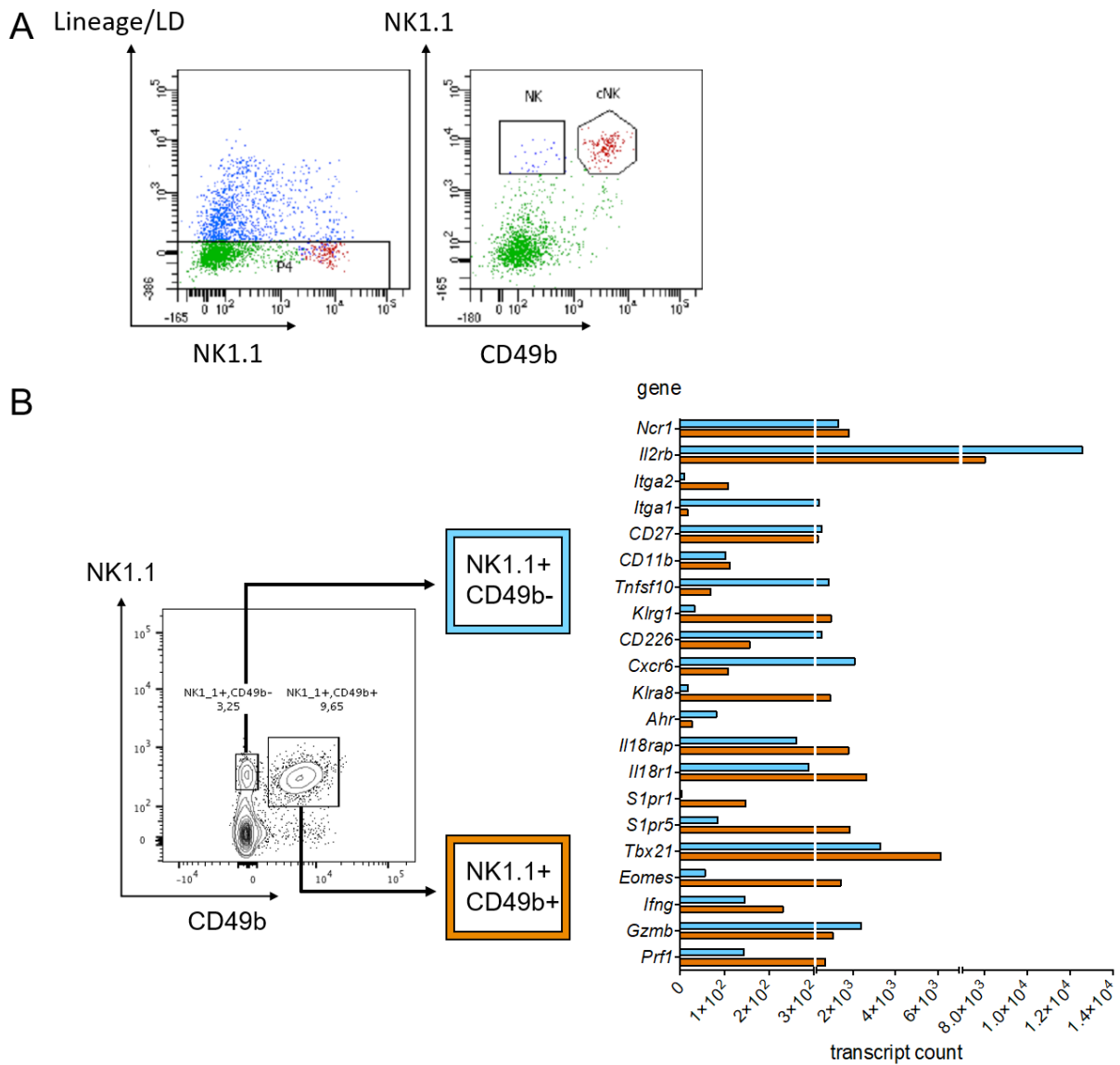


**Figure 8: 3'-RNA bulk sequencing of the mature hepatic NK cell subsets.** Lymphocytes were isolated from naïve mice and viable lineage negative (CD3-, CD19-, Ter119-) cells (gate P4) were sorted with respect to their expression of NK1.1 and CD49b (A). For each NK cell subset  $4 \times 10^4$  cells were analyzed in biological triplicates and the average transcript count/gene depicted (B).

Gene expression of *CD49a* (*Itga1*) coincided with the lack of *CD49b* expression (*Itga2*), presence of transcripts for TRAIL (*Tnfsf10*), DNAM-I (*CD226*), CXCR6, the aryl hydrocarbon receptor (*Ahr*), T-bet, IFN- $\gamma$  (*Ifng*), granzyme B (*Gzmb*) and perforin (*Prf1*). In contrast, gene expression of *CD49b* conformed with the expression of the *KLRG1* gene, transcripts for Ly49H (*Klra8*), genes encoding the IL-18 receptor subunits (*IL18rap*, *IL18r1*), cell mobility genes *S1pr1* and *S1pr5*, *T-bet* and *Eomes* in addition to the IFN- $\gamma$ , granzyme B, and perforin encoding genes (Figure 8B).

### 3.2 Elicitation response of MBEH-sensitized mice

#### 3.2.1 Ear swelling as indicator of successful MBEH sensitization

Following the general protocol of abdominal MBEH sensitization for four days (d0 - d3) and two days of MBEH application on the ear on d7 and d8 (elicitation), the induced ear swelling can be measured on d8 and d9 and compared to the ear thickness of naïve mice on d7 (Figure 9).

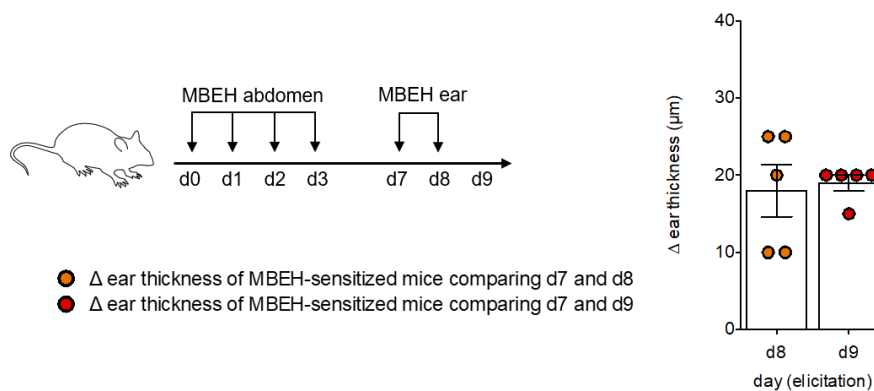


**Figure 9: Ear swelling response upon elicitation of MBEH-sensitized mice.** Mice were MBEH-sensitized on d0 - d3 and elicited on d7 and d8 to induce the recall response. Here, the difference in ear thickness between d7 and d8/d9 was measured. The ear thickness of all mice on d7 prior to elicitation ranged between 150 - 175  $\mu\text{m}$  and the difference to the ear thickness during elicitation is depicted ( $\Delta$ ) as mean  $\pm$  SEM (n=4).

As illustrated by Figure 9, previously sensitized mice developed a significant ear swelling upon re-challenge. Although ear thickness measurement in CHS is common,

this experiment demonstrates that the reliability of this readout extends to MBEH-induced CHS.

### **3.2.2 Multiple immune cell subsets respond during MBEH-induced elicitation**

To study the NK cell response strength during elicitation (d7 - d9) of MBEH-sensitized mice, the number of NK1.1+,CD49b- and NK1.1+,CD49b+ NK cells was measured in the liver, inguinal lymph node (ILN), and the targeted ear (Figure 10).

Altogether, the lymphocyte quantity in the liver was extenuated upon elicitation on d8 and d9. In the liver, the NK1.1+,CD49b- NK subset increased slightly from d7 to d8 and decreased between d8 and d9, whereas the NK1.1+,CD49b+ NK cell population decreased upon elicitation between d7 and d8 and was further diminished on d9 (Figure 10A). However, the NK cell alterations were not statistically significant. As expected for the recall response, a lymphocyte influx was observed in the ILN on d8 and both NK cell populations (NK1.1+,CD49b-; NK1.1+,CD49b+) were recruited to the ILN. Further, lymphocytes were recruited into the elicited ear, including NK1.1+,CD49b- and NK1.1+,CD49b+ NK cells, with tissue infiltration of NK1.1+,CD49b+ NK cells being stronger by comparison (Figure 10C).

For a more comprehensive overview of the events during elicitation of MBEH-sensitized mice, the quantities of T cells, DCs and neutrophils were analyzed and their CD103 expression investigated. CD103 expression was described on murine and human CD8+ T cells that were found in the intestine, bronchoalveolar fluid, and allograft tissues (Pauls et al., 2001; Rihs et al., 1996; Sarnacki et al., 1992), where this integrin directs lymphocytes to their ligand E-cadherin that is expressed on epithelial cells (Cepek et al., 1994; Karecla et al., 1995). In addition, CD103 is described as a target of Foxp3 (Hori et al., 2003), which is also expressed on CD4+ T<sub>regs</sub> (Banz et al., 2003; Lehmann et al., 2002), as a marker for alloantigen-induced CD8+ T<sub>regs</sub> (Uss et al., 2006), and as a hallmark of tumor-infiltrating Foxp3+ T<sub>regs</sub> (Anz et al., 2011). Thus, we wanted to identify whether MBEH elicitation induces CD103 expression on immune cells.

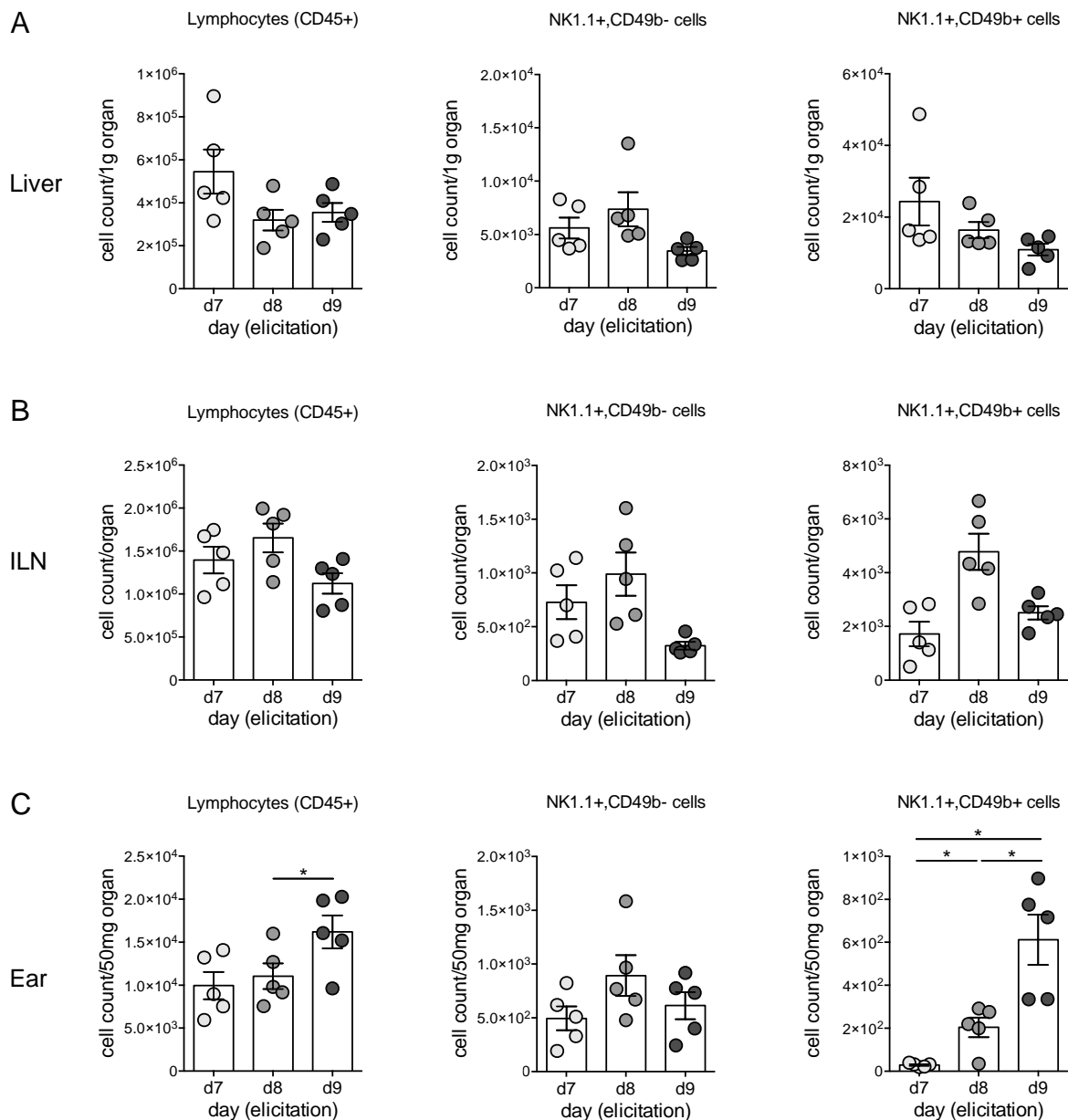


**Figure 10: Variations of lymphocyte and NK cell quantity in the liver, ILN, and ear of MBEH-sensitized mice during elicitation.** Lymphocytes and NK cells of sensitized mice were analyzed on d7, d8 and d9 to assess the effect of elicitation with MBEH on lymphocyte recruitment and the NK cell populations. Cell count was performed by FACS analysis and is shown as mean  $\pm$  SEM (n=2) with  $p < 0.05$  (\*) indicating statistically significant changes.

T cells were characterized through their receptors CD4 and CD8, whereas DCs and neutrophils were distinguished by the surface markers SSC-A and Gr-1 (neutrophils) or MHCII and CD11c (DCs) (Figure 11).

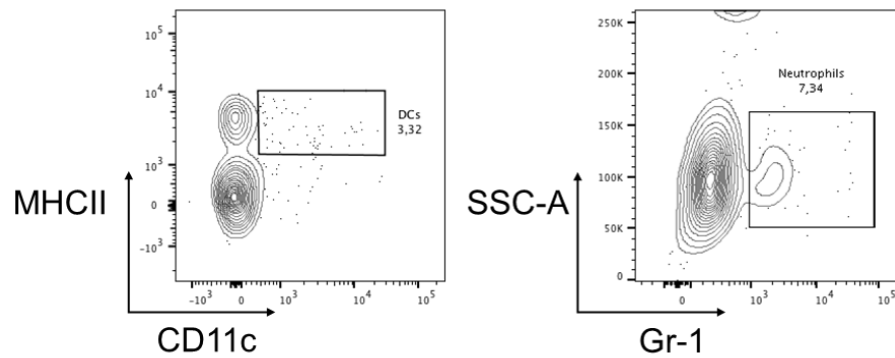


**Figure 11: Gating strategy for DCs and neutrophils.** Single, live and CD45+ lymphocytes were further discriminated through expression of MHCII and CD11c (DCs) and SSC-A intermediate and Gr-1 expression (neutrophils). This gating shows a sample from the elicited ear on d9.

Immune cell population analysis of the liver, ILN, and elicited ear on d7, d8 and d9 revealed significant changes in the immune cell quantities/organ during elicitation with MBEH (Figures 12 - 14). In the liver, the total lymphocyte count was reduced. On d8 and d9, CD4+ T cells, CD8+ T cells and DCs decreased in number, whereas the amount of CD103+ T cells was increased. While CD4+,CD103+ T cell numbers were significantly elevated on d8, the cell counts of d7 prior to elicitation and d9 after elicitation were similar. However, CD8+,CD103+ T cell numbers increased from d7 to d8 and were further elevated on d9 (Figure 12).

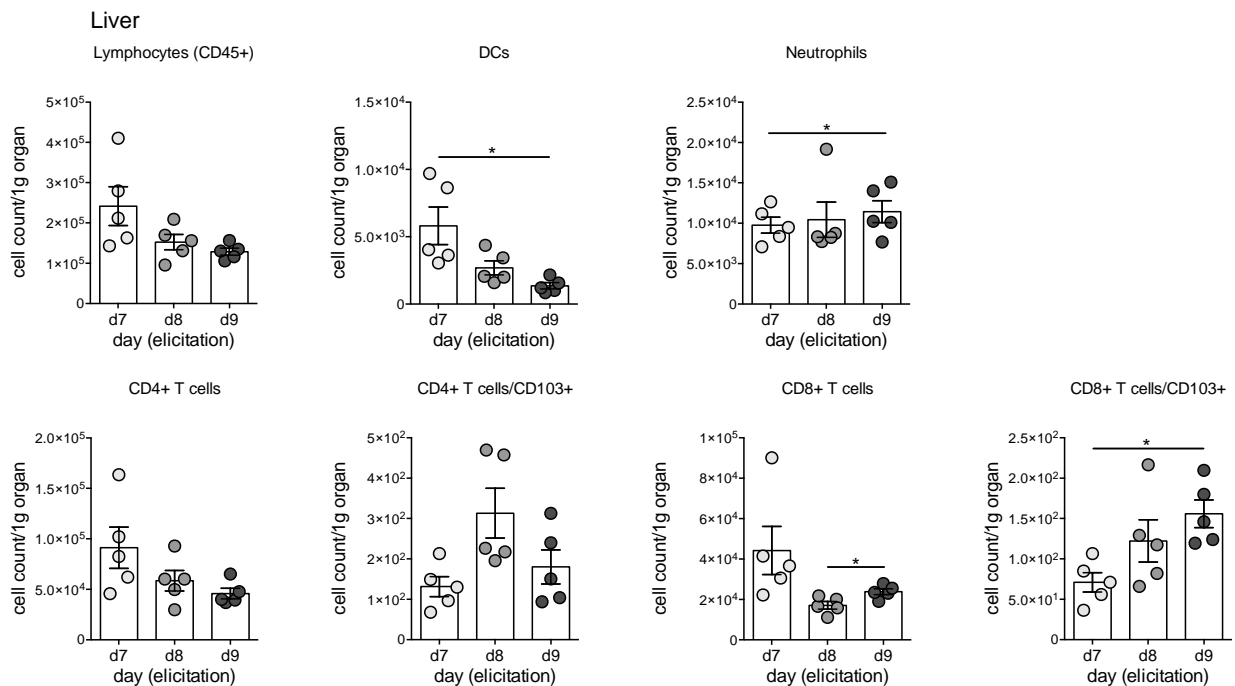


**Figure 12: Liver lymphocyte response during elicitation.** To characterize immune cell subset changes in the liver on d7, d8, and d9 during elicitation of MBEH-sensitized mice, livers were FACS-analyzed with respect to immune cell quantities. Therefore, viable and CD45 expressing cells were further gated to distinguish CD4+ T cells, CD8+ T cells, DCs and neutrophils. The cell numbers depicted represent the mean  $\pm$  SEM (n=2) and  $p < 0.05$  (\*) indicates a statistically significant difference between two datasets.

In the ILN, more lymphocytes were counted on d8 following elicitation with MBEH (Figure 13). On d8, a slight increase in the CD4+ and CD8+ T cell subsets was observed with a strong gain in CD103 expression in both T cell populations. Here, CD4+,CD103+ T cell numbers increased significantly on d8 and strongly decreased on d9, representing a short and strong gain in cell number, whereas CD8+,CD103+ T cells were clearly increased by d8 and remained elevated on d9, indicating a more persistent immune response than by the CD4+,CD103+ T cells. DCs increased slightly on d8 and on d9 a strong neutrophil influx was measured (Figure 13).



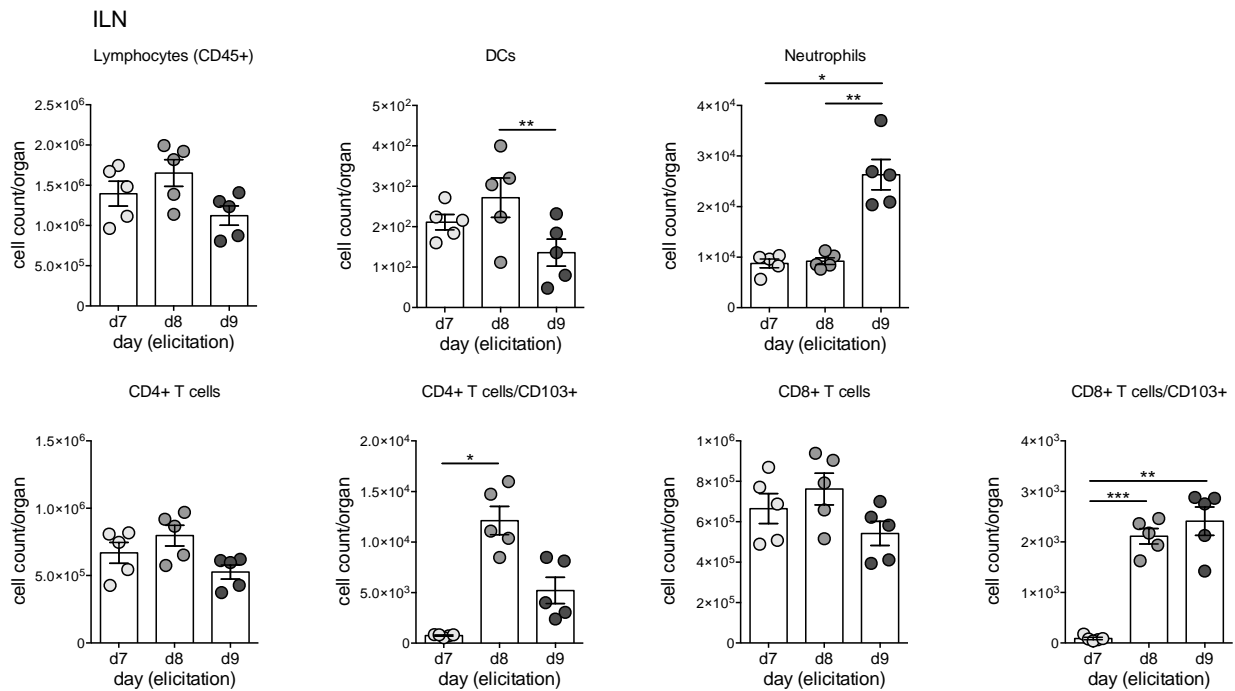


**Figure 13: Variation of lymphocyte quantity in the ILN upon elicitation of MBEH-sensitized mice.** ILNs were harvested on d7, d8, and d9 and FACS analyzed with respect to their immune cell quantity. Single, live, and CD45+ cells were further gated to distinguish CD4+ T cells, CD8+ T cells, DCs, and neutrophils, aiming to collect evidence of MBEH-induced lymphocyte trafficking and cell subset modulation. The cell numbers are indicated by the mean  $\pm$  SEM (n=2) and significant changes are indicated by  $p < 0.05$  (\*);  $p < 0.01$  (\*\*);  $p < 0.001$  (\*\*\*)

According to Figure 14, elicitation with MBEH rarely increased the lymphocyte amount in the elicited ear on d8 but resulted in a significant lymphocyte influx by d9. In the ear, CD4+ T cell counts were similar on d7 and d8 but gained in number on d9, while CD8+ T cell numbers decreased during elicitation. In both T cell populations, the amount of CD103 expressing cells was increased on d8 and d9. On d8, CD4+,CD103+ T cells were slightly elevated and increased on d9, whereas CD8+,CD103+ T cell numbers were significantly raised by d8 and remained elevated on d9. DCs and particularly CD103+ DCs increased in the tissue during elicitation comparing d7 to d9 and neutrophil numbers in the tissue were clearly elevated on d9 (Figure 14).

Of note, cellular subset counts in the liver, ILN, and ear (Figure 12 - 14) varied between both experiments but confirmed the respective cellular variations of CD45+ cells, DCs, neutrophils and CD4+/CD8+ T cells.

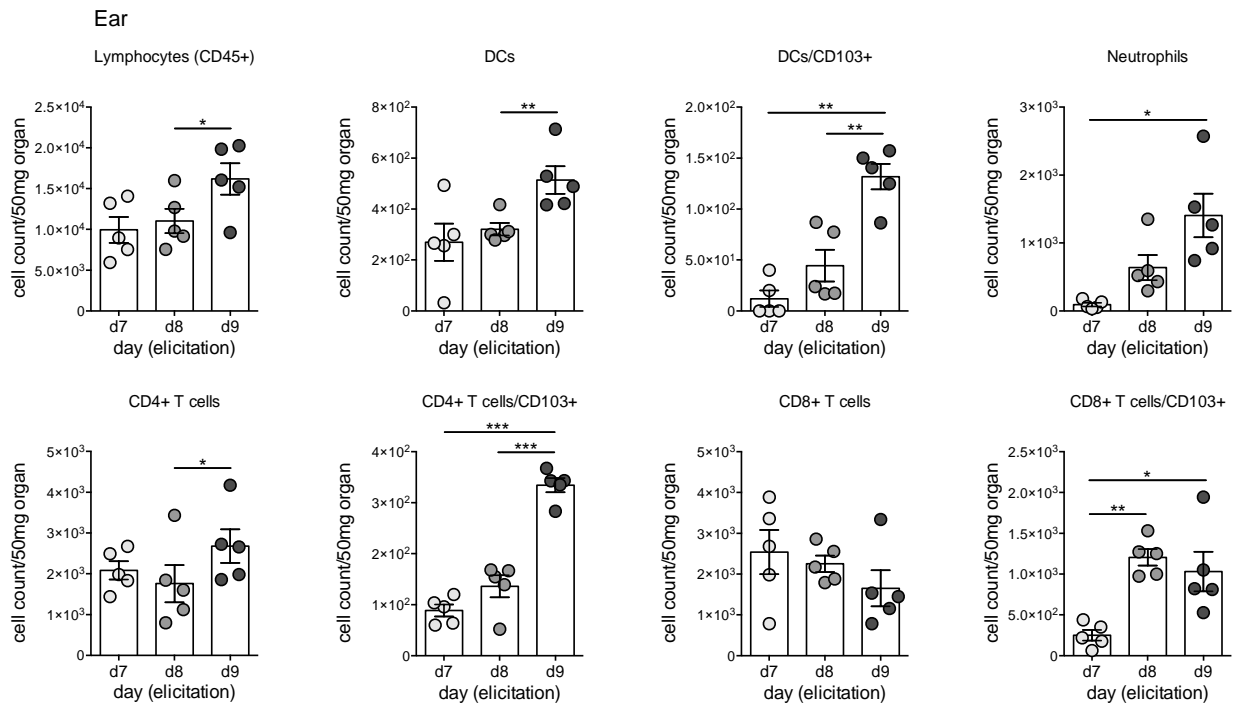


**Figure 14: Alterations of lymphocyte quantity in the ear during elicitation.** MBEH-treated ears were harvested on d7, d8, d9 and FACS analyzed. Viable and CD45+ cells were distinguished as CD4+ T cells, CD8+ T cells, DCs and neutrophils. Increases and decreases of these cellular subsets (mean  $\pm$  SEM) were measured to discriminate between responsive and unresponsive cell subsets in the ear during MBEH-induced elicitation (n=2). T cells and DCs were further analyzed with respect to their CD103 expression. Statistical significance is indicated by  $p < 0.05$  (\*);  $p < 0.01$  (\*\*);  $p < 0.001$  (\*\*\*)

### 3.3 Local and systemic immune cell signaling during MBEH elicitation

#### 3.3.1 The cytokine and chemokine milieu in the elicited ear

LEGENDplex™ assays were conducted to examine the local cytokine and chemokine milieu in the ear, comparing the ear homogenate prior to elicitation (d7), during elicitation (d8), and one day after MBEH elicitation of the ear (d9). Whereas type I and type II IFNs were not significantly elevated, TNF- $\alpha$  and IL-1 $\beta$  were verifiably increased on d8 and d9. Additionally, CCL2, CCL17, GM-CSF, IP-10, and IL-18 accumulated in the ear during elicitation. Especially CCL2, CCL17, CCL3, and IL-18 were even more enriched in the ear on d9 (Figure 15). Since TNF- $\alpha$ , IL-1 $\beta$ , CCL2, CCL17, GM-CSF, IP-10, and IL-10 were enriched in the ear homogenate on d8, these demonstrate to be important mediators for the early phase of the MBEH-induced ear swelling response during elicitation.

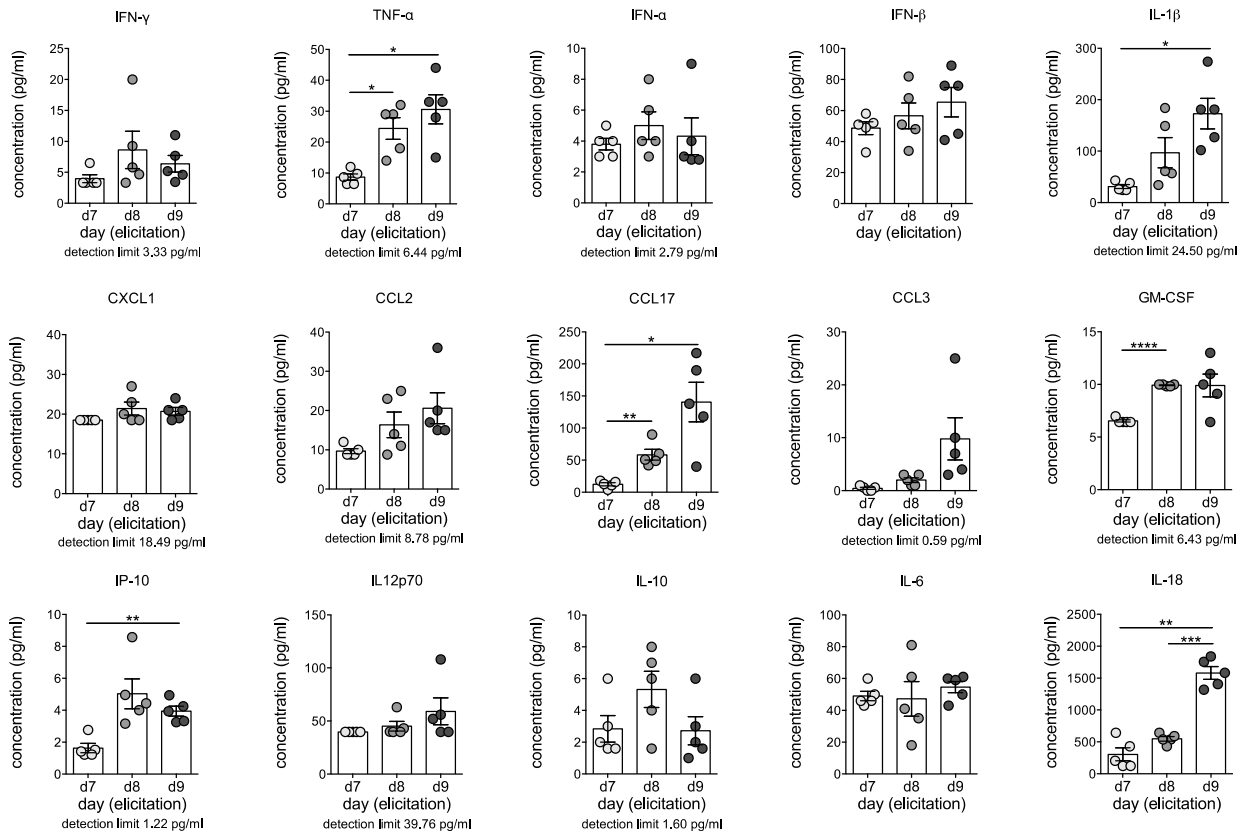


**Figure 15: Cytokine and chemokine quantity in the ear homogenate during elicitation.** For cell traffic and local immunity analysis, the ear homogenate of the elicited ear was analyzed on d7, d8, and d9 in MBEH-sensitized and elicited mice with respect to their cytokine and chemokine content, which is shown as mean  $\pm$  SEM (n=2) with significant alterations marked as  $p < 0.05$  (\*);  $p < 0.01$  (\*\*);  $p < 0.001$  (\*\*\*).

### 3.3.2 Cytokine and chemokine concentration in the serum

Aiming to shed light on the systemic response upon MBEH treatment, the serum of mice was analyzed, comparing d7 prior to elicitation with d8 of elicitation and d9 after elicitation. Upon elicitation we found elevated amounts of CCL2, CXCL1, CCL17, GM-CSF, and IP-10 in the serum of previously MBEH-sensitized mice on d8 (Figure 16). On d9, the amount of CCL2 and GM-CSF was again similar to d7 prior to elicitation, whereas the CXCL1 and CCL17 levels remained elevated. IL-18 was not found more abundantly in the serum throughout elicitation which points towards a local distribution and effect of this cytokine.

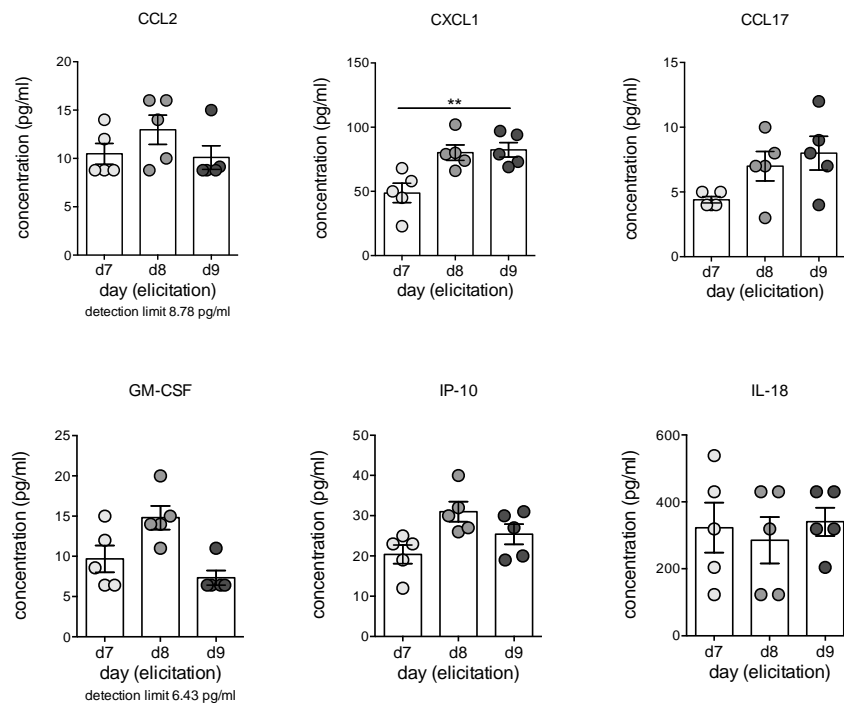


**Figure 16: Cytokine and chemokine quantities in the serum during elicitation.** For a more comprehensive analysis of MBEH-induced CHS the serum was analyzed with respect to its cytokine and chemokine content on d7, d8, and d9 to draw a broader picture of the MBEH-induced systemic immune response. Data are shown as mean  $\pm$  SEM ( $n=2$ ) and  $p < 0.01$  (\*\*) indicates a statistically significant alteration.

Overall, during elicitation of MBEH-sensitized mice several cytokines and chemokines were secreted in higher amounts locally at the target side (ear) or systemically (serum), with the amounts of CCL2, CCL17, GM-CSF, and IP-10 being elevated in the ear homogenate and the serum.

### 3.4 Adoptive transfer of hepatic NK cell populations and initiation of MBEH-induced CHS

#### 3.4.1 Adoptive transfer of mature hepatic NK cell populations reveals subset specificity in MBEH-induced CHS

Due to the fact that MBEH sensitization and elicitation change the amount of NK1.1<sup>+</sup>,CD49b<sup>-</sup> and NK1.1<sup>+</sup>,CD49b<sup>+</sup> NK cells in the liver (Figure 5), ILN and targeted ear (Figure 10), we investigated whether adoptive transfer of these two MBEH-primed cell

subsets can induce a MBEH-specific recall response in naïve mice. We thereby addressed two open questions: if hepatic NK1.1+,CD49b- NK cells can develop into memory cells in MBEH-induced CHS and whether the MBEH-reactive cells transferred in a previous study (van den Boorn et al., 2016) had been hepatic CD49b+ cells, which could be cNK cells, or other immune cells that had not been cleared from the sample by MACS purification. In general, MACS purification yielded approximately 85 % pure CD49b+ samples. Consequently, upon transfer of  $1 \times 10^5$  cells,  $1.5 \times 10^4$  cells were not necessarily CD49b+ innate immune cells. Hence, both mature NK cell populations were isolated from the livers of MBEH-sensitized mice and adoptively transferred into naïve mice (Figure 17). The MBEH-specific recall response was measured as ear swelling upon elicitation.

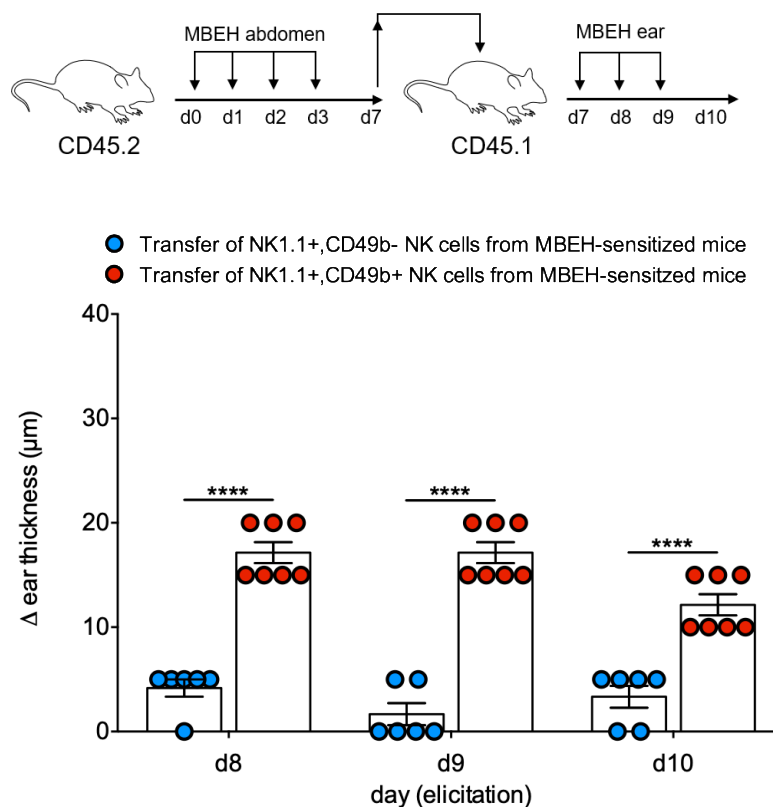


**Figure 17: Ear thickness measurement upon transfer of hepatic NK1.1+,CD49b- and NK1.1+,CD49b+ NK cells from MBEH-sensitized donors into naïve recipient mice.** Both NK cell subsets were isolated from MBEH-sensitized mice and sorted on d7. Naïve recipient mice received the first MBEH treatment on the ear immediately before i.v. transfer of the NK cells ( $8 \times 10^4$  cells/mouse). Elicitation was delivered on d8 and d9. Two pooled datasets of the ear thickness measurement upon transfer of NK1.1+,CD49b- and NK1.1+,CD49b+ NK cells are depicted (n=3). Ears measured prior to treatment ranged between 150 - 170  $\mu\text{m}$  in size and served as reference for the calculation of the  $\Delta$  ear thickness on d8, d9, and d10, shown as mean  $\pm$  SEM with  $p < 0.0001$  (\*\*\*\*).

After sensitization, liver lymphocytes were isolated and both hepatic NK cell subsets were purified by FACS-based cell sort according to Figure 8A. Next,  $8 \times 10^4$  cells of each NK cell subset were injected into each CD45.1 recipient mouse (Figure 17). Straight before cell transfer, the naïve recipient mice received the first MBEH application on the ear (d7), followed by elicitation of the ear on d8 and d9. As indicated by the ear swelling response upon adoptive transfer of hepatic NK1.1+,CD49b- and NK1.1+,CD49b+ cNK cells, only the transfer of NK1.1+,CD49b+ NK cells from MBEH-sensitized donors into naïve recipient mice could provide these mice with the competence of a strong recall response upon elicitation (Figure 17). The weak tissue response following transfer of NK1.1+,CD49b- cells and elicitation may link back to a low responsiveness of these cells or the acetone used as MBEH solvent, which can induce a slight inflammation of the skin. Thus, this experiment revealed that only the adoptive transfer of hepatic NK1.1+,CD49b+ NK cells induced an ear swelling in unsensitized recipient mice.

### **3.4.2 The ear swelling upon adoptive transfer of hepatic NK1.1+,CD49b+ cells from MBEH-sensitized mice arises from cell specificity**

Merely the transfer of hepatic NK1.1+,CD49b+ NK cells provided naïve recipient mice with a competent recall response upon MBEH challenge on the ear. Thus, we wanted to determine whether the recall competence after transfer of NK1.1+,CD49b+ NK cells was established by the change in population size through the injection of additional cells, or if these NK cells from MBEH-sensitized mice had gained a distinct functionality and responsive potential. Hence, the transfer experiment described in Figure 17 was applied to NK1.1+,CD49b+ NK cells, which were either isolated from naïve or MBEH-sensitized mice on d7. Following adoptive NK cell transfer, the ear thickness development upon MBEH challenge in both groups of mice was measured and compared to control-treated mice that were naïve, did not receive NK cells, but were treated with MBEH on the ear (Figure 18).

As illustrated by Figure 18, the transfer of naïve NK cells had a small effect on the ear swelling response upon elicitation when compared to the ear thickness of the control group on d8. Importantly, the recipient group provided with NK cells from sensitized mice responded with a stable and explicit ear swelling on d8 and d9, confirming that hepatic

MBEH-exposed NK1.1+,CD49b+ NK cells adoptively transfer the potential to specifically respond to MBEH challenge.

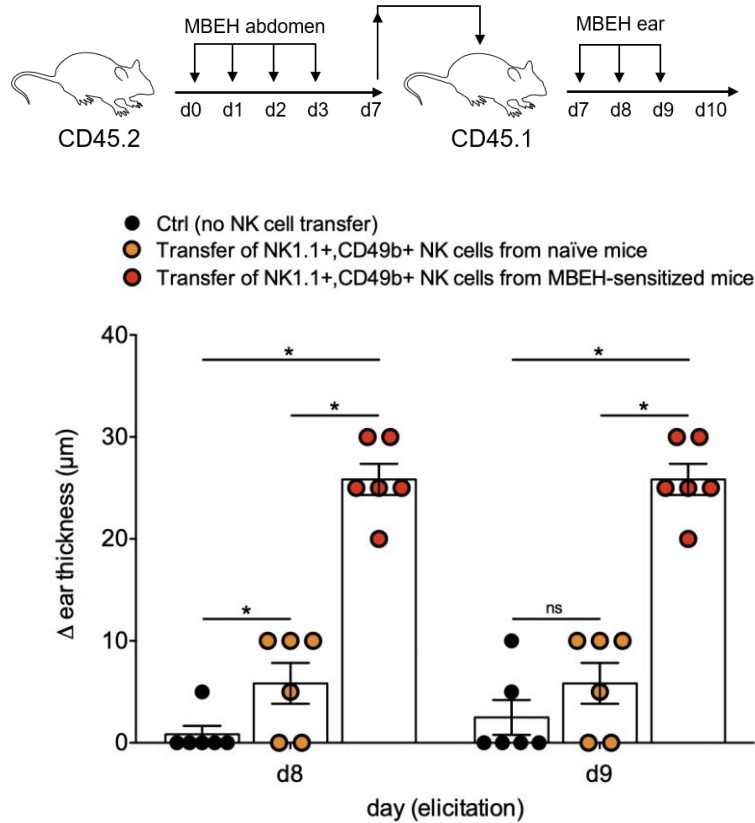


**Figure 18: CHS-induced ear swelling upon elicitation following transfer of NK1.1+,CD49b+ NK cells from naïve and MBEH-sensitized mice.** NK1.1+,CD49b+ NK cells were isolated from naïve and MBEH-sensitized mice, respectively, and sorted on d7. Recipient mice received the first MBEH treatment and NK cell injection ( $5 \times 10^4$  cells/mouse) i.v. on d7 and elicitation on the ear on d8 and d9. Two experiments are depicted, showing the ear thickness measurement upon transfer of naïve and MBEH-primed NK cells in comparison to naïve mice (Ctrl) that were elicited without previous NK cell transfer. The  $\Delta$  ear thickness calculation, depicted as mean  $\pm$  SEM, was performed for d8 and d9. On d7 the ear thickness of naïve mice ranged in all groups between 155 - 170  $\mu\text{m}$ . Significance is defined as  $p < 0.05$  (\*);  $p > 0.05$  (ns, not significant).

Cell purity checks were carried out upon cell sort for adoptive transfer experiments to provide evidence that the induced immune responses were induced by NK cells rather than a contaminating cell population not excluded by the applied FACS-based cell sort strategy (Figure 19).

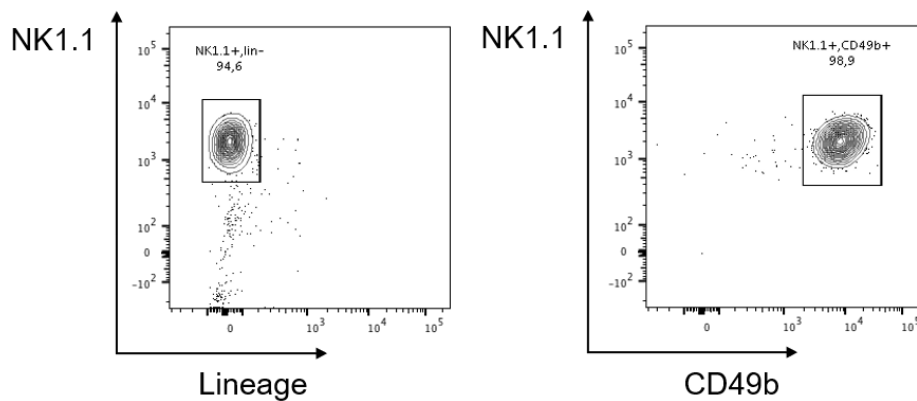


**Figure 19: Post-sort purity check of the cNK cell subset.** After the sort of hepatic cNK cells, purity checks were conducted to ensure a similar efficiency for transfer experiments. The gating for lineage negative (CD3<sup>-</sup>, Ter119<sup>-</sup>, CD19<sup>-</sup>) NK1.1<sup>+</sup>,CD49b<sup>+</sup> cNK cells is shown. In general, the average purity ranged between 92 - 96 %.

After adoptive cNK cell transfer (Figure 18), lymphocyte and NK cell counts were conducted for the liver, ILN, and elicited ear on d10 (Figure 20) in order to compare the effect of the respective cNK cell transfer (naïve vs. MBEH-treated). As depicted by Figure 20, the lymphocyte quantity in the liver was slightly reduced and the cNK cell count was minimally extenuated to similar. In the ILN a subtle increase in lymphocytes and NK1.1<sup>+</sup>,CD49b<sup>+</sup> NK cells was observed. With reference to the strong lymphocyte gain in the ear after sensitization and elicitation (Figure 10), the lymphocyte count after transfer differs since this increase was not retraced here (Figure 20). However, the tendency of a slight increase of the NK1.1<sup>+</sup>,CD49b<sup>+</sup> NK cell subset is supported by this analysis. Collectively, the cell number variations after adoptive transfer of cNK cells from sensitized mice are less pronounced than in the FACS-based analysis after complete sensitization and elicitation *in vivo* (Figure 10), but taken into account how many CHS mediator cells (e.g. KCs, mast cells, DCs, neutrophils, T cells) remained untreated in this experiment, the cNK cell transfer from MBEH-sensitized into naïve mice revealed a weak effect that could have been more distinct if we had analyzed the cells on d8 or d9.



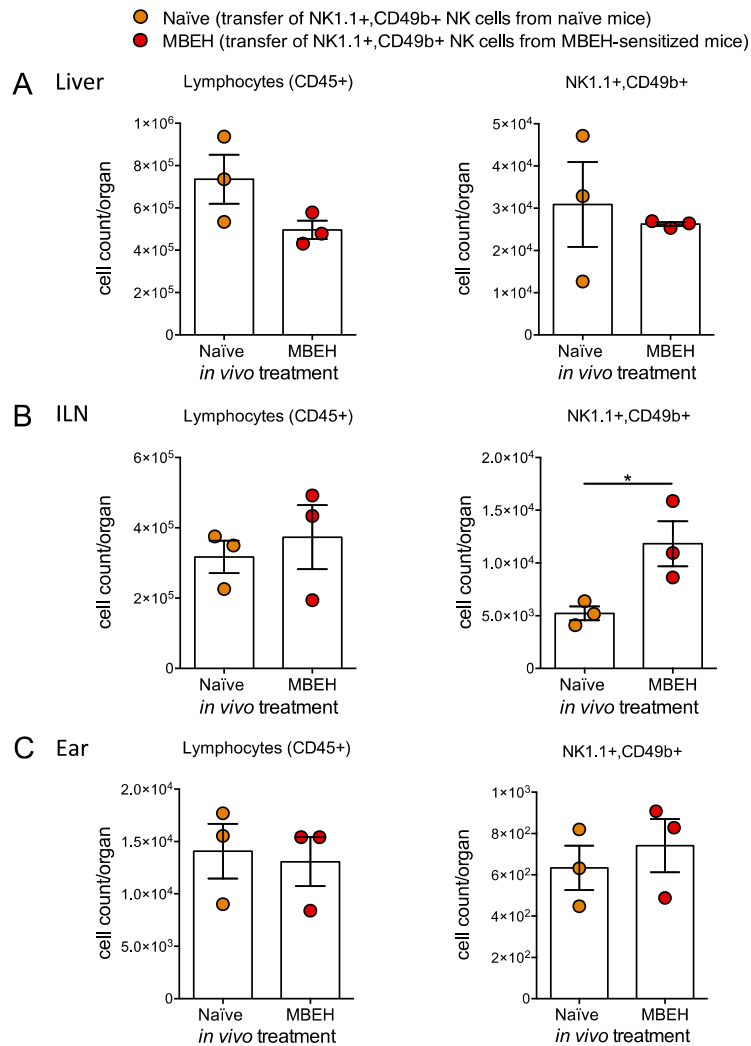


**Figure 20: Impact of hepatic NK1.1+,CD49b+ cell transfer on the lymphocyte and cNK cell count in the liver, ILN, and ear.** NK cells from naïve and MBEH-sensitized mice were isolated on d7 and naïve recipient mice received i.v.  $5 \times 10^4$  cells/mouse. MBEH was applied on d7, d8 and d9. On d10, the organs were harvested and analyzed by FACS. The analysis of one experiment included in Figure 18 is shown (mean  $\pm$  SEM), with  $p < 0.05$  (\*) revealing a statistically significant change.

### 3.5 Adoptive transfer of *in vitro* MBEH-exposed hepatic cNK cells can induce an elicitation response in naïve recipient mice

The *in vivo* priming effect of MBEH on hepatic NK1.1+,CD49b+ NK cells raised the question if the NK cell response is shaped indirectly through cellular activation and a variation in the cytokine/chemokine milieu, or whether MBEH as substance has a direct effect on exposed cNK cells. Therefore, hepatic NK1.1+,CD49b+ NK cells were isolated

from naïve mice and either incubated in standard cell culture medium or in medium supplemented with MBEH. Following this incubation, NK cells were washed. Prior to NK cell injection, naïve mice received the first MBEH treatment on the ear and were then, after i.v. NK cell injection, repeatedly elicited on d1, d2, d7, d8, and d14 (Figure 21), the ear thickness measured and the  $\Delta$  ear thickness calculated.

The transfer of MBEH-naïve (ctrl) NK cells did not induce an ear swelling on d1 - d4. One week later, a slight gain in ear thickness was recorded on d8 and d9 but it is highly possible that this was a response to the repeated acetone and contact sensitizer application itself. However, transfer of *ex vivo* to MBEH exposed cNK cells induced a distinct ear swelling in recipient mice. Already one day after transfer the ear thickness of the recipient mice was increased. Subsequently, the ear thickness gain remained steady on d2 and d3 and decreased by d4. One week after cell transfer and elicitation, the recall response was again induced by MBEH application to the ear to assess the specificity and stability of the recall response. As Figure 21 illustrates, the ear swelling response was even more pronounced one week after transfer of MBEH-exposed cNK cells, indicating modifications of hepatic NK1.1<sup>+</sup>,CD49b<sup>+</sup> NK cells through MBEH contact *ex vivo*.

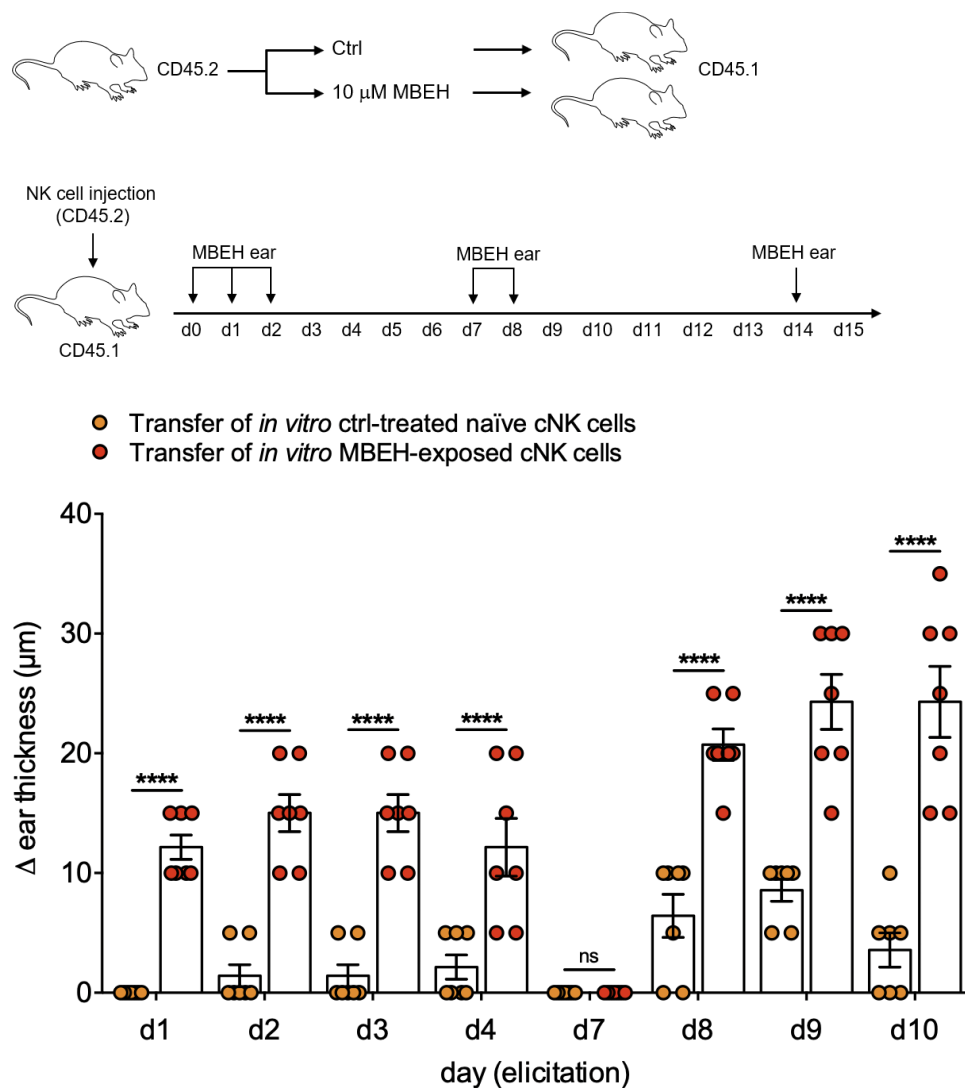


**Figure 21: Ear swelling upon transfer of *in vitro* ctrl-treated and MBEH-exposed cNK cells.** A different ear thickness development was traced between mice that received *in vitro* ctrl-treated MBEH-naïve and MBEH-treated cNK cells ( $2 \times 10^4$  cells/mouse) i.v. on d0, with MBEH application on the ear on d0 and elicitation on d1, d2, d7, and d8. The ear thickness of the untreated ear on d0 ranged between 160 - 180  $\mu\text{m}$  and the difference in ear thickness ( $\Delta$ ) was calculated and depicted as mean  $\pm$  SEM. The data of two experiments were pooled;  $p < 0.0001$  (\*\*\*\*);  $p > 0.05$  (ns, not significant).

These results suggest that hepatic cNK cells may either recognize MBEH directly or may serve as MBEH carriers, which would be impressive due to the minute amount of MBEH that in this case would be sufficient for CHS induction. However, these experiments imply that NK cell variations could be induced by *in vitro* exposure to MBEH and may thus function independent of cytokines, chemokines and additional cellular mediators.

Our attempt to track the cNK cells after transfer through the congenic marker CD45.2 was not successful, which is why the fate and longevity of the adoptively transferred cNK cells remain unclear.

### **3.6 MBEH sensitization of mice modifies hepatic NK cell features *in vitro***

#### **3.6.1 MBEH sensitization does not change the spontaneous IFN- $\gamma$ and granzyme B secretion of hepatic NK1.1<sup>+</sup>,CD49b<sup>+</sup> NK cells**

Hepatic MBEH-educated cNK cells were clearly capable of transferring the immune competence for a specific recall response upon challenge with MBEH (Figure 17, 18, 21), fostering the hypothesis that this cNK cell subset is activated and modified through sensitization with MBEH. To determine whether the spontaneous cytokine secretion after stimulation of naïve cNK cells differs from those of sensitized mice (d7), lymphocytes were isolated from both conditions and unspecifically stimulated *in vitro* using the Invitrogen™ eBioscience™ cell stimulation cocktail. By the use of GolgiPlug, cytokines produced by the NK cells accumulated in the cytoplasm and were measured by intracellular FACS staining. Figure 22 summarizes the secretion of IFN- $\gamma$  (Figure 22A) and granzyme B (Figure 22B) following *ex vivo* stimulation. To confirm the synthetic activation of naïve NK cells (d0) and NK cells from MBEH-sensitized mice (d7) *in vitro*, a control sample remained unstimulated. Interestingly, neither the spontaneous IFN- $\gamma$  secretion (Figure 22A) nor granzyme B release (Figure 22B) appeared to differ between cNK cells from naïve (d0) and MBEH-sensitized (d7) mice.

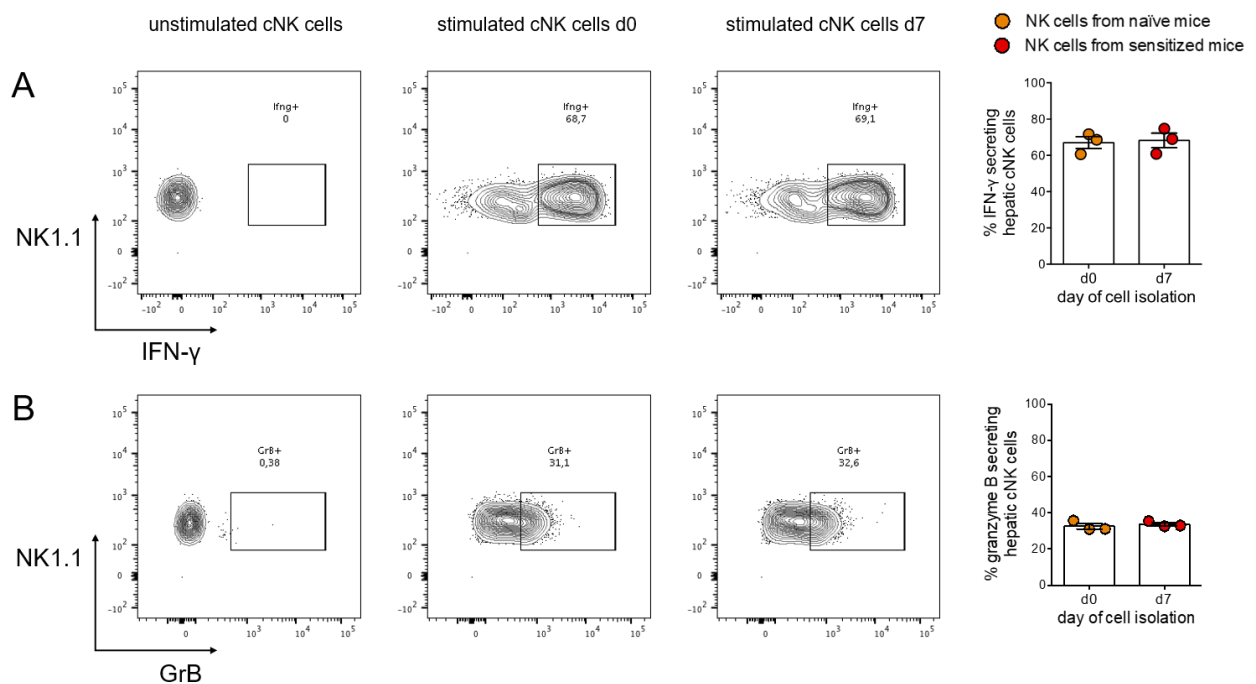


**Figure 22: IFN- $\gamma$  and granzyme B secretion by cNK cells upon re-stimulation *ex vivo*.** NK cells were isolated from naïve (d0) and MBEH-sensitized mice (d7). Upon isolation, NK cells were activated and stimulated for three hours *in vitro*. Then, cytokines were FACS-stained intracellularly to assess whether MBEH-priming affected the capacity of cNK cell cytokine secretion. The mean  $\pm$  SEM is indicated for these measurements (n=3).

General cell stimulation did not disclose an effect of *in vivo* sensitization with MBEH on the IFN- $\gamma$  or granzyme B secretion capacity of cNK cells. Based on this observation, the cNK cells of MBEH-sensitized mice may need a specific target or multiple stimuli to display acquired reactivity.

### 3.6.2 *In vivo* MBEH sensitization modulates NK cell control of B16.F10 melanoma cells *ex vivo*

As a result of the data shown in Figure 22, hepatic NK cells were provided with a different target *ex vivo*. Since MBEH treatment is reported to induce a specific autoimmune response against melanocytes *in vivo* and can protect from tumor outgrowth upon subcutaneous injection of B16.F10 melanoma cells (van den Boorn et al., 2016), this cell line was used for a co-culture experiment where we compared the reactivity of naïve (d0) NK cells and NK cells from MBEH-sensitized mice (d7) towards B16.F10 melanoma cells. With an effector to target ratio of 2:1,  $2 \times 10^4$  NK cells were added to  $1 \times 10^4$  seeded

melanoma cells. Subsequently, the B16.F10 melanoma cell survival was compared between the NK cell samples from naïve (d0) and sensitized mice (d7) (Figure 23) and the respective IFN- $\gamma$  (Figure 24) and granzyme B (Figure 25) release was quantified by ELISA. In this experiment, hepatic NK1.1+,CD49b- cells and NK1.1+,CD49b+ cNK cells were compared although NK1.1+,CD49b- NK cells were unable to induce a MBEH-specific recall response upon adoptive transfer (Figure 17). We wanted to assess if both NK subsets from naïve (d0) and MBEH-sensitized (d7) mice would behave similarly or different upon melanoma cell co-culture *ex vivo*.

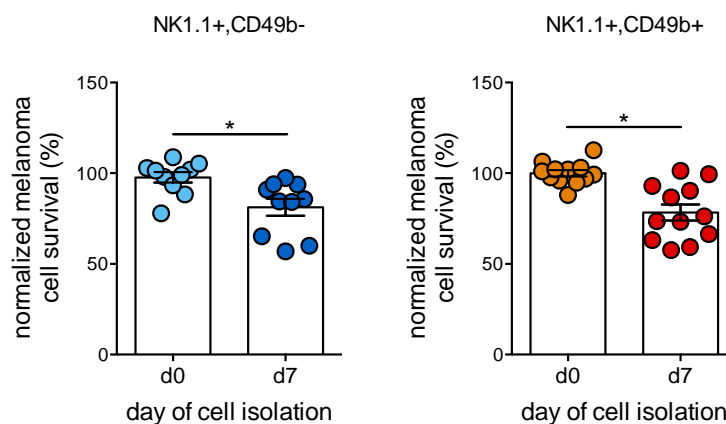


**Figure 23: B16.F10 melanoma cell survival upon co-culture with naïve and MBEH-primed NK cells.** Melanoma cells were seeded and NK cells added at the E:T ratio 2:1. The culture medium was supplemented with 100 U IL-2 and 10 ng IL-15. After 42 h, the CellTiter Blue<sup>®</sup> reagent was added and incubated for two hours prior to measurement. Data were normalized and depicted as mean  $\pm$  SEM (n=4) with p < 0.05 (\*) as indicator of statistical significance.

Normalization of the B16.F10 melanoma cell survival in the presence of NK cells from MBEH-sensitized (d7) and naïve (d0) mice showed that both hepatic NK cell subsets possessed an increased capacity to control melanoma cell growth and survival (Figure 23). Regarding the IFN- $\gamma$  (Figure 24) and granzyme B (Figure 25) release of NK1.1+,CD49b- and NK1.1+,CD49b+ NK cells disparities were recorded. As displayed by Figure 24, the co-cultured NK1.1+,CD49b+ NK cells secreted significantly more IFN- $\gamma$  when isolated from sensitized mice (d7), whereas the IFN- $\gamma$  secretion of NK1.1+,CD49b- NK cells was not explicitly changed.

Concerning the granzyme B release of both NK cell populations, NK1.1+,CD49b+ NK cells released significantly more granzyme B when taken from sensitized mice (d7), while granzyme B secretion of NK1.1+,CD49b- NK cells was steady (Figure 25).

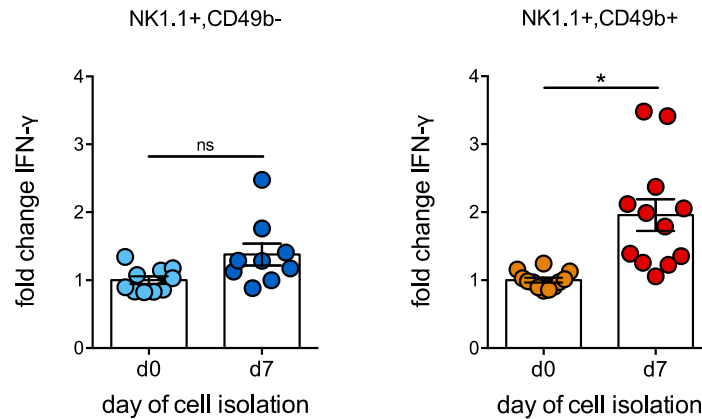


**Figure 24: IFN- $\gamma$  secretion by hepatic NK cells upon B16.F10 melanoma cell co-culture.** Melanoma cells were seeded and NK cells added with a ratio of 2:1. After 42 h of melanoma and NK cell co-culture in the presence of 100 U IL-2 and 10 ng IL-15, the IFN- $\gamma$  quantity in the medium was measured through ELISA and the fold change depicted as mean  $\pm$  SEM (n=4) with  $p < 0.05$  (\*) and  $p > 0.05$  (ns).

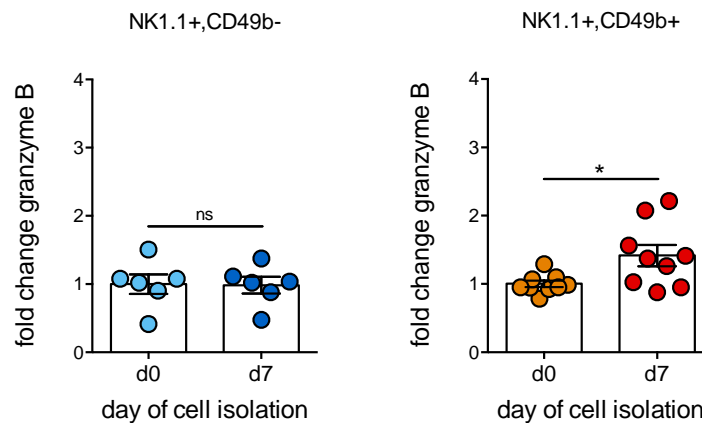


**Figure 25: Granzyme B secretion by hepatic NK cells during B16.F10 melanoma cell co-culture.** Melanoma cells were seeded and NK cells added at a E:T ratio of 2:1. After co-culture of naïve and MBEH-primed NK cells with B16.F10 melanoma cells in the presence of 100 U IL-2 and 10 ng IL-15 (42 h), the granzyme B concentration in the medium was measured by ELISA and calculated with the mean  $\pm$  SEM (n=3) with  $p < 0.05$  (\*) and  $p > 0.05$  (ns).

Taken together, these data suggest that both mature hepatic NK cell populations, NK1.1+,CD49b- and NK1.1+,CD49b+, control B16.F10 melanoma cell growth more efficiently when they were isolated from MBEH-sensitized mice. However, only the NK1.1+,CD49b+ NK cells from MBEH-sensitized mice secreted more IFN- $\gamma$  and granzyme B when exposed to B16.F10 melanoma cells.

### **3.7 RNA single cell sequencing reveals transcriptional identity of hepatic NK1.1+ cells from naïve and MBEH-sensitized mice**

Adoptive cell transfer experiments (Figure 17, 18), NK cell co-culture with B16.F10 melanoma cells (Figure 23 - 25), and transfer of *in vitro* MBEH-treated cNK cells (Figure 21) showed that MBEH affects cNK cell function and their faculty to provide a potent recall response upon antigen re-encounter. However, we wanted to test whether MBEH sensitization changed the NK cell transcriptome. By FACS-based cell sort we isolated viable lineage negative NK1.1+ cells (Figure 26A) and performed single RNA sequencing of NK1.1+ lymphocytes from naïve (d0) and MBEH-sensitized mice (d7) (Figure 26B).



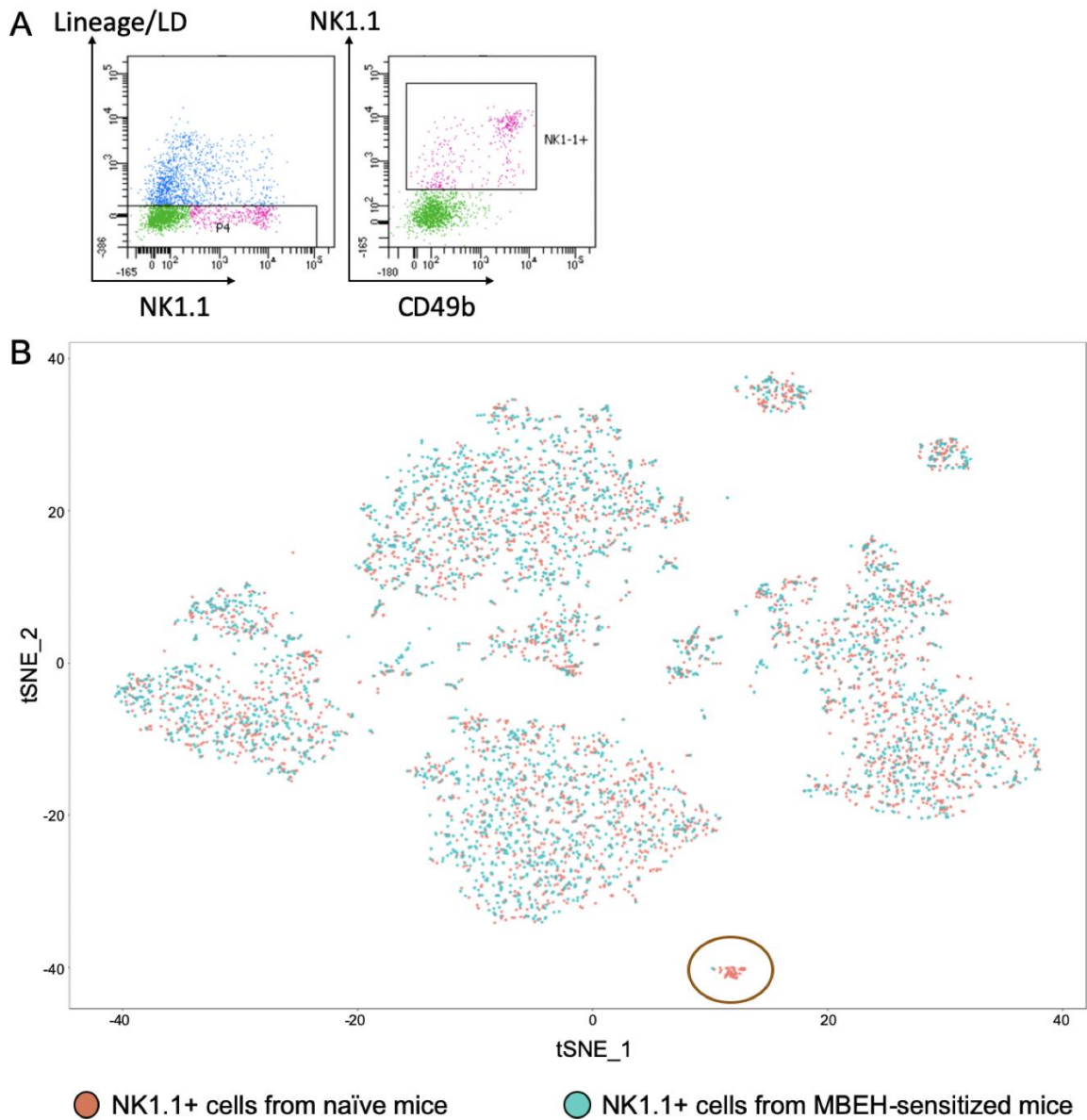


**Figure 26: RNA single cell sequencing of hepatic NK1.1+ cells shows transcriptional parity of cells from naïve and MBEH-sensitized mice.** Isolation and analysis of cells from naïve (d0) and MBEH-sensitized mice (d7) via cell sort of viable single hepatic cells that lacked the lineage markers CD3, CD19, and Ter119 (gate P4) and expressed NK1.1 (A). The analysis with a resolution of 0.6 is depicted, containing a total of 5819 analyzed cells (B). The brown circle indicates NKT cells which disappear from the liver upon MBEH sensitization.

RNA single cell analysis revealed the transcriptional identity of NK1.1+ lineage negative liver lymphocytes of naïve (d0) and MBEH-sensitized mice (d7) but also showed that one cellular subset, which we identified to be NKT cells, disappeared from the liver following sensitization (brown circle, Figure 26B).

As depicted by Figure 27, we could distinguish ten cellular clusters in the liver (0 - 9), with cluster two (blue circle) comprising the NK1.1+,CD49b- NK cell population and cluster one (orange circle) containing the NK1.1+,CD49b+ cNK cells.

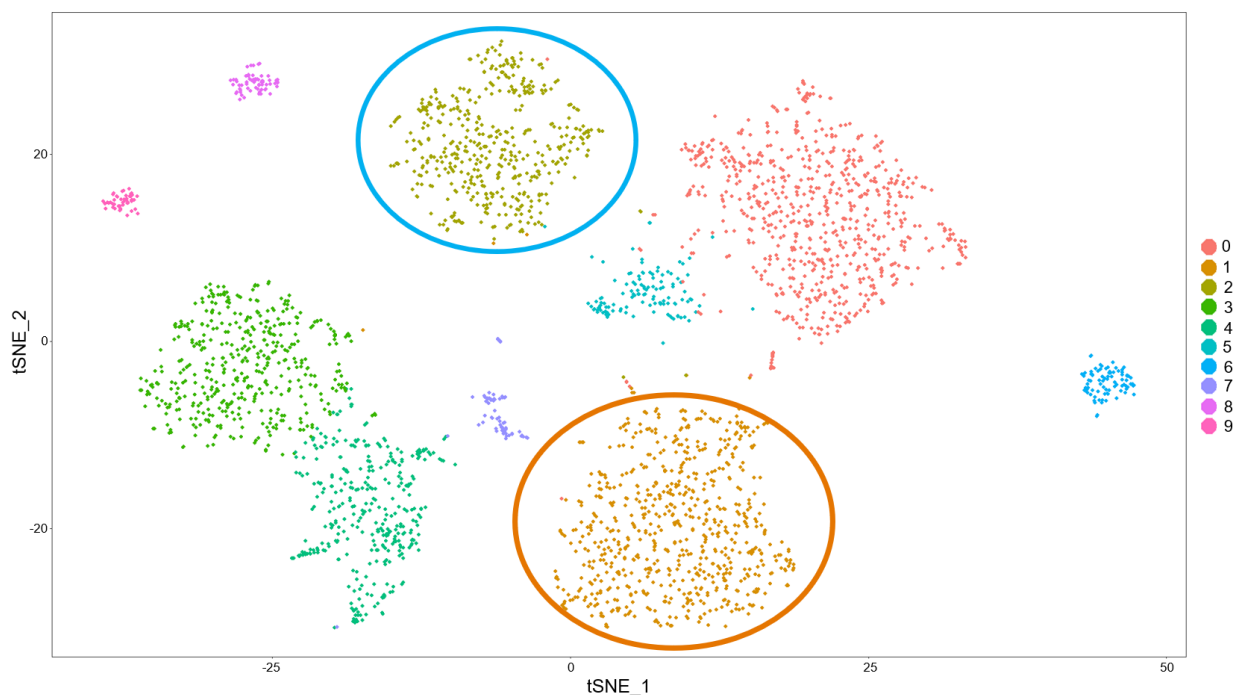


**Figure 27: Single cell RNA sequencing shows ten different hepatic NK1.1+ cell clusters of lineage negative cells.** Prior to sequencing, cells were sorted with respect to missing lineage markers (CD3, CD19, and Ter119) and NK1.1 expression. The analysis (resolution of 0.65 - 1.05) is depicted and shows ten different cellular clusters. While cluster 2 (blue circle) comprises the NK1.1+,CD49b- NK cells, cluster 1 (orange circle) represents the population of NK1.1+,CD49b+ cNK cells.

RNA single cell sequencing illustrated that the adoptively transferred naïve and MBEH-treated cNK cells were transcriptionally identical and that these cells' gain of function can not be explained by transcriptome analysis. Moreover, RNA single cell sequencing showed that MBEH treatment did not induce the formation of novel lineage negative NK1.1+ cell clusters in the liver.

### 3.8 Sensitization with MBEH *in vivo* induces transient transcriptional changes in hepatic cNK cells

For a better understanding of the intracellular processes that may be triggered in hepatic MBEH-exposed cNK cells, their transcriptome was analyzed at early timepoints during *in vivo* sensitization by 3'-RNA bulk sequencing. To confirm the single RNA sequencing result (Figure 26), three samples were sequenced for timepoints d0 and d7. In addition, two biological samples for timepoints d1, d2, d3, and d4 were sequenced to determine if at any point of time transcriptional changes were induced in hepatic cNK cells (Figure 28).

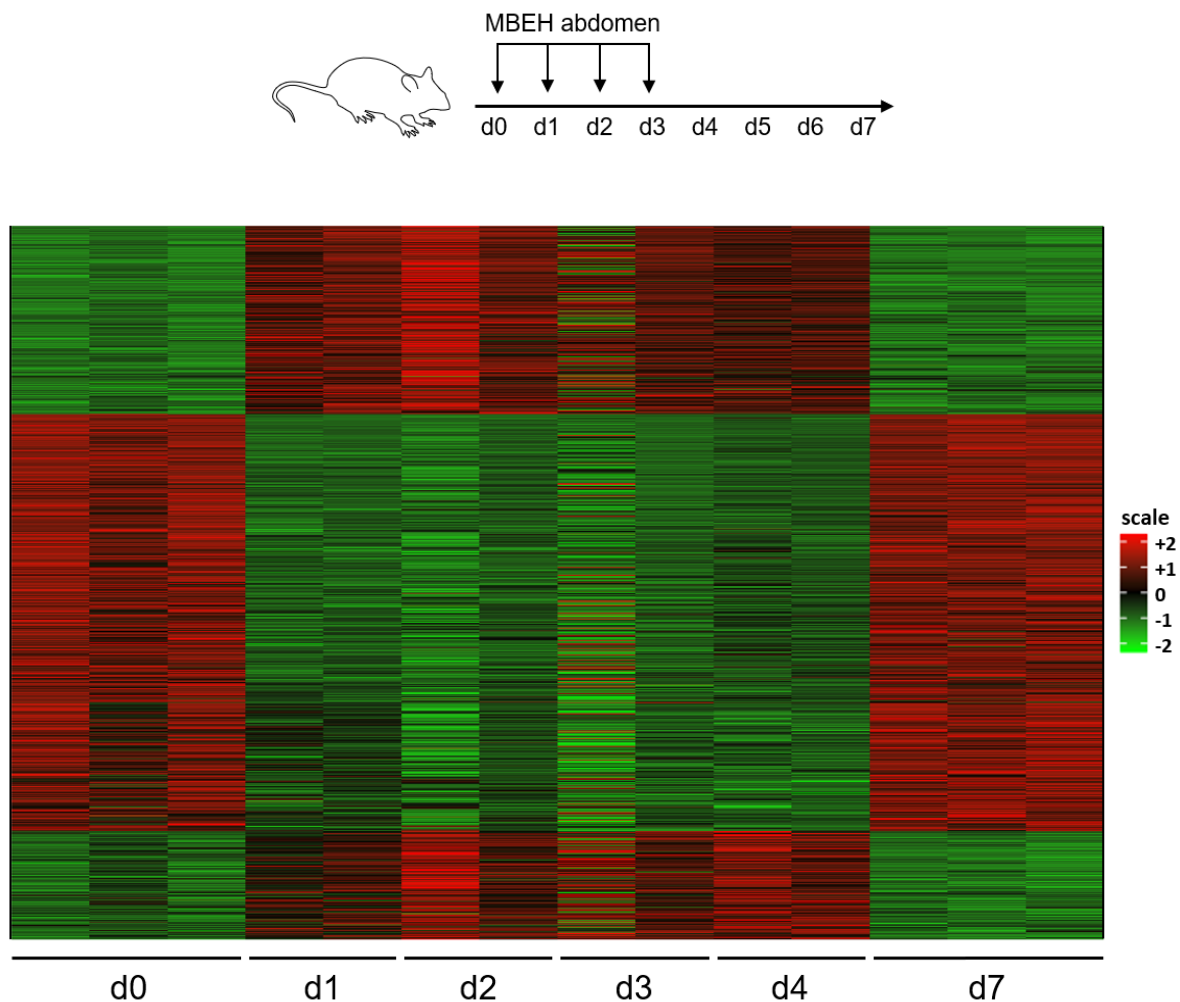


**Figure 28: 3'-RNA bulk sequencing of hepatic cNK cells reveals transient transcriptional changes upon sensitization with MBEH.**  $4 \times 10^4$  cells were sorted as lineage negative (CD3<sup>-</sup>, CD19<sup>-</sup>, Ter119<sup>-</sup>) cells, which expressed NK1.1 and CD49b. Whereas the single RNA sequencing comparing d0 and d7 was confirmed, analysis of timepoints d1 - d4 indicated significant transient transcriptional variations.

By 3'-RNA bulk sequencing we found multiple concise transcriptional changes between naïve cNK cells and cNK cells of mice that were being sensitized, with the transcriptional changes being most striking between d0 and d1, 24 hours after the first MBEH contact. Between d1 and d2 the overall quantity of transcriptional alterations remained similar but started to decrease on d3 and was even lower on d4. The most explicitly induced (Figure 29), repressed (Figure 30), and further genes of interest in the context of MBEH-induced cNK cells are shown and described based on the annotations and gene ontology available at the Mouse Genome Database (MGD) (Bult et al., 2019), UniProt (The UniProt Consortium, 2019), and the GeneCards® database (Stelzer et al., 2016).

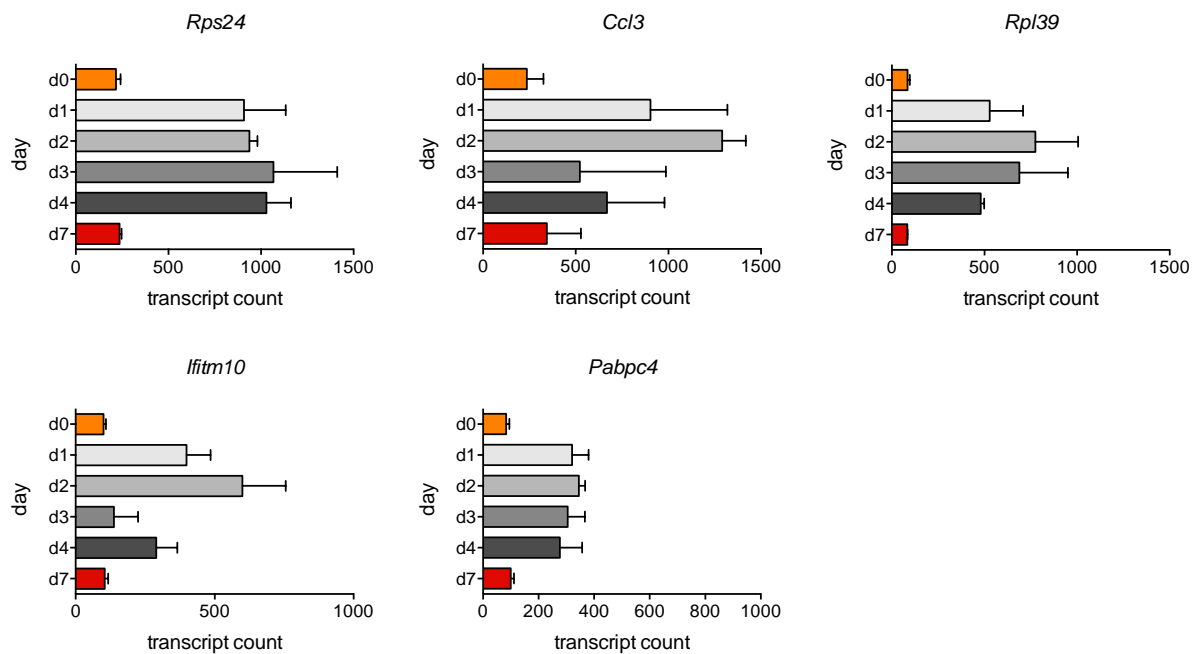


**Figure 29: The most significantly induced genes in cNK cells upon MBEH sensitization comparing d0 and d1.** Within 24 h upon first MBEH application to the abdomen, strong transcriptional changes of hepatic cNK cells were recorded. In total, these alterations were the strongest comparing d0 with d1 and declined subsequently. The most significantly induced genes of NK1.1+,CD49b+ NK cells are depicted as the mean  $\pm$  SEM of the respective transcript count per day.

Following MBEH application, *Rps24*, *Ccl3*, *Rpl39*, *Ifitm10* and *Pabpc4* (Figure 29) were the most significantly induced genes in cNK cells after 24 h (d1). *Rpl39* encodes the ribosomal protein L39, which is a constituent of the 60S ribosome that is located in the cytoplasm and according to gene ontology important in protein metabolic processes and

immune cell stimulation. Likewise, the ribosomal protein S24 encoded by *Rps24* is required for maturation of 40S ribosomes and is critical for mRNA translation. Further, the gene encoding an antiviral protein which prevents virus entry, induces cell cycle arrest, and mediates apoptosis (*Ifitm10*; interferon-induced transmembrane protein 10) was induced. The encoded protein is described to respond to IFN stimulation and to negatively regulate cell migration and proliferation, whereas the gene *Pabpc4* encodes the polyadenylate-binding protein 4 that is involved in the regulation of mRNA metabolism and mRNA stability. Additionally, transcription of *Ccl3* was highly induced. The CCL3 protein is involved in inflammatory responses through receptor binding of e.g. CCR5 and is reported to be secreted by activated NK cells with a higher cytotoxic capacity that secrete IFN- $\gamma$  during the antiviral NK response that aims to contain HIV infection (Roda et al., 2006). Especially due to the observed accumulation of CCL3 in the ear during elicitation on d9 (Figure 15) this transcriptional increase may link the elevated CCL3 amount in the ear during MBEH-induced CHS directly to the cNK cells involved in this immune response. In summary, these transcriptional changes show that hepatic cNK cells were severely stressed by *in vivo* sensitization with MBEH and aimed to adjust RNA metabolism, cell cycle regulation and cell signaling.

Moreover, a comprehensive reflection on the cNK cell fate upon sensitization required consideration not only of the strongly induced but also the most suppressed genes. These comprised *Dct*, *Tyrp1*, *Pmel*, *Rps27rt*, and *C1qa* (Figure 30). Here it was striking that particularly genes encoding proteins critical for melanin biosynthesis and regulation, namely *Dct* (dopachrome tautomerase) and *Tyrp1* (tyrosinase related protein 1) were completely suppressed. In addition, transcription of a lowly expressed gene encoding a melanocyte-specific transmembrane glycoprotein (*Pmel*) that is present in melanosomes and critical for their biogenesis, was repressed from d1 – d4. Further, transcription of the gene *Rps27rt* that encodes the ribosomal protein 27 involved in mRNA activation, viral mRNA translation, and rRNA processing was disabled, as was the gene from which a major constituent of the serum complement system subcomponent C1q results (*C1qa*).

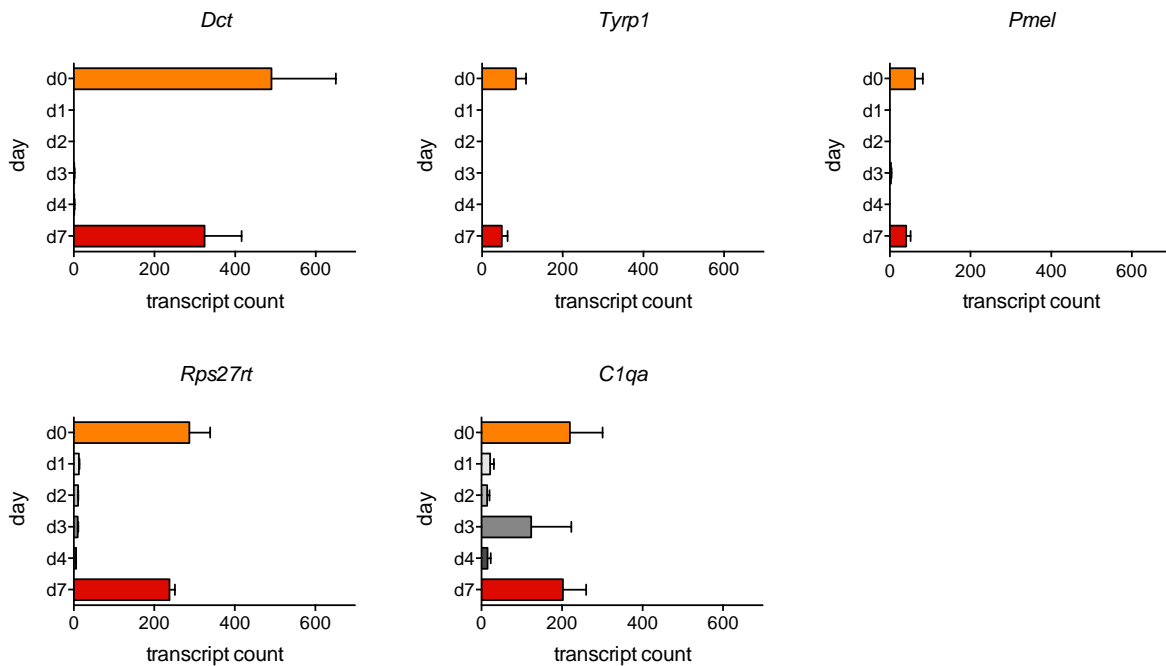


**Figure 30: The most significantly suppressed genes in cNK cells upon MBEH sensitization on d1.** 24 h after first MBEH application to the abdomen strong transcriptional changes of hepatic cNK cells were recorded. These changes are most significant between d0 and d1 and decline afterwards. The mean  $\pm$  SEM of the transcript count/day of cNK cells upon MBEH sensitization is depicted.

In addition to the cNK cell genes that showed the strongest induction or complete repression 24 h after MBEH treatment of mice, we investigated whether the expression of further genes relevant for NK cell function, development, and survival was transiently altered, too. With respect to the modified NK cytotoxicity upon sensitization revealed by co-culture of NK and melanoma cells (Figure 23) that coincided with a higher IFN- $\gamma$  secretion (Figure 24), the transcript quantities of the IFN- $\gamma$  and granzyme B encoding genes were both found to be increased on d1 and d2 in hepatic cNK cells (Figure 31A). Regarding the transcriptional regulators of NK cell development, the genes encoding *Id2* and *B2m* were analyzed (Figure 31B). *Id2* expression is crucial for NK and general ILC development and is described to regulate cellular growth, senescence, apoptosis, and differentiation. This gene was transcriptionally induced between d1 and d3, maybe due to the requirement to stabilize the NK cell fate upon MBEH-induced cellular stress. Similar to *Id2* transcription, *B2m* transcripts were elevated upon MBEH treatment (Figure 31B). These encode a component of MHC-I (*B2m*) which is involved in the presentation of

peptide antigens to the immune system and was induced in HUVEC, cells used for bystander cell assays, that were treated with medium conditioned by K562/HLA-E-activated adaptive NKG2C+ NK cells. Hence, transcription of this gene was indicated to be involved in antigen presentation when adaptive NK cells integrate inflammatory signals during target-cell encounter (Hammer et al., 2017).

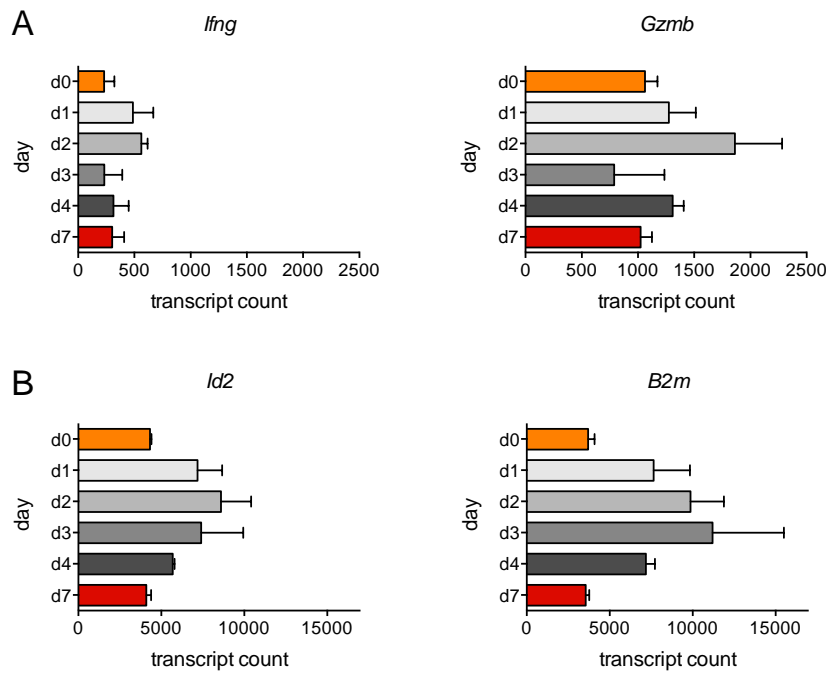


**Figure 31: Transiently fueled genes in hepatic cNK cells upon MBEH sensitization.** These gene transcript changes were not included in the statistically most significant transcriptomic alterations between d0 and d1 but their amount was changed and revealed further information about the processes triggered by MBEH in the cNK cell. For each day analyzed the gene transcript counts are depicted as mean  $\pm$  SEM.

Analysis of further genes that might be critically involved in MBEH-induced CHS revealed transiently elevated transcript quantities of *Rpp21*, *Gpx3*, *Ndr1*, *Hspa1a*, *Hspa1b* (Figure 32A), *Itgax*, *Nup210*, *Btg2*, and *Zap70* (Figure 32B) during sensitization. Four of these clearly differentially regulated genes are implicated in cellular stress responses (*Gpx3*, *Btg2*, *Ndr1*, *Rpp21*), with the BTG2 protein also being anti-proliferative and a negative regulator of cell cycle transition. Further, two induced genes encoded Hsp70 heat shock proteins (*Hspa1a*, *Hspa1b*) that function as molecular chaperones, are involved in stress protection of the proteome, polypeptide folding and transport, and proteolysis of misfolded proteins. In addition, transcription of the surface molecule CD11c (*Itgax*),

important for cellular adhesion, and *Zap70* that encodes an important protein for adaptive immune response regulation including adhesion, motility, and cytokine expression, were elevated on d1 and d2. Intriguingly, the group of transcriptionally induced genes also comprised the nucleoporin protein encoded by gene *Nup210*, which is a component of the nuclear pore complex that regulates the flow of macromolecules between the nucleus and cytoplasm and is essential for nuclear pore assembly, fusion, and structural integrity.

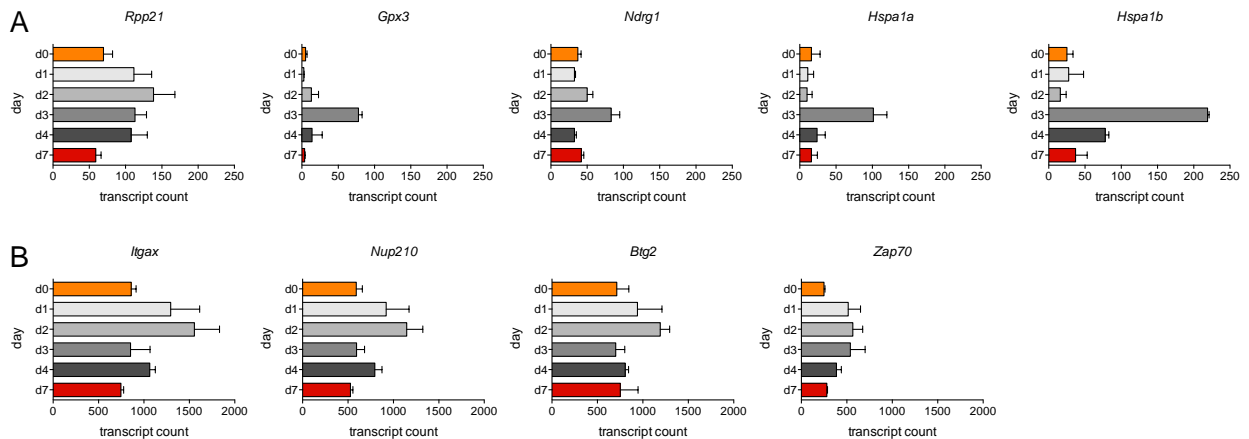


**Figure 32: Transiently transcriptionally up-regulated genes in hepatic cNK cells during MBEH sensitization.** These gene transcript changes are not included in the statistically most significantly altered genes between d0 and d1 but their amount was distinctly altered and the transcript count per day depicted as mean  $\pm$  SEM.

In summary, the transient transcriptional alterations following MBEH sensitization on d1 indicate that NK cells respond with a cellular stress response tailored to prevent apoptosis induction and cell cycle impairment and adapt the expression of genes encoding NK cell signaling proteins. However, these observations fuel the question how the long-term cNK cell specificity towards MBEH is conserved.

### 3.9 MBEH sensitization of mice establishes epigenetic changes in hepatic cNK cells

The transcriptional analysis illustrates how much MBEH sensitization challenges hepatic cNK cells but does not explain the functional differences observed following adoptive cell transfer and *ex vivo* analysis of cNK cells isolated from sensitized mice. However, one possibility would be that MBEH sensitization induces epigenetic changes that are



maintained by hepatic cNK cells. In order to test this hypothesis, hepatic cNK cells were purified by FACS-based cell sort from either naïve (d0) or sensitized (d7) mice and chromatin accessibilities were compared, revealing several significant differences between the cNK cell samples from d0 and d7 (Figure 33).

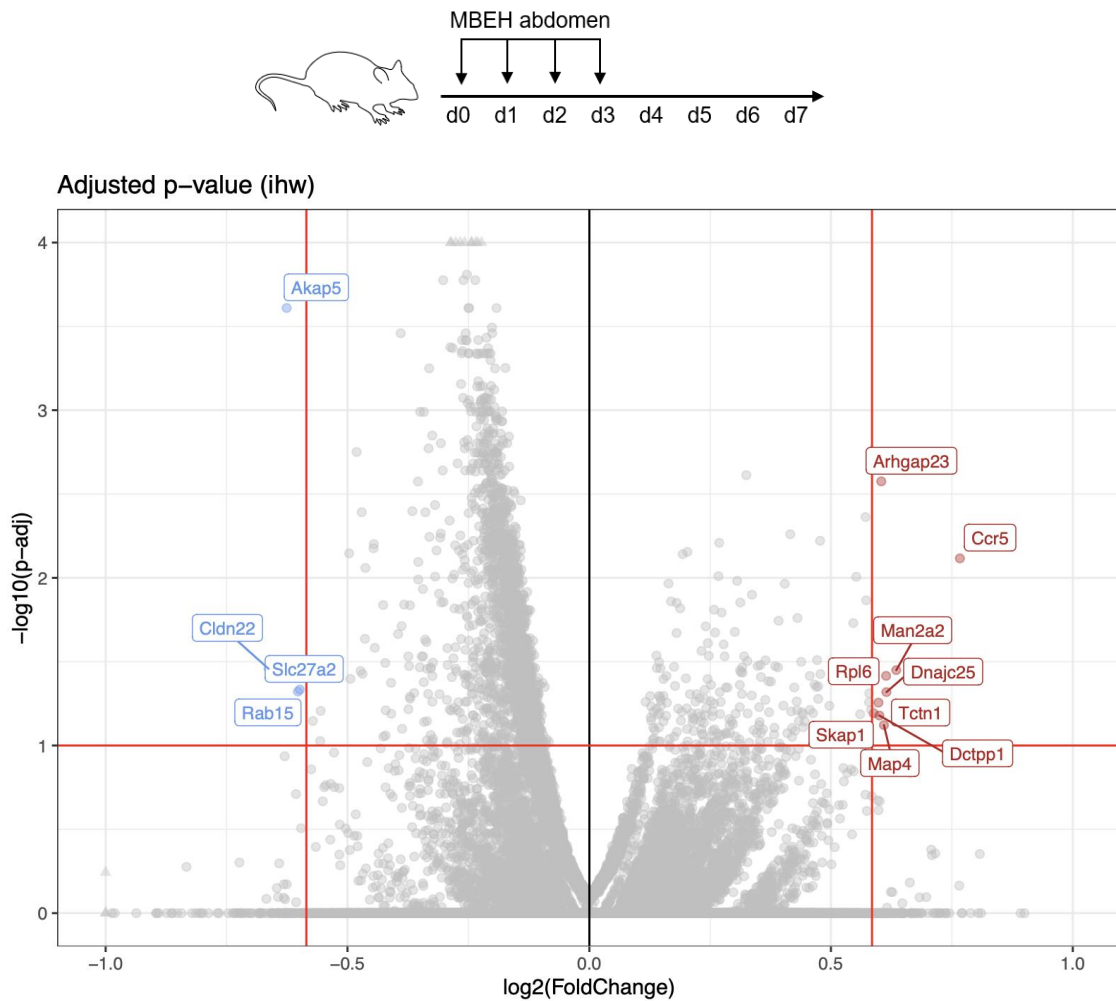


**Figure 33: Epigenetic changes distinguish hepatic cNK cells of naïve (d0) and MBEH-sensitized mice (d7).** Cell sorting of viable, lineage negative (CD3<sup>-</sup>, CD19<sup>-</sup>, Ter119<sup>-</sup>, TCR $\beta$ <sup>-</sup>) hepatic NK1.1<sup>+</sup>, CD49b<sup>+</sup> NK cells followed by ATAC sequencing revealed epigenetic differences between cells from untreated and MBEH-treated mice. For both timepoints four biological samples, each comprising  $1 \times 10^4$  -  $2 \times 10^4$  cNK cells, were included in the analysis.


When compared to cNKs from naïve mice (d0), MBEH-sensitized mice (d7) revealed chromatin modifications of which nine resulted in increased and four in decreased chromatin accessibilities. The genes revealing an increased chromatin accessibility

comprised *Arhgap23*, *Ccr5*, *Man2a2*, *Rpl6*, *Dnajc25*, *Skap1*, *Dctpp1*, *Map4*, and *Tctn1* while genes *Rab15*, *Cldn22*, *Akap5* and *Slc27a2* were found to obtain a reduced chromatin accessibility (Figure 33). Impacted genes are briefly described based on annotations and gene ontology by the Mouse Genome Database (MGD) (Bult et al., 2019), UniProt (The UniProt Consortium, 2019), and the GeneCards® database (Stelzer et al., 2016).

Intriguingly, *Ccr5* was among the genes with an increased chromatin accessibility after MBEH sensitization. This fits to the ear homogenate analysis during elicitation (Figure 15) and the transient transcriptional increase of *Ccl3* in hepatic cNK cells (Figure 29) because CCL3 binds as ligand to CCR5 that is involved in the control of granulocyte differentiation and lineage proliferation. In line with differentially expressed heat shock protein (Hsp)-encoding genes upon sensitization, the region encoding *Dnajc25* that results in a heat shock protein family (Hsp40) member influencing protein folding became more accessible by MBEH sensitization. Further, *Skap1* represents a T cell adaptor protein relevant for inside-out signaling, coupling T cell antigen receptor stimulation to integrin activation, allowing the optimal conjugation between T cells and APCs, whereas *Tctn1* encodes a component of the tectonic-like complex that is a regulator of the hedgehog signaling pathway.

In summary, four gene loci (*Rab15*, *Cldn22*, *Akap5*, *Slc27a2*) were recorded to be repressed by decreased chromatin accessibility after MBEH sensitization. *Rab15* is annotated as a GTP binding protein with GTPase activity that may regulate aspects of synaptic vesicle membrane flow, intracellular protein transport and protein secretion, whereas *Cldn22* encodes a claudin, which are integral membrane proteins and components of tight junction strands that serve as a physical barrier and prevent water and solutes from freely passing across the epithelium, contributing to the maintenance of signal transduction and cellular adhesion. Otherwise, *Akap5* encodes an A-kinase anchor protein which contains a group of proteins that bind to the regulatory subunit of protein kinase A (PKA) and plays a role in long-term synaptic potentiation through regulation of protein trafficking. Moreover, *Slc27a2* encodes the acyl-CoA synthetase that activates fatty acids with a (very) long chain, exhibits transport activity for these fatty acids and is described for its role in hepatic fatty acid uptake.

To characterize the cNK cell fate upon *in vivo* sensitization with MBEH in more detail, we used the generated ATAC sequencing data for a hallmark analysis (Figure 34). This analysis revealed TNF- $\alpha$  signaling via NF $\kappa$ B as most prevalent pathway in naïve mice (d0), followed by MTORC1 signaling and the p53 pathway. Reverse, hallmark analysis showed the IFN- $\gamma$  response to be the most significantly induced pathway on d7, followed by PI3K/AKT/MTOR signaling and the IFN- $\alpha$  response.



Count	Open in naïve cNK cells (d0)	Open in MBEH-primed cNK cells (d7)
	TNF- $\alpha$ signaling via NF $\kappa$ B	IFN- $\gamma$ response
	MTORC1 signaling	Mitotic spindle
	MYC targets V1	Allograft rejection
	G2M checkpoint	KRAS signaling
	E2F targets	MTOR signaling
	Hypoxia	IFN- $\alpha$ response
	p53 pathway	G2M checkpoint
	UV response	Oxidative phosphorylation
	IL2 STAT5 signaling	Adipogenesis
	Heme metabolism	Complement

**Figure 34: Hallmark analysis of accessible chromatin regions in naïve and MBEH-exposed cNK cells.** Cell sorting of live and CD3<sup>-</sup>, CD19<sup>-</sup>, Ter119<sup>-</sup>, TCR $\beta$ <sup>-</sup>, NK1.1<sup>+</sup>, CD49b<sup>+</sup> NK cells and ATAC sequencing allowed a hallmark analysis of these cNK cells. Both conditions comprise four biological samples of  $1 \times 10^4$  -  $2 \times 10^4$  cNK cells.

Conclusively, hallmark analysis of cNK cells with the IFN- $\gamma$  response as most significantly enhanced pathway after MBEH sensitization and gene ontology analysis revealing negative regulation of immune system processes, ribosome biogenesis, cell-substrate adhesion, rRNA processing, and cell killing as preferential cellular actions, suited the transient transcriptional modulations found after MBEH application to the skin of mice and the co-culture data of cNK with B16.F10 melanoma cells, where melanoma outgrowth was controlled more efficiently and more IFN- $\gamma$  and granzyme B were secreted by the MBEH-educated NK cells. As final assessment, experiments throughout this study, comprising the sensitization/elicitation of mice and analysis of transcription and chromatin accessibility of cNK cells accentuated the importance of CCL3-CCR5 signaling for MBEH-induced CHS in mice.

## 4. Discussion

Innate lymphocytes without RAG recombinase are classified as ILCs, which include NKs, ILC1s, ILC2s, ILC3s, and lymphoid tissue-inducer (LTi) cells. ILCs and NK cells can provide early defense against pathogens, tumor evolution and progression (Cella et al., 2009; Fuchs et al., 2013; Klose et al., 2014; Trinchieri, 1989; Vivier et al., 2018) and possess, despite their origin and classification as innate lymphocytes, the ability to develop adaptive features (Cooper et al., 2009; O'Leary et al., 2006; Paust et al., 2010; Peng et al., 2013; Sun et al., 2009; Wang et al., 2018; Wang et al., 2019).

To date, liver-resident CD49a<sup>+</sup>,CXCR6<sup>+</sup> NK cells and circulating CD49b<sup>+</sup>,Ly49C/I<sup>+</sup> cNK cells were shown to develop hapten-specific responses, implying the co-evolution of two distinct mechanisms for hapten-specific NK cells. It has been reported that only CD49a<sup>+</sup>,CXCR6<sup>+</sup> NK cells adoptively transferred memory upon Oxa-induced challenge (Peng et al., 2013; Zhang et al., 2016), whereas my study here shows that MBEH-induced CHS primarily involves cNK cells (NK1.1<sup>+</sup>,CD49b<sup>+</sup>). Other than murine CD49a<sup>+</sup> NKs, cNK cells express high amounts of the transcription factor *Eomes* that is described to facilitate the development of memory cells like CD8<sup>+</sup> T cells (Intlekofer et al., 2005), to provide the potential for homeostatic proliferation (Banerjee et al., 2010), support the maintenance of the mature NK phenotype and foster NK effector functions by supporting Ly49 receptor expression (Gordon et al., 2012). In line with these findings reported for *Eomes* expressing cells, a clinical study with human liver transplants revealed that liver-resident *Eomes*<sup>high</sup> donor NK cells possessed a long-term renewal capacity and were found to reside in recipient livers for up to 13 years (Cuff et al., 2016).

Immune cell population analysis of the liver, ILN, and ear upon elicitation revealed significantly altered immune cell quantities with an influx of lymphocytes and cNK cells in the ILN and at the target site (ear). In the ear tissue especially CD103<sup>+</sup> immune cells accumulated, probably because this integrin directed them to their ligand E-cadherin present on epithelial cells (Cepek et al., 1994; Karecla et al., 1995). This molecule is described as a hallmark of tumor-infiltrating T<sub>regs</sub> (Anz et al., 2011) and the presence of CD103<sup>+</sup> tissue-resident memory T cells coincided with the protection from viral infection (Park et al., 2018). Overall, the dominant and sustained response of CD8<sup>+</sup>,CD103<sup>+</sup> T cells in the ILN and ear during elicitation suites previous reports in which

MBEH-induced depigmentation was driven by antigen-specific CD8<sup>+</sup> T cells (van den Boorn et al., 2009). In addition, the explicit accumulation of a specific DC fraction (CD103<sup>+</sup> DCs), which is specialized in the cross-presentation of KC-derived self-antigens to cytotoxic T cells (Henri et al., 2010), was distinct and an analogy to other CHS responses.

To better characterize the local and systemic implications of MBEH treatment, the cytokine and chemokine levels were measured in the ear homogenate throughout elicitation. Immediate increases of IL-1 $\beta$  and TNF- $\alpha$ , CCL2, CCL17, GM-CSF, IP-10, IL-18, and to a lesser extent type I IFNs, with CCL2, CCL17, CCL3, GM-CSF, and IL-18 accumulating over both days (d8/d9) following antigen contact, were found. These data confirm KC activation and cytokine as well as chemokine secretion following hapten contact (Mori et al., 2008) and IL-18 and type I IFN secretion, which are potent activators of NK cell effector function (Walzer et al., 2005). Further, upon elicitation with MBEH the CCL17 concentration was elevated in the ear homogenate. This observation suites reports on increased CCL17 induction in inflamed human and murine skin (Kusumoto et al., 2007; Riis et al., 2011) and on the critical role for CCL17 in DNFB-induced CHS (Alferink et al., 2003), with CCL17-deficient mice developing weaker CHS (Fülle et al., 2018; Stutte et al., 2010). Given that chemokine receptor expression (e.g. CCR5) plays an important role during NK cell development and homeostasis in mice and humans (Grégoire et al., 2007), the measurement of its ligand CCL3 in the ear homogenate may be connected to the NK cell response itself. This hypothesis is supported by the transient transcriptional induction of *CCL3* in cNK cells upon MBEH treatment and the increased chromatin accessibility of the gene encoding the receptor CCR5 following complete MBEH sensitization.

Through adoptive transfer experiments we could show that only hepatic NK1.1<sup>+</sup>,CD49b<sup>+</sup> NK cells from MBEH-sensitized donors provided naïve recipient mice with the competence of a recall response upon elicitation. Additionally, adoptive transfer of hepatic cNK cells after *in vitro* incubation with MBEH mimicked adoptive transfer of cNKs from sensitized mice. This result implies that a MBEH-induced cNK cell response may to some extent function independent of helper cells and cellular mediators through recognition or an immediate effect of this molecule on cNK cells. However, MBEH could have also entered

the NK cells during incubation *in vitro* and either been secreted in the recipient mice or could have attached to NK cell surface receptors, leading to multiple recognition options in the recipient mice. In addition, the secretion of extracellular vesicles (EVs) by NK cells could play a role in this context because these can reflect NK cell stimulatory functions. Whether EV secretion by cNK cells accounts for the results of adoptively transferred cells in this study has not been tested, but their importance for immunomodulatory functions was illustrated when an NK cell EV ELISA was established to detect NK cell status changes in cancer patients, measuring plasma NK cell-derived EVs (Federici et al., 2020).

Aiming to test target specificity and reactivity of NK cells from MBEH-sensitized mice, hepatic NK1.1<sup>+</sup>,CD49b<sup>-</sup> and NK1.1<sup>+</sup>,CD49b<sup>+</sup> cells were co-cultured with B16.F10 melanoma cells and the melanoma cell survival and IFN- $\gamma$  and granzyme B secretion were measured. Although both hepatic NK cell populations slightly increased their ability to control B16.F10 melanoma cell growth and survival *in vitro* upon *in vivo* MBEH sensitization, solely the cNK cells exhibited a higher IFN- $\gamma$  and granzyme B secretion when previously sensitized *in vivo*. With respect to the transient transcriptional induction of the *Ifng* and *Gzmb* genes upon sensitization on d1 and d2 and advanced chromatin accessibility facilitating IFNG signaling upon sensitization on d7, we conclude that transcriptional induction of *Ifng* by MBEH is followed by chromatin modulation where it remains conserved and could explain a quicker and stronger cNK cell response upon re-challenge. Nevertheless, the measured variations of NK-induced melanoma cell killing are small and may indicate that the ideal target of MBEH-sensitized NKs remains to be determined or that NK cells may require a re-exposition to MBEH *in vitro* to respond explicitly. In the light of the results obtained it should be considered that MBEH treatment may facilitate NK cell signaling but not their cytotoxic function.

Based on the capability of *in vivo* and *in vitro* MBEH-exposed cNK cells to adoptively transfer MBEH-responsiveness to naïve mice, it was unexpected when RNA single cell and bulk sequencing revealed transcriptional identity of cNK cells in naïve (d0) and sensitized mice (d7). Nonetheless, RNA bulk sequencing showed multiple concise transcriptional changes that mostly occurred 24 h after first MBEH sensitization and revealed the induction of genes encoding ribosomal proteins that respond in the course of immune cell stimulation, antimicrobial and antibacterial responses (*Rpl39*), are critical

for mRNA translation (*Rps24*), antiviral host defense (*Ifitm10*), the regulation of mRNA metabolism and mRNA stability (*Pabpc4*) and the signaling molecule CCL3. The most suppressed genes comprised particularly genes encoding proteins critical for melanin biosynthesis and regulation (*Dct*, *Tyrp1*, *Pmel*), a ribosomal protein involved in mRNA activation, viral mRNA translation, and rRNA processing (*Rps27rt*) and a major constituent of the serum complement system subcomponent C1q (*C1qa*).

Analysis of further genes critical for NK effector function illustrated that the genes coding for IFN- $\gamma$  and granzyme B were transcriptionally induced and intriguingly, as upon MBEH sensitization, transcriptionally induced in NK cells post MCMV infection (Bezman et al., 2012). Also, the transcript count of the gene encoding B2M was elevated, which is involved in antigen presentation and exhibits an increased expression when adaptive NK cells integrate inflammatory signals during target-cell encounter (Hammer et al., 2017). In addition, elevated transcript quantities were recorded for genes encoding proteins that are implicated in responses towards cellular stress (*Gpx3*, *Btg2*, *Ndrp1*, *Rpp21*, *Nup210*), cell damage protection (*Hspa1a*, *Hspa1b*), cellular adhesion (*CD11c*), lymphocyte activation and regulation of adhesion, motility, and cytokine expression (*Zap70*), with differential *Zap70* regulation reported for activated NK and T cells that showed components of the ITAM (immunoreceptor tyrosine-based activation motif) signaling pathway to be enriched (Bezman et al., 2012). Of note, only two biological samples were sequenced for the early timepoints of MBEH sensitization (d1, d2, d3, d4), which circumvented a pathway analysis, but due to the implication of multiple differentially transcribed genes in translational processes (e.g. *Rps24*) and RNA stability (e.g. *Pabpc4*), in the future proteomics should be included in the characterization of MBEH-educated NK cells because protein expression and stability changes may critically shape the NK cell reactivity in MBEH-induced CHS.

Beside changes of the transcriptome, programmed lineage differentiation can be modulated by epigenetic modifications which can provide novel markers to track cell fate decisions (Bird, 2002; Calvanese et al., 2012). Here, methylation studies were already conducted with e.g. differentiating T lymphocytes (Kitagawa et al., 2013; Komori et al., 2015), erythroid cells (Yu et al., 2013) and myeloid cells (Karpurapu et al., 2014). In this context, the demethylation within the *FOXP3* gene that characterizes CD4<sup>+</sup> T<sub>regs</sub>

has been revealed as crucial epigenetic immune cell lineage marker (Wieczorek et al., 2009). With respect to NK cell biology, high demethylation in activated NK cells and low demethylation in naïve NKs provided evidence that the human NK methylome is modifiable in order to adapt to immune response requirements (Wiencke et al., 2016). For example, in human NK cells isolated from the blood of cancer patients and healthy individuals, demethylation of a region of the activating receptor gene locus *NCR1/NKp46* was found to be lower in the cancer patients (Accomando et al., 2012).

In general, NK cells were found to undergo strong epigenetic transformations upon activation, including an elevated expression of genes encoding IFN- $\gamma$  and *CCL3* (Li et al., 2017b), which we demonstrate to be critical mediators of MBEH-primed cNK cells. We could show that the IFN- $\gamma$  signaling was clearly enhanced through MBEH-induced chromatin modulation, which blends into reported NK cell degranulation and cytokine production alterations depending on the chromatin state (Li et al., 2017b). In consequence of the recognition of the MCMV-encoded glycoprotein m157 by murine Ly49H<sup>+</sup> NK cells, followed by their clonal expansion, contraction and long-lived memory NK cell formation, these had been examined epigenetically. In comparison to CD8<sup>+</sup> T cells, ATAC- and RNA sequencing of Ly49H<sup>+</sup> NK cells during MCMV infection revealed distinct epigenetic signatures of NK- and CD8<sup>+</sup> T cells (Lau et al., 2018). Upon MCMV infection, memory NK cells upregulated *Ifng* and *Dusp10* and increased the chromatin accessibility of *Gzmb*, *CCL9*, and *Prf1* and pathway analysis showed the NK cell-mediated cytotoxicity pathway and by majority pathways comprising cytokine- or antigen-receptor signaling to be the most enriched pathways (Lau et al., 2018). This finding correlates to the elevated NK cell-mediated cytotoxicity of MBEH-sensitized cells towards B16.F10 melanoma cells, the transiently induced cNK cell transcription of *Ifng* and *Gzmb* upon MBEH treatment, and the ATAC sequencing result of cNK cells from MBEH-sensitized mice. As this study shows, chromatin modulations of hepatic cNK cells in MBEH-sensitized mice resulted in more accessible regions promoting the IFN- $\gamma$  response (hallmark analysis) and cell killing (gene ontology).

However, recent studies revealed the critical role of NK metabolism for the function and survival of conventional and adaptive NK cells (O'Brien and Finlay, 2019). This prompted us to do some analysis in this direction because our ATAC sequencing data also indicated



that MBEH sensitization decreased the chromatin accessibility of *Slc27a2* in cNK cells. This acyl-CoA synthetase is described to be relevant for hepatic fatty acid uptake. Due to the limited amount of experiments with which we investigated NK metabolism upon MBEH exposure, these are not included in this thesis but they implicated that the quantity of mitochondria of cNK cells was reduced upon MBEH exposure *in vitro* and *in vivo* and cNK cells showed variations in their fatty acid uptake. These experiments could be worth to follow up on.

In the light of the evolving evidence for an important role of ILCs in health and disease, the development of adaptive features by ILCs during CHS and their impact on the outcome of hapten-induced immunity raise attention (Wang et al., 2018; Wang et al., 2020). Following Oxa treatment, IL-7R $\alpha$ + ILC1s were recruited to skin-draining LNs, did not express Ly49C/I but exited draining LNs via S1PR1 and resided in the liver through CXCR6-CXCL16 interaction (Wang et al., 2018), sharing some features with murine hepatic CD49a+ NK cells. In humans, CD56<sup>bright</sup> NK cells were observed to accumulate in skin lesions of ACD patients, produced high levels of IFN- $\gamma$  and TNF, expressed the receptor CCR5 (Carbone et al., 2010), that was also differentially regulated on transcription level in murine cNK cells during MBEH-induced CHS, and like murine Oxa-induced liver-resident ILC1s, expressed CXCR3 (Carbone et al., 2010; Wang et al., 2018). Moreover, depletion of all ILC subsets during elicitation of mice following hapten sensitization with TNCB increased the ear swelling response and especially ILC2-deficient mice showed strongly elevated ear thickness development upon challenge, suggesting ILC2s as negative regulators in this type 1-driven CHS response that influence the counterbalance between type I and type II immune responses in allergic skin diseases (Rafei-Shamsabadi et al., 2018; Rafei-Shamsabadi et al., 2019).

As aforementioned, the engagement of memory-like NK cells in CHS (O'Leary et al., 2006; Peng et al., 2013), upon cytokine stimulation (Cooper et al., 2009; Romee et al., 2016), and MCMV infection (Arase et al., 2002; Smith et al., 2002) is well-established and also applies for respiratory influenza virus infection in mice, which induced CD49a+ memory-like liver NK cells (Li et al., 2017a). Nevertheless, increasing evidence assigns immature NK cells a critical role in health protection. For example, a xenograft animal model with ovarian cancer tumor grafts showed that CD56<sup>bright</sup> or CD56<sup>superbright</sup> cell populations had

a more potent antitumor function than the mature CD56<sup>dim</sup> cells. Also, intratumoral CD56<sup>bright</sup> NK cells in bladder cancer revealed a higher cytotoxicity, cytokine production and increased survival more efficiently than NK cells of the mature phenotype (Mukherjee et al., 2018). Similarly, less mature NK cells were found to be involved in protection from leukemia relapse (Björklund et al., 2016).

Shifting the focus on the therapeutic use of NK cells, multiple advancements were achieved lately. For instance, human NK cells were shown to express the receptor RIG-I and specifically increased the expression of TRAIL upon RIG-I stimulation, which accentuates the potential of RIG-I activation in NK cells to improve melanoma immunotherapy (Daßler-Plenker et al., 2019). Further, using outbred pigs, hapten-specific CHS memory was proven to exist in a non-rodent model. In this study, DNFB and Oxa were used for initial sensitization, followed by challenges that revealed induced ear swellings to be significant for up to 32 days post sensitization (Putz et al., 2019).

In addition, the role of liver-resident NK cells has been investigated lately with respect to their impact on T cell immunity in the context of viral infection with lymphocytic choriomeningitis virus (LCMV) and adenoviruses. Here, the amount of virus-specific T cells increased in mice deficient of liver-resident NK cells during LCMV infection and upon adenovirus infection and transfer of liver-resident NK cells into mice that lacked these cells or wildtype mice inhibited hepatic T cell function and impaired viral clearance. In these experiments, liver-resident NK cells controlled the antiviral activity of hepatic T cells via the PD-1-PD-L1 axis, whereas transfer of cNK cells promoted the antiviral T cell response (Zhou et al., 2019). However, multiple studies investigate the relevance of the PD-1/PD-L1 interaction of NK and cancer cells and could show that blockade of this interplay could induce a powerful NK cell response (Hsu et al., 2018) and that expanded NK cells developed an improved antitumor efficacy when combined with an anti-PD-L1 antibody in an ovarian cancer model (Oyer et al., 2018). Anyhow, the impact of the PD-1/PD-L1 interaction of MBEH-induced cNK cells with melanoma cells has not been tested and could, with respect to *in vitro* studies that revealed the PD-L1 antibody avelumab to augment ADCC by NK cells that target breast cancer cells (Juliá et al., 2018), be considered in the future.

With a focus on virus-specific memory NK cells it was recently demonstrated that upon isolation from livers of humanized mice vaccinated with HIV-encoded envelope protein, human NK cells displayed antigen-specific and vaccination-dependent recall responses *in vitro* (Nikzad et al., 2019). Further, in varicella-zoster virus (VZV)-experienced human volunteers, a large number of cytotoxic NK cells with a tissue-resident phenotype were recruited to sites of challenge performed with a test antigen. These NK cell-mediated recall responses in humans were elicited decades after initial VZV challenge and demonstrate long-lived NK memory in humans (Nikzad et al., 2019), fueling the aspiration to use the potential of NK cells in the clinic to contain or prevent from viral infections and improve diseases like ACD and cancer.

## 5. Abstract

Contact hypersensitivity (CHS) mimics atopic dermatitis in a mouse model where haptens are applied to the skin. Several haptens are reported to induce CHS, but as indicated by the comparison of DNFB, Oxa and MBEH, not all of them activate, involve, and require the same immune cell subpopulations. Whereas hepatic tissue-resident CD49a+ NK cells are required for Oxa-induced CHS (Peng et al., 2013; Zhang et al., 2016), MBEH was reported to depend on hepatic CD49b+ innate cells (van den Boorn et al., 2016).

This study identifies the hepatic innate immune cells found to develop adaptive features upon *in vivo* MBEH sensitization as neither ILC1, nor CD49a+ NK cells, but mature conventional NK cells (cNKs). Upon adoptive transfer and elicitation, mice receiving hepatic cNK cells from sensitized mice responded similar to mice that had been sensitized to MBEH. These mice mounted a stable recall response, whereas transfer of hepatic CD49a+ NK cells from sensitized mice could not provide naïve mice with a recall response upon elicitation. Thus, these transfer experiments clarify that only the hepatic cNK cells develop a gain of function by *in vivo* sensitization with MBEH. Similarly, *in vitro* exposure to MBEH of cNK cells, followed by adoptive transfer into naïve recipient mice, was sufficient to cause ear swelling upon MBEH elicitation.

The comparison of immune cell recruitment in the liver, ILN, and ear, and measurement of the cytokine/chemokine levels in the elicited ear and serum during MBEH-induced CHS are consistent with previous reports on CHS and highlighted the importance of TNF- $\alpha$ , CCL17, IL-1 $\beta$ , GM-CSF, IP-10, IL-18, and type I IFN locally at the elicitation target site (ear).

By RNA single cell sequencing we identified that all clusters of hepatic NK1.1+ cells share the same transcriptome before (d0) and after (d7) MBEH sensitization. However, during and one day after sensitization with MBEH (d1, d2, d3, d4), hepatic cNK cells exhibited substantial changes in numerous levels of transcripts known to be associated with NK cell activation and effector function, virus-induced processes and ROS, while genes associated with melanin biosynthesis were strongly repressed.

Epigenetic analysis of *in vivo* sensitized hepatic cNK cells showed chromatin modifications, including genes involved in the IFN- $\gamma$  response and cell killing. These epigenetic changes suggest that MBEH application to the skin induces long-term

modifications of hepatic cNK cells that seem to drive potent recall responses towards this specific hapten.

In the future, proteomics will help to characterize MBEH-educated NK cells because many genes that revealed a transient differential transcriptional regulation during MBEH sensitization were found to be critical for translational processes and RNA stability.

## 6. List of figures

Figure 1: Overview of NK cell effector mechanisms.....	14
Figure 2: Schematized ILC development. ....	16
Figure 3: Chemical principle of MBEH attachment to the tyrosinase enzyme. ....	29
Figure 4: Hypothesized cell signaling upon MBEH application to the skin of mice.....	31
Figure 5: NK population size before, during, and after MBEH sensitization. ....	48
Figure 6: FACS gating scheme for NK cell analysis.....	49
Figure 7: Features of hepatic lineage (CD3, TCR $\beta$ , CD19, Ter119) negative mature NK subsets (NK1.1+,CD49b-; NK1.1+,CD49b+).....	50
Figure 8: 3'-RNA bulk sequencing of the mature hepatic NK cell subsets. ....	51
Figure 9: Ear swelling response upon elicitation of MBEH-sensitized mice. ....	52
Figure 10: Variations of lymphocyte and NK cell quantity in the liver, ILN, and ear of MBEH-sensitized mice during elicitation. ....	54
Figure 11: Gating strategy for DCs and neutrophils. ....	55
Figure 12: Liver lymphocyte response during elicitation.....	56
Figure 13: Variation of lymphocyte quantity in the ILN upon elicitation of MBEH- sensitized mice. ....	57
Figure 14: Alterations of lymphocyte quantity in the ear during elicitation.....	58
Figure 15: Cytokine and chemokine quantity in the ear homogenate during elicitation.....	59
Figure 16: Cytokine and chemokine quantities in the serum during elicitation. ....	60
Figure 17: Ear thickness measurement upon transfer of hepatic NK1.1+,CD49b- and NK1.1+,CD49b+ NK cells from MBEH-sensitized donors into naïve recipient mice.....	61
Figure 18: CHS-induced ear swelling upon elicitation following transfer of NK1.1+,CD49b+ NK cells from naïve and MBEH-sensitized mice.....	63
Figure 19: Post-sort purity check of the cNK cell subset. ....	64
Figure 20: Impact of hepatic NK1.1+,CD49b+ cell transfer on the lymphocyte and cNK cell count in the liver, ILN, and ear. ....	65
Figure 21: Ear swelling upon transfer of <i>in vitro</i> ctrl-treated and MBEH-exposed cNK cells.....	67

Figure 22: IFN- $\gamma$ and granzyme B secretion by cNK cells upon re-stimulation <i>ex vivo</i> .....	69
Figure 23: B16.F10 melanoma cell survival upon co-culture with naïve and MBEH- primed NK cells.....	70
Figure 24: IFN- $\gamma$ secretion by hepatic NK cells upon B16.F10 melanoma cell co-culture. ....	71
Figure 25: Granzyme B secretion by hepatic NK cells during B16.F10 melanoma cell co-culture.....	71
Figure 26: RNA single cell sequencing of hepatic NK1.1+ cells shows transcriptional parity of cells from naïve and MBEH-sensitized mice.....	73
Figure 27: Single cell RNA sequencing shows ten different hepatic NK1.1+ cell clusters of lineage negative cells. ....	74
Figure 28: 3'-RNA bulk sequencing of hepatic cNK cells reveals transient transcriptional changes upon sensitization with MBEH.....	75
Figure 29: The most significantly induced genes in cNK cells upon MBEH sensitization comparing d0 and d1.....	76
Figure 30: The most significantly suppressed genes in cNK cells upon MBEH sensitization on d1. ....	78
Figure 31: Transiently fueled genes in hepatic cNK cells upon MBEH sensitization.....	79
Figure 32: Transiently transcriptionally up-regulated genes in hepatic cNK cells during MBEH sensitization.....	80
Figure 33: Epigenetic changes distinguish hepatic cNK cells of naïve (d0) and MBEH-sensitized mice (d7).....	81
Figure 34: Hallmark analysis of accessible chromatin regions in naïve and MBEH-exposed cNK cells.....	83

## 7. List of tables

Table 1: Antibodies for immune cell FACS analysis .....	33
Table 2: Chemicals, reagents, and enzymes.....	34
Table 3: Kits.....	36
Table 4: Buffers .....	36
Table 5: Equipment .....	37
Table 6: Software for data analysis and illustration and databases .....	47



## 8. References

- Abdul-Careem MF, Lee AJ, Pek EA, Gill N, Gillgrass AE, Chew MV, Reid S, Ashkar AA. 2012. Genital HSV-2 infection induces short-term NK cell memory. *PLoS One* 7:e32821
- Accomando WP, Wiencke JK, Houseman EA, Butler R, Zheng S, Nelson HH, Kelsey KT. 2012. Decreased NK cells in patients with head and neck cancer determined in archival DNA. *Clin Cancer Res* 18:6147–6154
- Adams S, O'Neill DW, Nonaka D, Hardin E, Chiriboga L, Siu K, Cruz CM, Angiulli A, Angiulli F, Ritter E, Holman RM, Shapiro RL, Berman RS, Berner N, Shao Y, Manches O, Pan L, Venhaus RR, Hoffman EW, Jungbluth A, Gnjjatic S, Old L, Pavlick AC, Bhardwaj N. 2008. Immunization of malignant melanoma patients with full-length NY-ESO-1 protein using TLR7 agonist imiquimod as vaccine adjuvant. *J Immunol* 181:776–784
- Alferink J, Lieberam I, Reindl W, Behrens A, Weiß S, Hüser N, Gerauer K, Ross R, Reske-Kunz AB, Ahmad-Nejad P, Wagner H, Förster I. 2003. Compartmentalized production of CCL17 in vivo: strong inducibility in peripheral dendritic cells contrasts selective absence from the spleen. *J Exp Med* 197:585–599
- Aliahmad P, de la Torre B, Kaye J. 2010. Shared dependence on the DNA-binding factor TOX for the development of lymphoid tissue-inducer cell and NK cell lineages. *Nat Immunol* 11:945–952
- Anderson DC, Springer TA. 1987. Leukocyte adhesion deficiency: an inherited defect in the Mac-1, LFA-1, and p150,95 glycoproteins. *Annu Rev Med* 38:175–194
- Anfossi N, André P, Guia S, Falk CS, Roetynck S, Stewart CA, Bresó V, Frassati C, Reviron D, Middleton D, Romagné F, Ugolini S, Vivier E. 2006. Human NK cell education by inhibitory receptors for MHC class I. *Immunity* 25:331–342
- Anz D, Mueller W, Golic M, Kunz WG, Rapp M, Koelzer VH, Ellermeier J, Ellwart JW, Schnurr M, Bourquin C, Endres S. 2011. CD103 is a hallmark of tumor-infiltrating regulatory T cells. *Int J Cancer* 129:2417–2426
- Arase H, Mocarski ES, Campbell AE, Hill AB, Lanier LL. 2002. Direct recognition of cytomegalovirus by activating and inhibitory NK cell receptors. *Science* 296:1323–1326

- Artis D, Spits H. 2015. The biology of innate lymphoid cells. *Nature* 517:293–301
- Banerjee A, Gordon SM, Intlekofer AM, Paley MA, Mooney EC, Lindsten T, Wherry EJ, Reiner SL. 2010. The transcription factor eomesodermin enables CD8<sup>+</sup> T cells to compete for the memory cell niche. *J Immunol* 185:4988–4992
- Banz A, Peixoto A, Pontoux C, Cordier C, Rocha B, Papiernik M. 2003. A unique subpopulation of CD4<sup>+</sup> regulatory T cells controls wasting disease, IL-10 secretion and T cell homeostasis. *Eur J Immunol* 33:2419–2428
- Bauer S, Groh V, Wu J, Steinle A, Philips JH, Lanier LL, Spies T. 1999. Activation of NK cells and T cells by NKG2D, a receptor for stress-inducible MICA. *Science* 285:727–729
- Becker Jr. SW, Spencer MC. 1962. Evaluation of monobenzene. *JAMA* 180:279–284
- Beima KM, Miazgowicz MM, Lewis MD, Yan PS, Huang TH-M, Weinmann AS. 2006. T-bet binding to newly identified target gene promoters is cell type-independent but results in variable context-dependent functional effects. *J Biol Chem* 281:11992–12000
- Bernink JH, Peters CP, Munneke M, te Velde AA, Meijer SL, Weijer K, Hreggvidsdottir HS, Heinsbroek SE, Legrand N, Buskens CJ, Bemelman WA, Mjösberg JM, Spits H. 2013. Human type 1 innate lymphoid cells accumulate in inflamed mucosal tissues. *Nat Immunol* 14:221–229
- Bezman NA, Kim CC, Sun JC, Min-Oo G, Hendricks DW, Kamimura Y, Best JA, Goldrath AW, Lanier LL, Immunological Genome Project Consortium. 2012. Molecular definition of the identity and activation of natural killer cells. *Nat Immunol* 13:1000–1009
- Biedermann T, Kneilling M, Mailhammer R, Maier K, Sander CA, Kollias G, Kunkel SL, Hültner L, Röcken M. 2000. Mast cells control neutrophil recruitment during T cell-mediated delayed-type hypersensitivity reactions through tumor necrosis factor and macrophage inflammatory protein 2. *J Exp Med* 192:1441–1452
- Bird A. 2002. DNA methylation patterns and epigenetic memory. *Genes Dev* 16:6–21

- Björklund AT, Clancy T, Goodridge JP, Beziat V, Schaffer M, Hovig E, Ljunggren HG, Ljungman PT, Malmberg KJ. 2016. Naive Donor NK Cell Repertoires Associated with Less Leukemia Relapse after Allogeneic Hematopoietic Stem Cell Transplantation. *J Immunol* 196:1400–1411
- de Boer RJ, Hogeweg P. 1987. Immunological discrimination between self and non-self by precursor depletion and memory accumulation. *J Theor Biol* 124:343–369
- Bogoslowski A, Kubes P. 2018. Lymph nodes: the unrecognized barrier against pathogens. *ACS Infect Dis* 4:1158–1161
- Boissy RE, Manga P. 2004. On the etiology of contact/occupational vitiligo. *Pigment Cell Res* 17:208–214
- Bonneville M, Chavagnac C, Vocanson M, Rozieres A, Benetiere J, Pernet I, Denis A, Nicolas J-F, Hennino A. 2007. Skin contact irritation conditions the development and severity of allergic contact dermatitis. *J Invest Dermatol* 127:1430–1435
- van den Boorn JG, Konijnenberg D, DelleMijn TAM, van der Veen JP, Bos JD, Melief CJM, Vyth-Dreese FA, Luiten RM. 2009. Autoimmune destruction of skin melanocytes by perilesional T cells from vitiligo patients. *J Invest Dermatol* 129:2220–2232
- van den Boorn JG, Jakobs C, Hagen C, Renn M, Luiten RM, Melief CJM, Tüting T, Garbi N, Hartmann G, Hornung V. 2016. Inflammasome-dependent induction of adaptive NK cell memory. *Immunity* 44:1406–1421
- van den Boorn JG, Konijnenberg D, Tjin EPM, Picavet DI, Meeuwenoord NJ, Filippov DV, van der Veen JP, Bos JD, Melief CJM, Luiten RM. 2010. Effective melanoma immunotherapy in mice by the skin-depigmenting agent monobenzone and the adjuvants imiquimod and CpG. *PLoS One* 5:e10626
- van den Boorn JG, Picavet DI, van Swieten PF, van Veen HA, Konijnenberg D, van Veelen PA, van Capel T, de Jong EC, Reits EA, Drijfhout JW, Bos JD, Melief CJM, Luiten RM. 2011. Skin-depigmenting agent monobenzone induces potent T-cell autoimmunity toward pigmented cells by tyrosinase haptentation and melanosome autophagy. *J Invest Dermatol* 131:1240–1251

- Bouchery T, Kyle R, Camberis M, Shepherd A, Filbey K, Smith A, Harvie M, Painter G, Johnston K, Ferguson P, Jain R, Roediger B, Delahunt B, Weninger W, Forbes-Blom E, Le Gros G. 2015. ILC2s and T cells cooperate to ensure maintenance of M2 macrophages for lung immunity against hookworms. *Nat Commun* 6:6970
- Bour H, Peyron E, Gaucherand M, Garrigue JL, Desvignes C, Kaiserlian D, Revillard JP, Nicolas JF. 1995. Major histocompatibility complex class I-restricted CD8+ T cells and class II-restricted CD4+ T cells, respectively, mediate and regulate contact sensitivity to dinitrofluorobenzene. *Eur J Immunol* 25:3006–3010
- Buchmann K. 2014. Evolution of innate immunity: clues from invertebrates via fish to mammals. *Front Immunol* 5:459
- Buenrostro JD, Giresi PG, Zaba LC, Chang HY, Greenleaf WJ. 2013. Transposition of native chromatin for fast and sensitive epigenomic profiling of open chromatin, DNA-binding proteins and nucleosome position. *Nat Methods* 10:1213–1218
- Buentke E, Heffler LC, Wilson JL, Wallin RPA, Löfman C, Chambers BJ, Ljunggren H-G, Scheynius A. 2002. Natural killer and dendritic cell contact in lesional atopic dermatitis skin--Malassezia-influenced cell interaction. *J Invest Dermatol* 119:850–857
- Bult CJ, Blake JA, Smith CL, Kadin JA, Richardson JE, the Mouse Genome Database Group. 2019. Mouse Genome Database (MGD) 2019. *Nucleic Acids Res* 47:D801–D806
- Bursch LS, Wang L, Igyarto B, Kissenpfennig A, Malissen B, Kaplan DH, Hogquist KA. 2007. Identification of a novel population of Langerin+ dendritic cells. *J Exp Med* 204:3147–3156
- Calvanese V, Fernández AF, Urdinguio RG, Suárez-Alvarez B, Mangas C, Pérez-García V, Bueno C, Montes R, Ramos-Mejía V, Martínez-Cambor P, Ferrero C, Assenov Y, Bock C, Menendez P, Carrera AC, Lopez-Larrea C, Fraga MF. 2012. A promoter DNA demethylation landscape of human hematopoietic differentiation. *Nucleic Acids Res* 40:116–131

- Campos RA, Szczepanik M, Lisbonne M, Itakura A, Leite-de-Moraes M, Askenase PW. 2006. Invariant NKT cells rapidly activated via immunization with diverse contact antigens collaborate in vitro with B-1 cells to initiate contact sensitivity. *J Immunol* 177:3686–3694
- Campos RA, Szczepanik M, Itakura A, Lisbonne M, Dey N, Leite-de-Moraes MC, Askenase PW. 2006. Interleukin-4-dependent innate collaboration between iNKT cells and B-1 B cells controls adaptative contact sensitivity. *Immunology* 117:536–547
- Carbone T, Nasorri F, Pennino D, Eyerich K, Foerster S, Cifaldi L, Traidl-Hoffmann C, Behrendt H, Cavani A. 2010. CD56<sup>high</sup>CD16<sup>-</sup>CD62L<sup>-</sup> NK cells accumulate in allergic contact dermatitis and contribute to the expression of allergic responses. *J Immunol* 184:1102–1110
- Carlyle JR, Michie AM, Furlonger C, Nakano T, Lenardo MJ, Paige CJ, Zuniga-Pflucker JC. 1997. Identification of a novel developmental stage marking lineage commitment of progenitor thymocytes. *J Exp Med* 186:173–182
- Catona A, Lanzer D. 1987. Monobenzene, Superfade, vitiligo and confetti-like depigmentation. *Med J Aust* 146:320–321
- Cella M, Fuchs A, Vermi W, Facchetti F, Otero K, Lennerz JKM, Doherty JM, Mills JC, Colonna M. 2009. A human natural killer cell subset provides an innate source of IL-22 for mucosal immunity. *Nature* 457:722–725
- Cepek KL, Shaw SK, Parker CM, Russell GJ, Morrow JS, Rimm DL, Brenner MB. 1994. Adhesion between epithelial cells and T lymphocytes mediated by E-cadherin and the alpha E beta 7 integrin. *Nature* 372:190–193
- Chan A, Hong D-L, Atzberger A, Kollnberger S, Filer AD, Buckley CD, McMichael A, Enver T, Bowness P. 2007. CD56<sup>bright</sup> human NK cells differentiate into CD56<sup>dim</sup> cells: role of contact with peripheral fibroblasts. *J Immunol* 179:89–94
- Chiossone L, Chaix J, Fuseri N, Roth C, Vivier E, Walzer T. 2009. Maturation of mouse NK cells is a 4-stage developmental program. *Blood* 113:5488–5496
- Christensen AD, Haase C. 2012. Immunological mechanisms of contact hypersensitivity in mice. *APMIS* 120:1–27

- Colucci F, Samson SI, DeKoter RP, Lantz O, Singh H, Di Santo JP. 2001. Differential requirement for the transcription factor PU.1 in the generation of natural killer cells versus B and T cells. *Blood* 97:2625–2632
- Constantinides MG, McDonald BD, Verhoef PA, Bendelac A. 2014. A committed hemopoietic precursor to innate lymphoid cells. *Nature* 508:397–401
- Cooksey C, Jimbow K, Land EJ, Riley PA. 1992. Reactivity of orthoquinones involved in tyrosinase-dependent cytotoxicity: differences between alkylthio- and alkoxy-substituents. *Melanoma Res* 2:283–293
- Cooper MA, Elliott JM, Keyel PA, Yang L, Carrero JA, Yokoyama WM. 2009. Cytokine-induced memory-like natural killer cells. *Proc Natl Acad Sci U S A* 106:1915–1919
- Cooper MA, Fehniger TA, Turner SC, Chen KS, Ghaheri BA, Ghayur T, Carson WE, Caligiuri MA. 2001. Human natural killer cells: a unique innate immunoregulatory role for the CD56 (bright) subset. *Blood* 97:3146–3151
- Crotta S, Gkioka A, Male V, Duarte JH, Davidson S, Nisoli I, Brady HJM, Wack A. 2014. The transcription factor E4BP4 is not required for extramedullary pathways of NK cell development. *J Immunol* 192:2677–2688
- Cuff AO, Robertson FP, Stegmann KA, Pallett LJ, Maini MK, Davidson BR, Male V. 2016. Eomeshi NK cells in human liver are long-lived and do not recirculate but can be replenished from the circulation. *J Immunol* 197:4283–4291
- Cuff AO, Sillito F, Dertschnig S, Hall A, Luong TV, Chakraverty R, Male V. 2019. The obese liver environment mediates conversion of NK cells to a less cytotoxic ILC1-like phenotype. *Front Immunol* 10:2180
- Cumberbatch M, Kimber I. 1995. Tumour necrosis factor-alpha is required for accumulation of dendritic cells in draining lymph nodes and for optimal contact sensitization. *Immunology* 84:31–35
- Daßler-Plenker J, Paschen A, Putschli B, Rattay S, Schmitz S, Goldeck M, Bartok E, Hartmann G, Coch C. 2019. Direct RIG-I activation in human NK cells induces TRAIL-dependent cytotoxicity toward autologous melanoma cells. *Int J Cancer* 144:1645–1656

- Daussy C, Faure F, Mayol K, Viel S, Gasteiger G, Charrier E, Bienvenu J, Henry T, Debien E, Hasan UA, Marvel J, Yoh K, Takahashi S, Prinz I, de Bernard S, Buffat L, Walzer T. 2014. T-bet and Eomes instruct the development of two distinct natural killer cell lineages in the liver and in the bone marrow. *J Exp Med* 211:563–577
- Davis AH, Guseva NV, Ball BL, Heusel JW. 2008. Characterization of murine cytomegalovirus m157 from infected cells and identification of critical residues mediating recognition by the NK cell receptor, Ly49H. *J Immunol* 181:265–275
- Dearman RJ, Basketter DA, Kimber I. 1996. Characterization of chemical allergens as a function of divergent cytokine secretion profiles induced in mice. *Toxicol Appl Pharmacol* 138:308–316
- DeFranco AL. 1987. Molecular aspects of B-lymphocyte activation. *Annu Rev Cell Biol* 3:143–178
- Dilulio NA, Engeman T, Armstrong D, Tannenbaum C, Hamilton TA, Fairchild RL. 1999. G $\alpha$ -mediated recruitment of neutrophils is required for elicitation of contact hypersensitivity. *Eur J Immunol* 29:3485–3495
- Divkovic M, Pease CK, Gerberick GF, Basketter DA. 2005. Hapten-protein binding: from theory to practical application in the in vitro prediction of skin sensitization. *Contact Dermatitis* 53:189–200
- Dokun AO, Kim S, Smith HR, Kang HS, Chu DT, Yokoyama WM. 2001. Specific and nonspecific NK cell activation during virus infection. *Nat Immunol* 2:951–956
- Dudeck A, Dudeck J, Scholten J, Petzold A, Surianarayanan S, Köhler A, Peschke K, Vöhringer D, Waskow C, Krieg T, Müller W, Waisman A, Hartmann K, Gunzer M, Roers A. 2011. Mast cells are key promoters of contact allergy that mediate the adjuvant effects of haptens. *Immunity* 34:973–984
- Elices MJ, Osborn L, Takada Y, Crouse C, Luhowskyj S, Hemler ME, Lobb RR. 1990. VCAM-1 on activated endothelium interacts with the leukocyte integrin VLA-4 at a site distinct from the VLA-4/fibronectin binding site. *Cell* 60:577–584
- Engeman T, Gorbachev AV, Kish DD, Fairchild RL. 2004. The intensity of neutrophil infiltration controls the number of antigen-primed CD8 T cells recruited into cutaneous antigen challenge sites. *J Leukoc Biol* 76:941–949

- Ewens S, Wulferink M, Goebel C, Gleichmann E. 1999. T cell-dependent immune reactions to reactive benzene metabolites in mice. *Arch Toxicol* 73:159–167
- Fauriat C, Long EO, Ljunggren H-G, Bryceson YT. 2010. Regulation of human NK-cell cytokine and chemokine production by target cell recognition. *Blood* 115:2167–2176
- Federici C, Shahaj E, Cecchetti S, Camerini S, Casella M, Iessi E, Camisaschi C, Paolino G, Calvieri S, Ferro S, Cova A, Squarcina P, Bertuccini L, Iosi F, Huber V, Lugini L. 2020. Natural-killer-derived extracellular vesicles: immune sensors and interactors. *Front Immunol* 11:262
- Fernandez NC, Treiner E, Vance RE, Jamieson AM, Lemieux S, Raulet DH. 2005. A subset of natural killer cells achieves self-tolerance without expressing inhibitory receptors specific for self-MHC molecules. *Blood* 105:4416–4423
- Fink PJ, Hendricks DW. 2011. Post-thymic maturation: young T cells assert their individuality. *Nat Rev Immunol* 11:544–549
- Flier J, Boorsma DM, van Beek PJ, Nieboer C, Stoof TJ, Willemze R, Tensen CP. 2001. Differential expression of CXCR3 targeting chemokines CXCL10, CXCL9, and CXCL11 in different types of skin inflammation. *J Pathol* 194:398–405
- Foley B, Cooley S, Verneris MR, Curtsinger J, Luo X, Waller EK, Anasetti C, Weisdorf D, Miller JS. 2012. Human cytomegalovirus (CMV)-induced memory-like NKG2C(+) NK cells are transplantable and expand in vivo in response to recipient CMV antigen. *J Immunol* 189:5082–5088
- Foley B, Cooley S, Verneris MR, Pitt M, Curtsinger J, Luo X, Lopez-Vergès S, Lanier LL, Weisdorf D, Miller JS. 2012. Cytomegalovirus reactivation after allogeneic transplantation promotes a lasting increase in educated NKG2C+ natural killer cells with potent function. *Blood* 119:2665–2674
- Forman, L. 1953. A note on the depigmentary properties of monobenzylether of hydroquinone. *Br J Dermatol* 65:406–409
- Fuchs A, Vermi W, Lee JS, Lonardi S, Gilfillan S, Newberry RD, Cella M, Colonna M. 2013. Intraepithelial type I innate lymphoid cells are a unique subset of IL-12- and IL-15-responsive IFN-gamma-producing cells. *Immunity* 38:769–781



- Fukunaga A, Khaskhely NM, Sreevidya CS, Byrne SN, Ullrich SE. 2008. Dermal dendritic cells, and not Langerhans cells, play an essential role in inducing an immune response. *J Immunol* 180:3057–3064
- Fülle L, Steiner N, Funke M, Gondorf F, Pfeiffer F, Siegl J, Opitz FV, Haßel SK, Erazo AB, Schanz O, Stunden HJ, Blank M, Gröber C, Händler K, Beyer M, Weighardt H, Latz E, Schultze JL, Mayer G, Förster I. 2018. RNA aptamers recognizing murine CCL17 inhibit T cell chemotaxis and reduce contact hypersensitivity in vivo. *Mol Ther* 26:95–104
- Gao Y, Souza-Fonseca-Guimaraes F, Bald T, Ng SS, Young A, Ngiow SF, Rautela J, Straube J, Waddell N, Blake SJ, Yan J, Bartholin L, Lee JS, Vivier E, Takeda K, Messaoudene M, Zitvogel L, Teng MWL, Belz GT, Engwerda CR, Huntington ND, Nakamura K, Hölzel M, Smyth MJ. 2017. Tumor immunoevasion by the conversion of effector NK cells into type 1 innate lymphoid cells. *Nat Immunol* 18:1004–1015
- Gascoyne DM, Long E, Veiga-Fernandes H, de Boer J, Williams O, Seddon B, Coles M, Kioussis D, Brady HJM. 2009. The basic leucine zipper transcription factor E4BP4 is essential for natural killer cell development. *Nat Immunol* 10:1118–1124
- Geiger TL, Sun JC. 2016. Development and maturation of natural killer cells. *Curr Opin Immunol* 39:82–89
- Gillard GO, Bivas-Benita M, Hovav A-H, Grandpre LE, Panas MW, Seaman MS, Haynes BF, Letvin NL. 2011. Thy1+ NK cells from vaccinia virus-primed mice confer protection against vaccinia virus challenge in the absence of adaptive lymphocytes. *PLoS Pathog* 7:e1002141
- Glässner A, Eisenhardt M, Krämer B, Körner C, Coenen M, Sauerbruch T, Spengler U, Nattermann J. 2012. NK cells from HCV-infected patients effectively induce apoptosis of activated primary human hepatic stellate cells in a TRAIL-, FasL- and NKG2D-dependent manner. *Lab Invest* 92:967–977
- Gocinski BL, Tigelaar RE. 1990. Roles of CD4+ and CD8+ T cells in murine contact sensitivity revealed by in vivo monoclonal antibody depletion. *J Immunol* 144:4121–4128

- Gogas H, Ioannovich J, Dafni U, Stavropoulou-Giokas C, Frangia K, Tsoutsos D, Panagiotou P, Polyzos A, Papadopoulos O, Stratigos A, Markopoulos C, Bafaloukos D, Pectasides D, Fountzilias G, Kirkwood JM. 2006. Prognostic significance of autoimmunity during treatment of melanoma with interferon. *N Engl J Med* 354:709–718
- Gorbachev AV, Fairchild RL. 2001. Induction and regulation of T-cell priming for contact hypersensitivity. *Crit Rev Immunol* 21:451–472
- Gordon SM, Chaix J, Rupp LJ, Wu J, Madera S, Sun JC, Lindsten T, Reiner SL. 2012. The transcription factors T-bet and Eomes control key checkpoints of natural killer cell maturation. *Immunity* 36:55–67
- Grabbe S, Steinbrink K, Steinert M, Luger TA, Schwarz T. 1995. Removal of the majority of epidermal Langerhans cells by topical or systemic steroid application enhances the effector phase of murine contact hypersensitivity. *J Immunol* 155:4207–4217
- Grabbe S, Steinert M, Mahnke K, Schwarz A, Luger TA, Schwarz T. 1996. Dissection of antigenic and irritative effects of epicutaneously applied haptens in mice. Evidence that not the antigenic component but nonspecific proinflammatory effects of haptens determine the concentration-dependent elicitation of allergic contact dermatitis. *J Clin Invest* 98:1158–1164
- Grégoire C, Chasson L, Luci C, Tomasello E, Geissmann F, Vivier E, Walzer T. 2007. The trafficking of natural killer cells. *Immunol Rev* 220:169–182
- Grojean MF, Thivolet J, Perrot H. 1982. Acquired leukomelanoderma caused by topical depigmenting agents. *Ann Dermatol Venereol* 109:641–647
- Hammer Q, Rückert T, Dunst J, Romagnani C. 2017. Adaptive Natural Killer cells integrate Interleukin-18 during target-cell encounter. *Front Immunol* 8:1967
- Harada D, Takada C, Tsukumo Y, Takaba K, Manabe H. 2005. Analyses of a mouse model of the dermatitis caused by 2,4,6-trinitro-1-chlorobenzene (TNCB)-repeated application. *J Dermatol Sci* 37:159–167
- Hatton RD, Harrington LE, Luther RJ, Wakefield T, Janowski KM, Oliver JR, Lallone RL, Murphy KM, Weaver CT. 2006. A distal conserved sequence element controls *Irfng* gene expression by T cells and NK cells. *Immunity* 25:717–729

- Hayakawa Y, Smyth MJ. 2006. CD27 dissects mature NK cells into two subsets with distinct responsiveness and migratory capacity. *J Immunol* 176:1517–1524
- van Helden MJG, de Graaf N, Boog CJP, Topham DJ, Zaiss DMW, Sijts AJAM. 2012. The bone marrow functions as the central site of proliferation for long-lived NK cells. *J Immunol* 189:2333–2337
- Hemler ME. 1990. VLA proteins in the integrin family: structures, functions, and their role on leukocytes. *Annu Rev Immunol* 8:365–400
- Heng TSP, Painter MW, Immunological Genome Project Consortium. 2008. The Immunological Genome Project: networks of gene expression in immune cells. *Nat Immunol* 9:1091–1094
- Henri S, Poulin LF, Tamoutounour S, Ardouin L, Guilliams M, de Bovis B, Devilard E, Viret C, Azukizawa H, Kissenpfennig A, Malissen B. 2010. CD207<sup>+</sup> CD103<sup>+</sup> dermal dendritic cells cross-present keratinocyte-derived antigens irrespective of the presence of Langerhans cells. *J Exp Med* 207:189–206
- Hepworth MR, Fung TC, Masur SH, Kelsen JR, McConnell FM, Dubrot J, Withers DR, Hugues S, Farrar MA, Reith W, Eberl G, Baldassano RN, Laufer TM, Elson CO, Sonnenberg GF. 2015. Immune tolerance. Group 3 innate lymphoid cells mediate intestinal selection of commensal bacteria-specific CD4<sup>+</sup> T cells. *Science* 348:1031–1035
- Herberman RB, Nunn ME, Lavrin DH. 1975. Natural cytotoxic reactivity of mouse lymphoid cells against syngeneic and allogeneic tumors. I. Distribution of reactivity and specificity. *Int J Cancer* 16:216–229
- Homey B, Alenius H, Müller A, Soto H, Bowman EP, Yuan W, McEvoy L, Lauerma AI, Assmann T, Bünemann E, Lehto M, Wolff H, Yen D, Marxhausen H, To W, Sedgwick J, Ruzicka T, Lehmann P, Zlotnik A. 2002. CCL27-CCR10 interactions regulate T cell-mediated skin inflammation. *Nat Med* 8:157–165
- Honda T, Matsuoka T, Ueta M, Kabashima K, Miyachi Y, Narumiya S. 2009. Prostaglandin E(2)-EP(3) signaling suppresses skin inflammation in murine contact hypersensitivity. *J Allergy Clin Immunol* 124:809–818

- Honda T, Nakajima S, Egawa G, Ogasawara K, Malissen B, Miyachi Y, Kabashima K. 2010. Compensatory role of Langerhans cells and langerin-positive dermal dendritic cells in the sensitization phase of murine contact hypersensitivity. *J Allergy Clin Immunol* 125:1154–1156
- Honda T, Otsuka A, Tanizaki H, Minegaki Y, Nagao K, Waldmann H, Tomura M, Hori S, Miyachi Y, Kabashima K. 2011. Enhanced murine contact hypersensitivity by depletion of endogenous regulatory T cells in the sensitization phase. *J Dermatol Sci* 61:144–147
- Honda T, Egawa G, Grabbe S, Kabashima K. 2013. Update of immune events in the murine contact hypersensitivity model: toward the understanding of allergic contact dermatitis. *J Invest Dermatol* 133:303–315
- Hori S, Nomura T, Sakaguchi S. 2003. Control of regulatory T cell development by the transcription factor Foxp3. *Science* 299:1057–1061
- Hsu J, Hodgins JJ, Marathe M, Nicolai CJ, Bourgeois-Daigneault M-C, Trevino TN, Azimi CS, Scheer AK, Randolph HE, Thompson TW, Zhang L, Iannello A, Mathur N, Jardine KE, Kirn GA, Bell JC, McBurney MW, Raulet DH, Ardolino M. 2018. Contribution of NK cells to immunotherapy mediated by PD-1/PD-L1 blockade. *J Clin Invest* 128:4654–4668
- Huntington ND, Tabarias H, Fairfax K, Brady J, Hayakawa Y, Degli-Esposti MA, Smyth MJ, Tarlinton DM, Nutt SL. 2007. NK cell maturation and peripheral homeostasis is associated with KLRG1 up-regulation. *J Immunol* 178:4764–4770
- Ignatiadis N, Klaus B, Zaugg JB, Huber W. 2016. Data-driven hypothesis weighting increases detection power in genome-scale multiple testing. *Nat Methods* 13:577–580
- Igyártó BZ, Jenison MC, Dudda JC, Roers A, Müller W, Koni PA, Campbell DJ, Shlomchik MJ, Kaplan DH. 2009. Langerhans cells suppress contact hypersensitivity responses via cognate CD4 interaction and langerhans cell-derived IL-10. *J Immunol* 183:5085–5093

- Intlekofer AM, Takemoto N, Wherry EJ, Longworth SA, Northrup JT, Palanivel VR, Mullen AC, Gasink CR, Kaech SM, Miller JD, Gapin L, Ryan K, Russ AP, Lindsten T, Orange JS, Goldrath AW, Ahmed R, Reiner SL. 2005. Effector and memory CD8 + T cell fate coupled by T-bet and eomesodermin. *Nat Immunol* 6:1236–1244
- Janeway Jr. CA. 1989. Approaching the asymptote? Evolution and revolution in immunology. *Cold Spring Harb Symp Quant Biol* 54:1–13
- Jenne CN, Enders A, Rivera R, Watson SR, Brankovich AJ, Pereira JP, Xu Y, Roots CM, Beilke JN, Banerjee A, Reiner SL, Miller SA, Weinmann AS, Goodnow CC, Lanier LL, Cyster JG, Chun J. 2009. T-bet-dependent S1P<sub>5</sub> expression in NK cells promotes egress from lymph nodes and bone marrow. *J Exp Med* 206:2469–2481
- Juliá EP, Amante A, Pampena MB, Mordoh J, Levy EM. 2018. Avelumab, an IgG1 anti-PD-L1 immune checkpoint inhibitor, triggers NK cell-mediated cytotoxicity and cytokine production against triple negative breast cancer cells. *Front Immunol* 9:2140
- Kaech SM, Cui W. 2012. Transcriptional control of effector and memory CD8+ T cell differentiation. *Nat Rev Immunol* 12:749–761
- Kahn G. 1970. Depigmentation caused by phenolic detergent germicides. *Arch Dermatol* 102:177–187
- Kallies A, Good-Jacobson KL. 2017. Transcription factor T-bet orchestrates lineage development and function in the immune system. *Trends Immunol* 38:287–297
- Kamizono S, Duncan GS, Seidel MG, Morimoto A, Hamada K, Grosveld G, Akashi K, Lind EF, Haight JP, Ohashi PS, Look AT, Mak TW. 2009. Nfil3/E4bp4 is required for the development and maturation of NK cells in vivo. *J Exp Med* 206:2977–2986
- Kaplan DH, Jenison MC, Saeland S, Shlomchik WD, Shlomchik MJ. 2005. Epidermal Langerhans cell-deficient mice develop enhanced contact hypersensitivity. *Immunity* 23:611–620
- Karecla PI, Bowden SJ, Green SJ, Kilshaw PJ. 1995. Recognition of E-cadherin on epithelial cells by the mucosal T cell integrin alpha M290 beta 7 (alpha E beta 7). *Eur J Immunol* 25:852–856

- Karlberg A-T, Bergström MA, Börje A, Luthman K, Nilsson JLG. 2008. Allergic contact dermatitis--formation, structural requirements, and reactivity of skin sensitizers. *Chem Res Toxicol* 21:53–69
- Karlhofer FM, Yokoyama WM. 1991. Stimulation of murine natural killer (NK) cells by a monoclonal antibody specific for the NK1.1 antigen. IL-2-activated NK cells possess additional specific stimulation pathways. *J Immunol* 146:3662–3673
- Karo JM, Schatz DG, Sun JC. 2014. The RAG recombinase dictates functional heterogeneity and cellular fitness in natural killer cells. *Cell* 159:94–107
- Karpurapu M, Ranjan R, Deng J, Chung S, Lee YG, Xiao L, Nirujogi TS, Jacobson JR, Park GY, Christman JW. 2014. Krüppel like factor 4 promoter undergoes active demethylation during monocyte/macrophage differentiation. *PLoS One* 9:e93362
- Kärre K, Ljunggren HG, Piontek G, Kiessling R. 1986. Selective rejection of H-2-deficient lymphoma variants suggests alternative immune defence strategy. *Nature* 319:675–678
- Karsak M, Gaffal E, Date R, Wang-Eckhardt L, Rehnelt J, Petrosino S, Starowicz K, Steuder R, Schlicker E, Cravatt B, Mechoulam R, Buettner R, Werner S, Di Marzo V, Tüting T, Zimmer A. 2007. Attenuation of allergic contact dermatitis through the endocannabinoid system. *Science* 316:1494–1497
- Kehren J, Desvignes C, Krasteva M, Ducluzeau MT, Assossou O, Horand F, Hahne M, Kägi D, Kaiserlian D, Nicolas JF. 1999. Cytotoxicity is mandatory for CD8+ T cell-mediated contact hypersensitivity. *J Exp Med* 189:779–786
- Kiessling R, Klein E, Wigzell H. 1975. „Natural” killer cells in the mouse. I. Cytotoxic cells with specificity for mouse Moloney leukemia cells. Specificity and distribution according to genotype. *Eur J Immunol* 5:112–117
- Kim S, Iizuka K, Kang H-SP, Dokun A, French AR, Greco S, Yokoyama WM. 2002. In vivo developmental stages in murine natural killer cell maturation. *Nat Immunol* 3:523–528
- Kim S, Poursine-Laurent J, Truscott SM, Lybarger L, Song Y-J, Yang L, French AR, Sunwoo JB, Lemieux S, Hansen TH, Yokoyama WM. 2005. Licensing of natural killer cells by host major histocompatibility complex class I molecules. *Nature* 436:709–713

- Kish DD, Gorbachev AV, Fairchild RL. 2005. CD8<sup>+</sup> T cells produce IL-2, which is required for CD4<sup>+</sup>CD25<sup>+</sup> T cell regulation of effector CD8<sup>+</sup> T cell development for contact hypersensitivity responses. *J Leukoc Biol* 78:725–735
- Kish DD, Volokh N, Baldwin III WM, Fairchild RL. 2011. Hapten Application to the skin induces an inflammatory program directing hapten-primed effector CD8 T cell interaction with hapten-presenting endothelial cells. *J Immunol* 186:2117–2126
- Kish DD, Li X, Fairchild RL. 2009. CD8 T cells producing IL-17 and IFN- $\gamma$  initiate the innate immune response required for responses to antigen skin challenge. *J Immunol* 182:5949–5959
- Kitagaki H, Fujisawa S, Watanabe K, Hayakawa K, Shiohara T. 1995. Immediate-type hypersensitivity response followed by a late reaction is induced by repeated epicutaneous application of contact sensitizing agents in mice. *J Invest Dermatol* 105:749–755
- Kitagaki H, Ono N, Hayakawa K, Kitazawa T, Watanabe K, Shiohara T. 1997. Repeated elicitation of contact hypersensitivity induces a shift in cutaneous cytokine milieu from a T helper cell type 1 to a T helper cell type 2 profile. *J Immunol* 159:2484–2491
- Kitagawa Y, Ohkura N, Sakaguchi S. 2013. Molecular determinants of regulatory T cell development: the essential roles of epigenetic changes. *Front Immunol* 4:106
- Klein J. 1989. Are invertebrates capable of anticipatory immune responses? *Scand J Immunol* 29:499–505
- Klose CSN, Flach M, Möhle L, Rogell L, Hoyler T, Ebert K, Fabiunke C, Pfeifer D, Sexl V, Fonseca-Pereira D, Domingues RG, Veiga-Fernandes H, Arnold SJ, Busslinger M, Dunay IR, Tanriver Y, Diefenbach A. 2014. Differentiation of type 1 ILCs from a common progenitor to all helper-like innate lymphoid cell lineages. *Cell* 157:340–356
- Komori HK, Hart T, LaMere SA, Chew PV, Salomon DR. 2015. Defining CD4 T cell memory by the epigenetic landscape of CpG DNA methylation. *J Immunol* 194:1565–1579
- Kondo M, Weissmann IL, Akashi K. 1997. Identification of clonogenic common lymphoid progenitors in mouse bone marrow. *Cell* 91:661–672

- Kruglov AA, Grivennikov SI, Kuprash DV, Winsauer C, Prepens S, Seleznik GM, Eberl G, Littman DR, Heikenwalder M, Tumanov AV, Nedospasov SA. 2013. Nonredundant function of soluble LTa3 cells in intestinal homeostasis. *Science* 342:1243–1246
- Kusumoto M, Xu B, Shi M, Matsuyama T, Aoyama K, Takeuchi T. 2007. Expression of chemokine receptor CCR4 and its ligands (CCL17 and CCL22) in murine contact hypersensitivity. *J Interferon Cytokine Res* 27:901–910
- Langmead B, Salzberg SL. 2012. Fast gapped-read alignment with Bowtie 2. *Nat Methods* 9:357–359
- Lanier LL, Philips JH, Hackett Jr J, Tutt M, Kumar V. 1986. Natural killer cells: definition of a cell type rather than a function. *J Immunol* 137:2735–2739
- Larson RP, Zimmerli SC, Comeau MR, Itano A, Omori M, Iseki M, Hauser C, Ziegler SF. 2010. Dibutyl phthalate-induced thymic stromal lymphopoietin is required for Th2 contact hypersensitivity responses. *J Immunol* 184:2974–2984
- Lau CM, Adams NM, Geary CD, Weizman O-E, Rapp M, Pritykin Y, Leslie CS, Sun JC. 2018. Epigenetic control of innate and adaptive immune memory. *Nat Immunol* 19:963–972
- Lawrence M, Huber W, Pagès H, Aboyoun P, Carlson M, Gentleman R, Morgan MT, Carey VJ. 2013. Software for computing and annotating genomic ranges. *PLoS Comput Biol* 9:e1003118
- Lazarevic V, Glimcher LH. 2011. T-bet in disease. *Nat Immunol* 12:597–606
- Lazarevic V, Glimcher LH, Lord GM. 2013. T-bet: a bridge between innate and adaptive immunity. *Nat Rev Immunol* 13:777–789
- Lehmann J, Huehn J, de la Rosa M, Maszyzna F, Kretschmer U, Krenn V, Brunner M, Scheffold A, Hamann A. 2002. Expression of the integrin  $\alpha\text{E}\beta\text{7}$  identifies unique subsets of CD25<sup>+</sup> as well as CD25<sup>-</sup> regulatory T cells. *Proc Natl Acad Sci U S A* 99:13031–13036
- Levitt LJ, Nagler A, Lee F, Abrams J, Shatsky M, Thompson D. 1991. Production of granulocyte/macrophage-colony-stimulating factor by human natural killer cells. Modulation by the p75 subunit of the interleukin 2 receptor and by the CD2 receptor. *J Clin Invest* 88:67–75



- Lewis MD, Miller SA, Miazgowiec MM, Beima KM, Weinmann AS. 2007. T-bet's ability to regulate individual target genes requires the conserved T-box domain to recruit histone methyltransferase activity and a separate family member-specific transactivation domain. *Mol Cell Biol* 27:8510–8521
- Li H, Handsaker B, Wysoker A, Fennell T, Ruan J, Homer N, Marth G, Abecasis G, Durbin R, 1000 Genome Project Data Processing Subgroup. 2009. The sequence alignment/map format and SAMtools. *Bioinformatics* 25:2078–2079
- Li T, Wang J, Wang Y, Chen Y, Wei H, Sun R, Tian Z. 2017. Respiratory influenza virus infection induces memory-like liver NK cells in mice. *J Immunol* 198:1242–1252
- Li Y, Wang J, Yin J, Liu X, Yu M, Li T, Yan H, Wang X. 2017. Chromatin state dynamics during NK cell activation. *Oncotarget* 8:41854–41865
- Long EO. 2007. Ready for prime time: NK cell priming by dendritic cells. *Immunity* 26:385–387
- Lonsdorf AS, Kuekrek H, Stern BV, Boehm BO, Lehmann PV, Tary-Lehmann M. 2003. Intratumor CpG-oligodeoxynucleotide injection induces protective antitumor T cell immunity. *J Immunol* 171:3941–3946
- Lopez-Vergès S, Milush JM, Schwartz BS, Pando MJ, Jarjoura J, York VA, Houchins JP, Miller S, Kang SM, Norris PJ, Nixon DF, Lanier LL. 2011. Expansion of a unique CD57<sup>+</sup>NKG2Chi natural killer cell subset during acute human cytomegalovirus infection. *Proc Natl Acad Sci U S A* 108:14725–14732
- Lotem J, Levanon D, Negreanu V, Leshkowitz D, Friedlander G, Groner Y. 2013. Runx3-mediated transcriptional program in cytotoxic lymphocytes. *PLoS One* 8:e80467
- Love MI, Huber W, Anders S. 2014. Moderated estimation of fold change and dispersion for RNA-seq data with DESeq2. *Genome Biol* 15:550
- Luiten RM, Kueter EW, Mooi W, Gallee MP, Rankin EM, Gerritsen WR, Clift SM, Nooijen WJ, Weder P, van de Kastele WF, Sein J, van den Berk PC, Nieweg OE, Berns AM, Spits H, de Gast GC. 2005. Immunogenicity, including vitiligo, and feasibility of vaccination with autologous GM-CSF-transduced tumor cells in metastatic melanoma patients. *J Clin Oncol* 23:8978–8991

- Lyon CC, Beck MH. 1998. Contact hypersensitivity to monobenzyl ether of hydroquinone used to treat vitiligo. *Contact Dermatitis* 39:132–133
- Ma A, Koka R, Burkett P. 2006. Diverse functions of IL-2, IL-15, and IL-7 in lymphoid homeostasis. *Annu Rev Immunol* 24:657–679
- Male V, Nisoli I, Kostrzewski T, Allan DSJ, Carlyle JR, Lord GM, Wack A, Brady HJM. 2014. The transcription factor E4bp4/Nfil3 controls commitment to the NK lineage and directly regulates Eomes and Id2 expression. *J Exp Med* 211:635–642
- Marchal G, Seman M, Milon G, Truffa-Bachi P, Zilberfarb V. 1982. Local adoptive transfer of skin delayed-type hypersensitivity initiated by a single T lymphocyte. *J Immunol* 129:954–958
- Mariathasan S, Weiss DS, Newton K, McBride J, O'Rourke K, Roose-Girma M, Lee WP, Weinrauch Y, Monack DM, Dixit VM. 2006. Cryopyrin activates the inflammasome in response to toxins and ATP. *Nature* 440:228–232
- Martin SF, Esser PR, Weber FC, Jakob T, Freudenberg MA, Schmidt M, Goebeler M. 2011. Mechanisms of chemical-induced innate immunity in allergic contact dermatitis. *Allergy* 66:1152–1163
- Martin SF, Dudda JC, Bachtanian E, Lembo A, Liller S, Dürr C, Heimesaat MM, Bereswill S, Fejer G, Vassileva R, Jakob T, Freudenberg N, Termeer CC, Johner C, Galanos C, Freudenberg MA. 2008. Toll-like receptor and IL-12 signaling control susceptibility to contact hypersensitivity. *J Exp Med* 205:2151–2162
- Martin S, Lappin MB, Kohler J, Delattre V, Leicht C, Preckel T, Simon JC, Weltzien HU. 2000. Peptide immunization indicates that CD8+ T cells are the dominant effector cells in trinitrophenyl-specific contact hypersensitivity. *J Invest Dermatol* 115:260–266
- Martinon F, Pétrilli V, Mayor A, Tardivel A, Tschopp J. 2006. Gout-associated uric acid crystals activate the NALP3 inflammasome. *Nature* 440:237–241
- Matloubian M, David A, Engel S, Ryan JE, Cyster JG. 2000. A transmembrane CXC chemokine is a ligand for HIV-coreceptor Bonzo. *Nat Immunol* 1:298–304
- McFadden JP, Dearman RJ, White JML, Basketter DA, Kimber I. 2011. The hapten-atopy hypothesis II: the 'cutaneous hapten paradox'. *Clin Exp Allergy* 41:327–337

- McMinn PC, Halliday GM, Muller HK. 1990. Effects of gliotoxin on Langerhans' cell function: contact hypersensitivity responses and skin graft survival. *Immunology* 71:46–51
- Medzhitov R, Preston-Hurlburt P, Janeway Jr CA. 1997. A human homologue of the *Drosophila* Toll protein signals activation of adaptive immunity. *Nature* 388:394–397
- Mehrotra PT, Donnelly RP, Wong S, Kanegane H, Geremew A, Mostowski HS, Furuke K, Siegel JP, Bloom ET. 1998. Production of IL-10 by human natural killer cells stimulated with IL-2 and/or IL-12. *J Immunol* 160:2637–2644
- Michishita M, Videm V, Arnaout MA. 1993. A novel divalent cation-binding site in the A domain of the beta 2 integrin CR3 (CD11b/CD18) is essential for ligand binding. *Cell* 72:857–867
- Miller SA, Huang AC, Miazgowiec MM, Brassil MM, Weinmann AS. 2008. Coordinated but physically separable interaction with H3K27-demethylase and H3K4-methyltransferase activities are required for T-box protein-mediated activation of developmental gene expression. *Genes Dev* 22:2980–2993
- Mjösberg J, Spits H. 2016. Human innate lymphoid cells. *J Allergy Clin Immunol* 138:1265-1276
- Mombaerts P, Iacomini J, Johnson RS, Herrup K, Tonegawa S, Papaioannou VE. 1992. RAG-1-deficient mice have no mature B and T lymphocytes. *Cell* 68:869–877
- Mori T, Kabashima K, Yoshiki R, Sugita K, Shiraishi N, Onoue A, Kuroda E, Kobayashi M, Yamashita U, Tokura Y. 2008. Cutaneous hypersensitivities to haptens are controlled by IFN-gamma-upregulated keratinocyte Th1 chemokines and IFN-gamma-downregulated langerhans cell Th2 chemokines. *J Invest Dermatol* 128:1719–1727
- Mosher DB, Parrish JA, Fitzpatrick TB. 1977. Monobenzylether of hydroquinone. A retrospective study of treatment of 18 vitiligo patients and a review of the literature. *Br J Dermatol* 97:669–679

- Mukherjee N, Ji N, Hurez V, Curiel TJ, Montgomery MO, Braun AJ, Nicolas M, Aguilera M, Kaushik D, Liu Q, Ruan J, Kendrick KA, Svatek RS. 2018. Intratumoral CD56<sup>bright</sup> natural killer cells are associated with improved survival in bladder cancer. *Oncotarget* 9:36492–36502
- Murphy K, Weaver C. 2016. *Janeway's Immunobiology* 9th edition. Garland Science
- Naish S, Riley PA. 1989. Studies on the kinetics of oxidation of 4-hydroxyanisole by tyrosinase. *Biochem Pharmacol* 38:1103–1107
- Najar HM, Dutz JP. 2008. Topical CpG enhances the response of murine malignant melanoma to dacarbazine. *J Invest Dermatol* 128:2204–2210
- Nakae S, Komiyama Y, Narumi S, Sudo K, Horai R, Tagawa Y, Sekikawa K, Matsushima K, Asano M, Iwakura Y. 2003. IL-1-induced tumor necrosis factor- $\alpha$  elicits inflammatory cell infiltration in the skin by inducing IFN- $\gamma$ -inducible protein 10 in the elicitation phase of the contact hypersensitivity response. *Int Immunol* 15:251–260
- Nazih A, Benezra C, Lepoittevin J-P. 1993. Bihaptens with 5- and 6-methyl-substituted alkylcatechols and methylene lactone functional groups: tools for hapten (allergen or tolerogen)-protein interaction studies. *Chem Res Toxicol* 6:215–222
- Nestle FO, Di Meglio P, Qin J-Z, Nickoloff BJ. 2009. Skin immune sentinels in health and disease. *Nat Rev Immunol* 9:679–691
- Ni J, Miller M, Stojanovic A, Garbi N, Cerwenka A. 2012. Sustained effector function of IL-12/15/18–preactivated NK cells against established tumors. *J Exp Med* 209:2351–2365
- Nikzad R, Angelo LS, Aviles-Padilla K, Le DT, Singh VK, Bimler L, Vukmanovic-Stejic M, Vendrame E, Ranganath T, Simpson L, Haigwood NL, Blish CA, Akbar AN, Paust S. 2019. Human natural killer cells mediate adaptive immunity to viral antigens. *Sci Immunol* 4:eaat8116
- Noordegraaf M, Flacher V, Stoitzner P, Clausen BE. 2010. Functional redundancy of langerhans cells and langerin<sup>+</sup> dermal dendritic cells in contact hypersensitivity. *J Invest Dermatol* 130:2752–2759

- Nordlund JJ, Forget B, Kirkwood J, Lerner AB. 1985. Dermatitis produced by applications of monobenzene in patients with active vitiligo. *Arch Dermatol* 121:1141–1144
- O'Brien KL, Finlay DK. 2019. Immunometabolism and natural killer cell responses. *Nat Rev Immunol* 19:282–290
- O'Leary JG, Goodarzi M, Drayton DL, von Andrian UH. 2006. T cell- and B cell-independent adaptive immunity mediated by natural killer cells. *Nat Immunol* 7:507–516
- O'Sullivan TE, Sun JC, Lanier LL. 2015. Natural killer cell memory. *Immunity* 43:634–645
- Ohno S, Sato T, Kohu K, Takeda K, Okumura K, Satake M, Habu S. 2008. Runx proteins are involved in regulation of CD122, Ly49 family and IFN-gamma expression during NK cell differentiation. *Int Immunol* 20:71–79
- Oliver EA, Schwartz L, Warren LH. 1939. Occupational leukoderma. *JAMA* 113:927–928
- Otsuka A, Kubo M, Honda T, Egawa G, Nakajima S, Tanizaki H, Kim B, Matsuoka S, Watanabe T, Nakae S, Miyachi Y, Kabashima K. 2011. Requirement of interaction between mast cells and skin dendritic cells to establish contact hypersensitivity. *PLoS One* 6:e25538
- Ottaviani C, Nasorri F, Bedini C, de Pità O, Girolomoni G, Cavani A. 2006. CD56bright CD16(-) NK cells accumulate in psoriatic skin in response to CXCL10 and CCL5 and exacerbate skin inflammation. *Eur J Immunol* 36:118–128
- Oyer JL, Gitto SB, Altomare DA, Copik AJ. 2018. PD-L1 blockade enhances anti-tumor efficacy of NK cells. *Oncoimmunology* 7:e1509819
- Parham P. 2005. MHC class I molecules and KIRs in human history, health and survival. *Nat Rev Immunol* 5:201–214
- Park SL, Zaid A, Hor JL, Christo SN, Prier JE, Davies B, Alexandre YO, Gregory JL, Russell TA, Gebhardt T, Carbone FR, Tschärke DC, Heath WR, Mueller SN, MacKay LK. 2018. Local proliferation maintains a stable pool of tissue-resident memory T cells after antiviral recall responses. *Nat Immunol* 19:183–191

- Pasparakis M, Haase I, Nestle FO. 2014. Mechanisms regulating skin immunity and inflammation. *Nat Rev Immunol* 14:289–301
- Pauls K, Schön M, Kubitza RC, Homey B, Wiesenborn A, Lehmann P, Ruzicka T, Parker CM, Schön MP. 2001. Role of integrin alphaE(CD103)beta7 for tissue-specific epidermal localization of CD8+ T lymphocytes. *J Invest Dermatol* 117:569–575
- Paust S, Gill HS, Wang B-Z, Flynn MP, Moseman EA, Senman B, Szczepanik M, Telenti A, Askenase PW, Compans RW, von Andrian UH. 2010. Critical role for the chemokine receptor CXCR6 in NK cell-mediated antigen-specific memory of haptens and viruses. *Nat Immunol* 11:1127–1135
- Peiser M, Tralau T, Heidler J, Api AM, Arts JH, Basketter DA, English J, Diepgen TL, Fuhlbrigge RC, Gaspari AA, Johansen JD, Karlberg AT, Kimber I, Lepoittevin JP, Liebsch M, Maibach HI, Martin SF, Merk HF, Platzek T, Rustemeyer T, Schnuch A, Vandebriel RJ, White IR, Luch A. 2011. Allergic contact dermatitis: epidemiology, molecular mechanisms, in vitro methods and regulatory aspects. Current knowledge assembled at an international workshop at BfR, Germany. *Cell Mol Life Sci* 69:763–781
- Peng H, Jiang X, Chen Y, Sojka DK, Wei H, Gao X, Sun R, Yokoyama WM, Tian Z. 2013. Liver-resident NK cells confer adaptive immunity in skin-contact inflammation. *J Clin Invest* 123:1444–1456
- Picelli S, Björklund AK, Reinius B, Sagasser S, Winberg G, Sandberg R. 2014. Tn5 transposase and tagmentation procedures for massively scaled sequencing projects. *Genome Res* 24:2033–2040
- Putz EJ, Putz AM, Boettcher A, Charley S, Sauer M, Palmer M, Phillips R, Hostetter J, Loving CL, Cunnick JE, Tuggle CK. 2019. Successful development of methodology for detection of hapten-specific contact hypersensitivity (CHS) memory in swine. *PLoS One* 14:e0223483
- Quaglino P, Marenco F, Osella-Abate S, Cappello N, Ortoncelli M, Salomone B, Fierro MT, Savoia P, Bernengo MG. 2010. Vitiligo is an independent favourable prognostic factor in stage III and IV metastatic melanoma patients: results from a single-institution hospital-based observational cohort study. *Ann Oncol* 21:409–414

- Rafei-Shamsabadi DA, Klose CSN, Halim TYF, Tanriver Y, Jakob T. 2019. Context dependent role of type 2 innate lymphoid cells in allergic skin inflammation. *Front Immunol* 10:2591
- Rafei-Shamsabadi DA, van de Poel S, Dorn B, Kunz S, Martin SF, Klose CSN, Arnold SJ, Tanriver Y, Ebert K, Diefenbach A, Halim TYF, McKenzie ANJ, Jakob T. 2018. Lack of type 2 innate lymphoid cells promotes a type I-driven enhanced immune response in contact hypersensitivity. *J Invest Dermatol* 138:1962–1972
- Ramírez F, Ryan DP, Grüning B, Bhardwaj V, Kilpert F, Richter AS, Heyne S, Dündar F, Manke T. 2016. deepTools2: a next generation web server for deep-sequencing data analysis. *Nucleic Acids Res* 44:W160–W165
- Rankin LC, Girard-Madoux MJH, Seillet C, Mielke LA, Kerdiles Y, Fenis A, Wieduwild E, Putoczki T, Mondot S, Lantz O, Demon D, Papenfuss AT, Smyth GK, Lamkanfi M, Carotta S, Renauld J-C, Shi W, Carpentier S, Soos T, Arendt C, Ugolini S, Huntington ND, Belz GT, Vivier E. 2016. Complementarity and redundancy of IL-22-producing innate lymphoid cells. *Nat Immunol* 17:179–186
- Ray CM, Kluk M, Grin CM, Grant-Kels JM. 2005. Successful treatment of malignant melanoma in situ with topical 5% imiquimod cream. *Int J Dermatol* 44:428–434
- Reiss Y, Proudfoot AE, Power CA, Campbell JJ, Butcher EC. 2001. CC chemokine receptor (CCR)4 and the CCR10 ligand cutaneous T cell-attracting chemokine (CTACK) in lymphocyte trafficking to inflamed skin. *J Exp Med* 194:1541–1547
- Ren S, Wang Q, Zhang Y, Zhang B, Zhao C, Dong X, Song Y, Zhang W, Qin X, Liu M. 2019. Imiquimod enhances DNFB mediated contact hypersensitivity in mice. *Int Immunopharmacol* 72:284–291
- Rihs S, Walker C, Virchow Jr JC, Boer C, Kroegel C, Giri SN, Braun RK. 1996. Differential expression of alpha E beta 7 integrins on bronchoalveolar lavage T lymphocyte subsets: regulation by alpha 4 beta 1-integrin crosslinking and TGF-beta. *Am J Respir Cell Mol Biol* 15:600–610
- Riis JL, Johansen C, Vestergaard C, Bech R, Kragballe K, Iversen L. 2011. Kinetics and differential expression of the skin-related chemokines CCL27 and CCL17 in psoriasis, atopic dermatitis and allergic contact dermatitis. *Exp Dermatol* 20:789–794

- Robbins SH, Tessmer MS, Van Kaer L, Brossay L. 2005. Direct effects of T-bet and MHC class I expression, but not STAT1, on peripheral NK cell maturation. *Eur J Immunol* 35:757–765
- Robert C, Kupper TS. 1999. Inflammatory skin diseases, T cells, and immune surveillance. *New Engl J Med* 341:1817–1828
- Robinette ML, Fuchs A, Cortez VS, Lee JS, Wang Y, Durum SK, Gilfillan S, Colonna M, Immunological Genome Consortium. 2015. Transcriptional programs define molecular characteristics of innate lymphoid cell classes and subsets. *Nat Immunol* 16:306–317
- Roda JM, Parihar R, Magro C, Nuovo GJ, Tridandapani S, Carson 3rd WE. 2006. Natural killer cells produce T cell-recruiting chemokines in response to antibody-coated tumor cells. *Cancer Res* 66:517–526
- Romagnani C, Juelke K, Falco M, Morandi B, D'Agostino A, Costa R, Ratto G, Forte G, Carrega P, Lui G, Conte R, Strowig T, Moretta A, Münz C, Thiel A, Moretta L, Ferlazzo G. 2007. CD56 bright CD16-killer Ig-like receptor-NK cells display longer telomeres and acquire features of CD56 dim NK cells upon activation. *J Immunol* 178:4947–4955
- Romee R, Rosario M, Berrien-Elliott MM, Wagner JA, Jewell BA, Schappe T, Leong JW, Abdel-Latif S, Schneider SE, Willey S, Neal CC, Yu L, Oh ST, Lee Y-S, Mulder A, Claas F, Cooper MA, Fehniger TA. 2016. Cytokine-induced memory-like natural killer cells exhibit enhanced responses against myeloid leukemia. *Sci Transl Med* 8:357ra123
- Romee R, Schneider SE, Leong JW, Chase JM, Keppel CR, Sullivan RP, Cooper MA, Fehniger TA. 2012. Cytokine activation induces human memory-like NK cells. *Blood* 120:4751–4760
- Röse L, Schneider C, Stock C, Zollner TM, Döcke W-D. 2012. Extended DNFB-induced contact hypersensitivity models display characteristics of chronic inflammatory dermatoses. *Exp Dermatol* 21:25–31
- Rosmaraki EE, Douagi I, Roth C, Colucci F, Cumano A, Di Santo JP. 2001. Identification of committed NK cell progenitors in adult murine bone marrow. *Eur J Immunol* 31:1900–1909



- Ruoslahti E, Pierschbacher MD. 1987. New perspectives in cell adhesion: RGD and integrins. *Science* 238:491–507
- Sánchez MJ, Muench MO, Roncarolo MG, Lanier LL, Phillips JH. 1994. Identification of a common T/natural killer cell progenitor in human fetal thymus. *J Exp Med* 180:569–576
- Sarnacki S, Bègue B, Buc H, Le Deist F, Cerf-Bensussan N. 1992. Enhancement of CD3-induced activation of human intestinal intraepithelial lymphocytes by stimulation of the beta 7-containing integrin defined by HML-1 monoclonal antibody. *Eur J Immunol* 22:2887–2892
- Scharton TM, Scott P. 1993. Natural killer cells are a source of interferon gamma that drives differentiation of CD4+ T cell subsets and induces early resistance to *Leishmania major* in mice. *J Exp Med* 178:567–577
- Schluns KS, Lefrancois L. 2003. Cytokine control of memory T-cell development and survival. *Nat Rev Immunol* 3:269–279
- Seillet C, Huntington ND, Gangatirkar P, Axelsson E, Minnich M, Brady HJM, Busslinger M, Smyth MJ, Belz GT, Carotta S. 2014. Differential requirement for Nfil3 during NK cell development. *J Immunol* 192:2667–2676
- Sekimata M, Pérez-Melgosa M, Miller SA, Weinmann AS, Sabo PJ, Sandstrom R, Dorschner MO, Stamatoyannopoulos JA, Wilson CB. 2009. CCCTC-binding factor and the transcription factor T-bet orchestrate T helper 1 cell-specific structure and function at the interferon-gamma locus. *Immunity* 31:551–564
- Shi L, Kraut RP, Aebersold R, Greenberg AH. 1992. A natural killer cell granule protein that induces DNA fragmentation and apoptosis. *J Exp Med* 175:553–566
- Shinkai Y, Rathbun G, Lam K-P, Oltz EM, Stewart V, Mendelsohn M, Charron J, Datta M, Young F, Stall AM, Alt FW. 1992. RAG-2-deficient mice lack mature lymphocytes owing to inability to initiate V(D)J rearrangement. *Cell* 68:855–867
- Sidky YA, Borden EC, Weeks CE, Reiter MJ, Hatcher JF, Bryan GT. 1992. Inhibition of murine tumor growth by an interferon-inducing imidazoquinolinamine. *Cancer Res* 52:3528–3533

- Sivori S, Falco M, Della Chiesa M, Carlomagno S, Vitale M, Moretta L, Moretta A. 2004. CpG and double-stranded RNA trigger human NK cells by Toll-like receptors: induction of cytokine release and cytotoxicity against tumors and dendritic cells. *Proc Natl Acad Sci U S A* 101:10116–10121
- Sivori S, Vitale M, Morelli L, Sanseverino L, Augugliaro R, Bottino C, Moretta L, Moretta A. 1997. p46, a novel natural killer cell-specific surface molecule that mediates cell activation. *J Exp Med* 186:1129–1136
- Smith HRC, Heusel JW, Mehta IK, Kim S, Dorner BG, Naidenko OV, Iizuka K, Furukawa H, Beckman DL, Pingel JT, Scalzo AA, Fremont DH, Yokoyama WM. 2002. Recognition of a virus-encoded ligand by a natural killer cell activation receptor. *Proc Natl Acad Sci U S A* 99:8826–8831
- Spits H, Cupedo T. 2012. Innate lymphoid cells: emerging insights in development, lineage relationships, and function. *Annu Rev Immunol* 30:647–675
- Spits H, Artis D, Colonna M, Diefenbach A, Di Santo JP, Eberl G, Koyasu S, Locksley RM, McKenzie ANJ, Mebius RE, Powrie F, Vivier E. 2013. Innate lymphoid cells - a proposal for uniform nomenclature. *Nat Rev Immunol* 13:145–149
- Spits H, Di Santo JP. 2011. The expanding family of innate lymphoid cells: regulators and effectors of immunity and tissue remodeling. *Nat Immunol* 12:21–27
- Springer TA. 1985. The LFA-1, Mac-1 glycoprotein family and its deficiency in an inherited disease. *Fed Proc* 44:2660–2663
- Springer TA. 1990. Adhesion receptors of the immune system. *Nature* 346:425–434
- Stelzer G, Rosen N, Plaschkes I, Zimmerman S, Twik M, Fishilevich S, Stein TI, Nudel R, Lieder I, Mazor Y, Kaplan S, Dahary D, Warshawsky D, Guan-Golan Y, Kohn A, Rappaport N, Safran M, Lancet D. 2016. The GeneCards suite: from gene data mining to disease genome sequence analyses. *Curr Protoc Bioinformatics* 54:1.30.1-1.30.33
- Stokic-Trtica V, Diefenbach A, Klose CSN. 2020. NK cell development in times of innate lymphoid cell diversity. *Front Immunol* 11:813

- Stutte S, Quast T, Gerbitzki N, Savinko T, Novak N, Reifenberger J, Homey B, Kolanus W, Alenius H, Förster I. 2010. Requirement of CCL17 for CCR7- and CXCR4-dependent migration of cutaneous dendritic cells. *Proc Natl Acad Sci U S A* 107:8736–8741
- Sun JC, Beilke JN, Lanier LL. 2010. Immune memory redefined: characterizing the longevity of natural killer cells. *Immunol Rev* 236:83–94
- Sun JC, Beilke JN, Lanier LL. 2009. Adaptive immune features of natural killer cells. *Nature* 457:557–561
- Sun JC, Lanier LL. 2010. *The immune response to infection*. ASM Press, Washington, D.C.
- Sun JC, Lanier LL. 2011. NK cell development, homeostasis and function: parallels with CD8<sup>+</sup> T cells. *Nat Rev Immunol* 11:645–57
- Sutterwala FS, Ogura Y, Szczepanik M, Lara-Tejero M, Lichtenberger GS, Grant EP, Bertin J, Coyle AJ, Galán JE, Askenase PW, Flavell RA. 2006. Critical role for NALP3/CIAS1/Cryopyrin in innate and adaptive immunity through its regulation of caspase-1. *Immunity* 24:317–327
- Szabo SJ, Kim ST, Costa GL, Zhang X, Fathman CG, Glimcher LH. 2000. A novel transcription factor, T-bet, directs Th1 lineage commitment. *Cell* 100:655–669
- Szczepanik M, Akahira-Azuma M, Bryniarski K, Tsuji RF, Kawikova I, Ptak W, Kiener C, Campos RA, Askenase PW. 2003. B-1 B cells mediate required early T cell recruitment to elicit protein-induced delayed-type hypersensitivity. *J Immunol* 171:6225–6235
- Szilvassy SJ. 2003. The biology of hematopoietic stem cells. *Arch Med Res* 34:446–460
- Takeda K, Kaisho T, Akira S. 2003. Toll-like receptors. *Annu Rev Immunol* 21:335–376
- Takeda K, Cretney E, Hayakawa Y, Ota T, Akiba H, Ogasawara K, Yagita H, Kinoshita K, Okumura K, Smyth MJ. 2005. TRAIL identifies immature natural killer cells in newborn mice and adult mouse liver. *Blood* 105:2082–2089

- Takeda K, Oshima H, Hayakawa Y, Akiba H, Atsuta M, Kobata T, Kobayashi K, Ito M, Yagita H, Okumura K. 2000. CD27-mediated activation of murine NK cells. *J Immunol* 164:1741–1745
- Tay SS, Roediger B, Tong PL, Tikoo S, Weninger W. 2013. The skin-resident immune network. *Curr Dermatol Rep* 3:13–22
- The UniProt Consortium. 2019. UniProt: a worldwide hub of protein knowledge. *Nucleic Acids Res* 47:D506–D515
- Tomura M, Honda T, Tanizaki H, Otsuka A, Egawa G, Tokura Y, Waldmann H, Hori S, Cyster JG, Watanabe T, Miyachi Y, Kanagawa O, Kabashima K. 2010. Activated regulatory T cells are the major T cell type emigrating from the skin during a cutaneous immune response in mice. *J Clin Invest* 120:883–893
- Townsend MJ, Weinmann AS, Matsuda JL, Salomon R, Farnham PJ, Biron CA, Gapin L, Glimcher LH. 2004. T-bet regulates the terminal maturation and homeostasis of NK and Valpha14i NKT cells. *Immunity* 20:477–494
- Trinchieri G. 1989. Biology of natural killer cells. *Adv Immunol* 47:187–376
- Tsuji RF, Kawikova I, Ramabhadran R, Akahira-Azuma M, Taub D, Hugli TE, Gerard C, Askenase PW. 2000. Early local generation of C5a initiates the elicitation of contact sensitivity by leading to early T cell recruitment. *J Immunol* 165:1588–1598
- Tsuji RF, Szczepanik M, Kawikova I, Paliwal V, Campos RA, Itakura A, Akahira-Azuma M, Baumgarth N, Herzenberg LA, Askenase PW. 2002. B cell-dependent T cell responses: IgM antibodies are required to elicit contact sensitivity. *J Exp Med* 196:1277–1290
- Uss E, Rowshani AT, Hooibrink B, Lardy NM, van Lier RAW, ten Berge IJM. 2006. CD103 is a marker for alloantigen-induced regulatory CD8<sup>+</sup> T cells. *J Immunol* 177:2775–2783
- Vivier E, Artis D, Colonna M, Diefenbach A, Di Santo JP, Eberl G, Koyasu S, Locksley RM, McKenzie ANJ, Mebius RE, Powrie F, Spits H. 2018. Innate lymphoid cells: 10 years on. *Cell* 174:1054–1066
- Vivier E, Nunès JA, Vély F. 2004. Natural killer cell signaling pathways. *Science* 306:1517–1519

- Vonarbourg C, Mortha A, Bui VL, Hernandez PP, Kiss EA, Hoyler T, Flach M, Bengsch B, Thimme R, Hölscher C, Hönig M, Pannicke U, Schwarz K, Ware CF, Finke D, Diefenbach A. 2010. Regulated expression of nuclear receptor ROR $\gamma$ t confers distinct functional fates to NK cell receptor-expressing ROR $\gamma$ t(+) innate lymphocytes. *Immunity* 33:736–751
- Walzer T, Chiossone L, Chaix J, Calver A, Carozzo C, Garrigue-Antar L, Jacques Y, Baratin M, Tomasello E, Vivier E. 2007. Natural killer cell trafficking in vivo requires a dedicated sphingosine 1-phosphate receptor. *Nat Immunol* 8:1337–1344
- Walzer T, Dalod M, Robbins SH, Zitvogel L, Vivier E. 2005. Natural-killer cells and dendritic cells: “l’union fait la force”. *Blood* 106:2252–2258
- Wang X, Fujita M, Prado R, Tousson A, Hsu H-C, Schottelius A, Kelly DR, Yang PA, Wu Q, Chen J, Xu H, Elmets CA, Mountz JD, Edwards 3rd CK. 2010. Visualizing CD4 T-cell migration into inflamed skin and its inhibition by CCR4/CCR10 blockades using in vivo imaging model. *Br J Dermatol* 162:487–496
- Wang X, Peng H, Cong J, Wang X, Lian Z, Wei H, Sun R, Tian Z. 2018. Memory formation and long-term maintenance of IL-7R $\alpha$ <sup>+</sup> ILC1s via a lymph node-liver axis. *Nat Commun* 9:4854
- Wang X, Peng H, Tian Z. 2019. Innate lymphoid cell memory. *Cell Mol Immunol* 16:423–429
- Wang X, Tian Z, Peng H. 2020. Tissue-resident memory-like ILCs: innate counterparts of T<sub>RM</sub> cells. *Protein Cell* 11:85–96
- Warren HS, Kinnear BF, Phillips JH, Lanier LL. 1995. Production of IL-5 by human NK cells and regulation of IL-5 secretion by IL-4, IL-10, and IL-12. *J Immunol* 154:5144–5152
- Watanabe H, Gehrke S, Contassot E, Roques S, Tschopp J, Friedmann PS, French LE, Gaide O. 2008. Danger signaling through the inflammasome acts as a master switch between tolerance and sensitization. *J Immunol* 180:5826–5832
- Webb EF, Tzimas MN, Newsholme SJ, Griswold DE. 1998. Intralésional cytokines in chronic oxazolone-induced contact sensitivity suggest roles for tumor necrosis factor alpha and interleukin-4. *J Invest Dermatol* 111:86–92

- Weber FC, Esser PR, Müller T, Ganesan J, Pellegatti P, Simon MM, Zeiser R, Idzko M, Jakob T, Martin SF. 2010. Lack of the purinergic receptor P2X<sub>7</sub> results in resistance to contact hypersensitivity. *J Exp Med* 207:2609–2619
- Werfel T, Uciechowski P, Tetteroo PA, Kurrle R, Deicher H, Schmidt RE. 1989. Activation of cloned human natural killer cells via Fc gamma RIII. *J Immunol* 142:1102–1106
- Werneck MBF, Lugo-Villarino G, Hwang ES, Cantor H, Glimcher LH. 2008. T-bet plays a key role in NK-mediated control of melanoma metastatic disease. *J Immunol* 180:8004–8010
- Wieczorek G, Asemissen A, Model F, Turbachova I, Floess S, Liebenberg V, Baron U, Stauch D, Kotsch K, Pratschke J, Hamann A, Loddenkemper C, Stein H, Volk HD, Hoffmüller U, Grützkau A, Mustea A, Huehn J, Scheibenbogen C, Olek S. 2009. Quantitative DNA methylation analysis of FOXP3 as a new method for counting regulatory T cells in peripheral blood and solid tissue. *Cancer Res* 69:599–608
- Wiencke JK, Butler R, Hsuang G, Eliot M, Kim S, Sepulveda MA, Siegel D, Houseman EA, Kelsey KT. 2016. The DNA methylation profile of activated human natural killer cells. *Epigenetics* 11:363–380
- Wight A, Mahmoud AB, Scur M, Tu MM, Rahim MMA, Sad S, Makrigiannis AP. 2018. Critical role for the Ly49 family of class I MHC receptors in adaptive natural killer cell responses. *Proc Natl Acad Sci U S A* 115:11579–11584
- Williams MA, Bevan MJ. 2007. Effector and memory CTL differentiation. *Annu Rev Immunol* 25:171–192
- Yokota Y, Mansouri A, Mori S, Sugawara S, Adachi S, Nishikawa S, Gruss P. 1999. Development of peripheral lymphoid organs and natural killer cells depends on the helix-loop-helix inhibitor Id2. *Nature* 397:702–706
- Yokoyama WM, Plougastel BFM. 2003. Immune functions encoded by the natural killer gene complex. *Nat Rev Immunol* 3:304–316
- Yokoyama WM, Kim S, French AR. 2004. The dynamic life of natural killer cells. *Annu Rev Immunol* 22:405–429
- Yu G, Wang L-G, He Q-Y. 2015. ChIPseeker: an R/Bioconductor package for ChIP peak annotation, comparison and visualization. *Bioinformatics* 31:2382–2383

- Yu J, Heller G, Chewning J, Kim S, Yokoyama WM, Hsu KC, Yu J, Heller G, Chewning J, Kim S, Yokoyama WM, Hsu KC. 2007. Hierarchy of the human natural killer cell response is determined by class and quantity of inhibitory receptors for self-HLA-B and HLA-C ligands. *J Immunol* 179:5977–5989
- Yu Y, Mo Y, Ebenezer D, Bhattacharyya S, Liu H, Sundaravel S, Giricz O, Wontakal S, Cartier J, Caces B, Artz A, Nischal S, Bhagat T, Bathon K, Maqbool S, Gligich O, Suzuki M, Steidl U, Godley L, Skoultchi A, Greally J, Wickrema A, Verma A. 2013. High resolution methylome analysis reveals widespread functional hypomethylation during adult human erythropoiesis. *J Biol Chem* 288:8805–8814
- Zhang LH, Shin JH, Haggadone MD, Sunwoo JB. 2016. The aryl hydrocarbon receptor is required for the maintenance of liver-resident natural killer cells. *J Exp Med* 213:2249–2257
- Zhang Y, Liu T, Meyer CA, Eeckhoute J, Johnson DS, Bernstein BE, Nusbaum C, Myers RM, Brown M, Li W, Liu XS. 2008. Model-based analysis of ChIP-Seq (MACS). *Genome Biol* 9:R137
- Zhou J, Peng H, Li K, Qu K, Wang B, Wu Y, Ye L, Dong Z, Wei H, Sun R, Tian Z. 2019. Liver-resident NK cells control antiviral activity of hepatic T cells via the PD-1-PD-L1 axis. *Immunity* 50:403–417